AFML-TR-75-207

AN INVESTIGATION OF STRUCTURE-PROPERTY CORRELATIONS IN POLYETHYLENE TEREPHTHALATE FILMS

POLYMER BRANCH
NONMETALLIC MATERIALS DIVISION

APRIL 1976

TECHNICAL REPORT AFML-TR-75-207
FINAL REPORT FOR PERIOD SEPTEMBER 1974 - OCTOBER 1975

AIR FORCE MATERIALS LABORATORY
AIR FORCE WRIGHT AERONAUTICAL LABORATORIES
Air Force Systems Command
Wright-Patterson Air Force Base, Ohio 45433

NOTICE

When Government drawings, specifications, or other data are used for any purpose other than in connection with a definitely related Government procurement operation, the United States Government thereby incurs no responsibility nor any obligation whatsoever; and the fact that the government may have formulated, furnished, or in any way supplied the said drawings, specifications, or other data, is not to be regarded by implication or otherwise as in any manner licensing the holder or any other person or corporation, or conveying any rights or permission to manufacture, use, or sell any patented invention that may in any way be related thereto.

This report was prepared in the Polymer Branch (MBP), Nonmetallic Materials Division, Air Force Materials Laboratory, Air Force Systems Command, Wright-Patterson Air Force Base, Ohio. The work was initiated under Project No. 7340, "Nonmetallic and Composite Materials", Task No. 734004, "New Organic and Inorganic Polymers", Subtask No. 73400465, "Polymer Bulk Properties and Morphology". Co-authors were Dr. A. Viswanathan, National Research Council, Senior Postdoctoral Resident Research Associate; Dr. D. R. Wiff, University of Dayton Research Institute; and W. W. Adams, Air Force Materials Laboratory.

This report covers research conducted from September 1974 to October 1975.

This report has been reviewed by the Information Office (ASD/OIP) and is releasable to the National Technical Information Service (NTIS). At NTIS, it will be available to the general public, including foreign nations.

This technical report has been reviewed and is approved for publication.

DR. I. GOLDFARB

FOR THE COMMANDER

DR. R. L. Van Deusen
Chief, Polymer Branch
Nonmetallic Materials Division

Copies of this report should not be returned unless return is required by security considerations, contractual obligations, or notice on a specific document.

AIR FORCE - 22 JULY 76 - 125

UNCLASSIFIED

SECURITY CLASSIFICATION OF THIS PAGE *(When Data Entered)*

REPORT DOCUMENTATION PAGE		READ INSTRUCTIONS BEFORE COMPLETING FORM
1. REPORT NUMBER AFML-TR-75-207	2. GOVT ACCESSION NO.	3. RECIPIENT'S CATALOG NUMBER
4. TITLE *(and Subtitle)* AN INVESTIGATION OF STRUCTURE-PROPERTY CORRELATIONS IN POLYETHYLENE TEREPHTHALATE FILMS		5. TYPE OF REPORT & PERIOD COVERED Sept 1974 - Oct 1975 Final 6. PERFORMING ORG. REPORT NUMBER
7. AUTHOR*(s)* Dr. A. Viswanathan Dr. D. R. Wiff W. W. Adams		8. CONTRACT OR GRANT NUMBER*(s)*
9. PERFORMING ORGANIZATION NAME AND ADDRESS Polymer Branch, (AFML/MBP) Air Force Materials Laboratory Wright-Patterson AFB, Ohio 45433		10. PROGRAM ELEMENT, PROJECT, TASK AREA & WORK UNIT NUMBERS 73400465
11. CONTROLLING OFFICE NAME AND ADDRESS Polymer Branch (AFML/MBP) Air Force Materials Laboratory Wright-Patterson AFB, Ohio 45433		12. REPORT DATE April 1976 13. NUMBER OF PAGES 127
14. MONITORING AGENCY NAME & ADDRESS*(if different from Controlling Office)*		15. SECURITY CLASS. *(of this report)* Unclassified 15a. DECLASSIFICATION/DOWNGRADING SCHEDULE

16. DISTRIBUTION STATEMENT *(of this Report)*

Approved for public release; distribution unlimited.

17. DISTRIBUTION STATEMENT *(of the abstract entered in Block 20, if different from Report)*

18. SUPPLEMENTARY NOTES

19. KEY WORDS *(Continue on reverse side if necessary and identify by block number)*

Polyethylene Terephthalate	Polymers	X-ray Diffraction
Hermans' Orientation Factor	Mylar Films	Birefringence
Paracrystallinity	Degree of Crystallinity	Computer Program
Disorder Parameter	Mechanical Properties	

20. ABSTRACT *(Continue on reverse side if necessary and identify by block number)*

Six characteristic types of polyethylene terephthalate (Mylar) films were studied by x-ray diffraction techniques. The degree of crystallinity, extent of preferred orientation, crystallite sizes, and paracrystalline disorder were evaluated. The tensile properties were measured in directions parallel and normal to the trace of the optic axial plane as well as in the machine and transverse directions of stretch.

DD FORM 1 JAN 73 1473 EDITION OF 1 NOV 65 IS OBSOLETE

UNCLASSIFIED

SECURITY CLASSIFICATION OF THIS PAGE *(When Data Entered)*

The influence of crystallite orientation on the mechanical properties is discussed. The exceptionally high strength in the machine direction of type 142T film may be associated with the high degree of orientation achieved by a two-way stretch followed by a post-stretch in the machine direction. The balanced, physical properties in type 1000S film are likewise attributable to the presence of two-way stretches in mutually perpendicular directions. The influence of crystallinity was masked by the anisotropic disorder arising from varying degrees of preferred orientation. The techniques employed are indicated to be applicable to other polymeric materials.

FOREWORD

This report was prepared in the Polymer Branch (MBP), Nonmetallic Materials Division, Air Force Materials Laboratory, Air Force Systems Command, Wright-Patterson Air Force Base, Ohio. The work was initiated under Project No. 7340, "Nonmetallic and Composite Materials", Task No. 734004, "New Organic and Inorganic Polymers", Subtask No. 73400465, "Polymer Bulk Properties and Morphology". Co-authors were Dr. A Viswanathan, National Research Council, Senior Postdoctoral Resident Research Associate; Dr. D. R. Wiff, University of Dayton Research Institute; and W. W. Adams, Air Force Materials Laboratory.

This report covers research conducted from September 1974 to October 1975.

Dr. A. Viswanathan is grateful to the National Research Council and Dr. M. T. Gehatia, Air Force Materials Laboratory for providing an opportunity to come to the United States as a Senior Postdoctoral Resident Research Associate. The authors wish to acknowledge the diligent assistance of Mr. D. E. Wright, University of Dayton Research Institute, in data collection on mechanical properties.

TABLE OF CONTENTS

TABLE OF CONTENTS (Contd)

LIST OF TABLES

LIST OF TABLES (Contd)

LIST OF ILLUSTRATIONS

LIST OF ILLUSTRATIONS (Contd)

LIST OF ILLUSTRATIONS (Contd)

SECTION I

INTRODUCTION

Polyester films are now being extensively used in the manufacture of electrical insulation tapes, base material for magnetic recording tapes and decorative laminations, dielectrics in high temperature capacitors, packaging material impermeable to moisture and gases, etc. Polyester resins have more recently found applications in reinforced plastics. Polyethylene terephthalate (herein after referred to as PET) dominates the field of industrial polyester films which are offered in commerce in a wide range of thicknesses. These films are made by various manufacturers under different trade names using varying patented techniques (a list is given in Appendix A). From among these, Mylar film manufactured by duPont was chosen for the current study for two reasons: first, many scientists are aware of one type or another of Mylar films and therefore their research results could be a point of reference to further work; second, by a fortuitous coincidence one of the Mylar film plants is located in Circleville, Ohio, close to the laboratory where the present investigation was carried out. The duPont scientist, Dr. C. J. Heffelfinger, was very cooperative in supplying us the needed material and explaining the general industrial melt processing conditions without divulging the trade secrets that give rise to the different types of Mylar films.

The success of PET to hold its own in industry may be attributed to the following characteristics: ability to permaset; hydrophobic nature; resistance to solvents and acids; indifference to moths, mildews, and microorganisms; resistance to tendering by light and weather conditions; recovery from bending; low creep; retention of properties at moderate and usefully high temperatures; ease of cleaning; etc. Films from PET are strong, tough and yet flexible, and have excellent dielectric properties. A summary of these properties from the work of Heffelfinger and Knox (Reference 1) is given in Appendix B.

The different types of films possess the listed characteristics to different degrees depending on their end-uses. Each end-use requires

highly specialized physical properties. This involves particular treatments during and possibly subsequent to final processing. Basically, these films consist of long molecular chains with varying degrees of orientation and ordered arrangements. Therefore, it is quite conceivable that the mechanical and other physical properties of the polyester (or any other polymer) films are a function of the crystalline structure of the material in question, in particular the degree of crystallinity, crystallite orientation, order, and crystallite sizes.

The present investigation has for its goal the characterization of these parameters for the different types of polyethylene terephthalate films and the possible influence they could have on certain mechanical properties. It is an attempt to infer from an understanding of the basic structural aspects what processing conditions would be needed in order to achieve the desired physical and mechanical properties.

The uniqueness of this approach lies in the fact that although there is reference in current literature to work done with a particular type of Mylar film, such as Mylar 142T or Mylar A, etc., the present study describes results obtained from a number of types of Mylar films thus giving an overview of the field. Also, in the analysis of x-ray data, specialized techniques used earlier with considerable success in cotton fibers have been adapted to the PET films in order to obtain the maximum information from each experiment.

SECTION II

CRYSTAL STRUCTURE OF POLYETHYLENE TEREPHTHALATE

The chemical formula of polyesters falls into three broad categories:

$$\left[-O\cdot R\cdot O\cdot OC\cdot R'\cdot CO-\right],\ \left[-O\cdot R\cdot CO-\right],\ \left[-O\cdot R\cdot O\cdot CO-\right],$$

the possible range of variance of the groups represented by R and R' being extremely wide including aliphatic, alicyclic, aromatic, and heterocyclic types. They may encompass units containing nitrogen, phosphorus, sulphur, silicon, or other atoms. Polyethylene terephthalate is an aromatic polymer of the first type mentioned above and has the chemical formula:

$$\left[O\cdot CH_2\cdot CH_2\cdot O\cdot OC\cdot C_6H_4\cdot CO-\right]_n \text{ or simply } \left[-C_{10}H_8O_4-\right]_n$$

Mylar films are manufactured by reacting dimethylester of terephthalic acid with ethylene glycol giving rise to dihydroxyethylene terephthalate (DHET) which is then treated with excess ethylene glycol in vacuo. In the process of DHET formation, methanol is evolved and during the reaction in vacuo DHET polymerizes by a condensation mechanism.

The crystal structure of polyethylene terephthalate has been determined to be triclinic, though the different workers from their investigations on Terylene (trade name for PET filaments made by ICI, Appendix A) have arrived at different unit cell dimensions as may be seen from Table 1. From the crystal structure, the monomer of PET would seem to possess a center of symmetry as seen from Figure 1 showing the projection of the molecules along c-axis and normal to (010) plane. The monomer itself could be described as:

$$\left[-CH_2-O-C_6H_4-C-O-CH_2-\right]_n$$

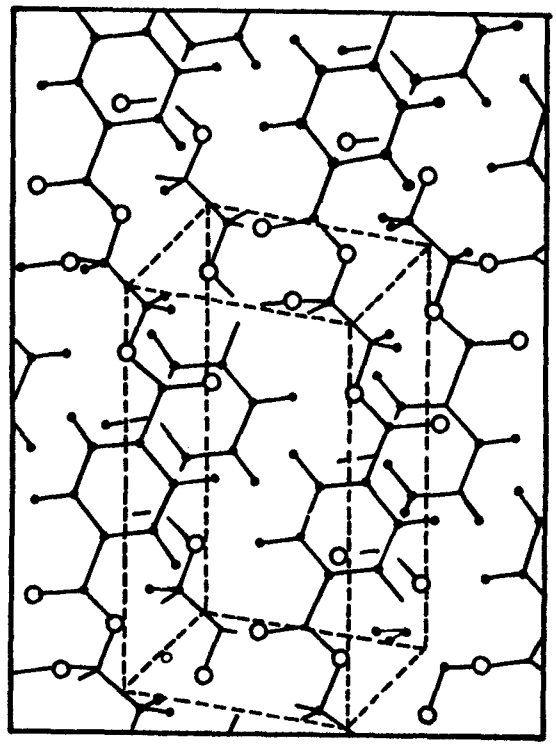

Projection Normal to (010) Plane

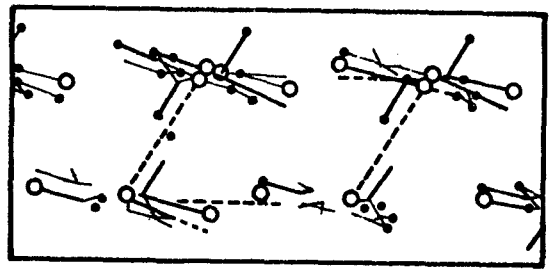

Projection Along C-Axis (Larger Dot, Carbon; Smaller Dot, Hydrogen; Open Circle, Oxygen)

Figure 1. Arrangement of Molecules in the Crystal of Polyethylene Terephthalate

TABLE 1

CRYSTAL STRUCTURE OF POLYETHYLENE TEREPHTHALATE
ACCORDING TO DIFFERENT AUTHORS

Unit Cell Parameters		Values taken from Reference 2	Reference 3	Reference 4
Length:	a:	5.54A	4.56A	4.52A
	b:	4.14A	5.94A	5.98A
	c:	10.86A	10.75A	10.77A
Angle:	α	107°5'	98°30'	101°
	β	112°24'	118°	118°
	γ	92°23'	112°	111°

The unit cell proposed by Astbury and Brown (Reference 2) could not account for the fourth layer reflections obtained for better oriented fiber specimens, so the crystal structure had to be revised. Daubeny et al. (Reference 3) from their x-ray investigation on Terylene fibers concluded that the molecules of PET were essentially flat and the plane of the molecule was roughly parallel to the (100) plane. The molecular axis was inclined by about 5° to the fiber axis. Tomashopolskii and Markova (Reference 4), studying films formed by evaporation of the solvent from a hot 1% solution of polyethylene terephthalate in m-cresol on the surface of water, confirmed, by means of electron diffraction, that the benzene ring was approximately parallel to the (100) plane. The inclination of the axis of the molecules to the c-axis of the crystal was very small, approximately 3°. Heffelfinger and Burton (Reference 5) applying an x-ray beam both normal and parallel to a stack of cast films established that there was no preferred orientation of the crystallites relative to the film surface. Upon orienting by stretching, however, the

(100) planes became parallel to the surface of the film, with the c-axis oriented parallel to the direction of stretch.

From the foregoing it is obvious that experiments involving the reflection from (100) planes would not differentiate between different films. These planes give rise to a peak at $2\theta = 25.75°$ when copper K_α radiation is used. Two other relatively strong peaks occur at $2\theta = 17.35°$ and $2\theta = 42.8°$, which are attributable to (010) and $(\bar{1}05)$ planes. The (010) reflection is in fact overlapping so much with the one from the (011) line profile ($2\theta = 16.5°$) that it is not a convenient base for computation of crystalline parameters. The reflection from $(\bar{1}05)$ is not seriously affected by any of its neighbors. Heffelfinger and Schmidt (Reference 6) attributed the discrepancy between the observed peak position ($2\theta = 42.8°$) of $(\bar{1}05)$ and the theoretically expected angle ($2\theta = 46.0°$) to minor variations in unit cell dimensions. However, upon recalculation with a computer program available in this laboratory, it was verified that $(\bar{1}05)$ reflection should occur at $2\theta = 43°$ and not $2\theta = 46°$. Dumbleton and Bowles (Reference 7) estimated that the normal to $(\bar{1}05)$ planes makes an angle of approximately 10° with the c-axis. Heffelfinger and Schmidt (Reference 6) inferred that the $(\bar{1}05)$ normal makes an angle of 2° with the c-axis. In any case it would be legitimate and convenient to assume the normals to $(\bar{1}05)$ planes to lie nearly parallel to the c-axis. Therefore, from the distribution of these normals, the extent of preferred orientation could be approximately estimated from the intensity distribution of $(\bar{1}05)$ planes, using the procedure described by Hermans and co-workers (Reference 8) for determining the orientation in the case of a diatropic reflection for cellulose. Therefore, it is this reflection that is used in the present work for evaluation of preferred orientation and also crystallite size.

SECTION III

EXPERIMENTAL

1. MATERIAL

Six types of Mylar films of varying thicknesses were investigated. These are designated A, C, D, M, S, and T by the manufacturer. Description of the individual samples is complete with a number (nominal thickness in mil multiplied by 100) followed by a letter denoting the type. Thus, 700D would refer to a film of type D, 7 mil (0.007") thick. M type has an additional numerical designation e.g. M24, M25 and M27, the significance of which is not obvious, but would seem to be related to the type of special coating on the film, applied for improved gas and moisture barrier properties (Reference 1). The actual thicknesses of the films were in substantial agreement with the nominal ones. All the Mylar films were obtained in 12" x 9" sheet form from a representative stock of commercial material (see Introduction).

2. X-RAY DIFFRACTION

A Jarrell-Ash microfocus generator with appropriate flat-film camera was employed to qualitatively study the variations between different types of Mylar films. For quantitative x-ray investigation, a Phillips vertical powder diffractometer was used with pole-figure attachment, semi-automatic electronics including a single channel pulse height analyzer and NaI scintillation detector and teletype output. This equipment offers both reflection and transmission capabilities. The latter was found more appropriate for the present study as Mylar consists of only light atoms (carbon, oxygen and hydrogen), all being poor scatterers of x-rays. All x-ray studies were performed with CuK_{α} Ni filtered radiation. The Phillips unit was operated at 40KV and 30MA, while the Jarrell-Ash unit was operated at 38KV and 6.5 MA.

Experiments on the diffractometer were performed with three objectives: 1) determination of crystallinity and disorder parameter, 2) evaluation of the degree of preferred orientation, and 3) estimation

of the crystallite size. For counting x-ray quanta, the continuous scan method was adopted. The advantages of the step-scan method have been recently emphasized by Blessing and co-workers (Reference 9), but cumulative counting with continuous rotation of the counting arm does not really present any serious loss of accuracy for polymeric materials such as Mylar film giving only a few broad reflections. Further, the scanning speed could be reduced in those experiments requiring higher precision.

a. Crystallinity and Disorder Parameter

Data were collected for crystallinity determination by scanning the x-rays scattered over a range of 2θ values from about 3° to 40° - 60° depending on the degree of crystallization in the material under investigation. After some preliminary work, a standard practice of five readings per minute was found most satisfactory, corresponding to an interval in 2θ of 0.2° with a 2θ = 1° per minute scan. After scanning the x-ray scattering from specimens according to the standard practice, the specimen was transferred to a position between the x-ray port and collimator where a second scan of x-ray scattering was carried out under identical operating conditions. In this way correction for specimen absorption and air scatter could be made in a simple manner, since customary theoretical estimates are not truly valid for polymers. This was noted by Ruck and Krassig (Reference 10). The values of intensities so obtained were corrected for polarization and plotted versus 2θ. These data were then transformed into corrected intensity versus reciprocal lattice coordinate profiles. Following Ruland's computational procedure (Reference 11), described in Appendix C, a consistent value for the degree of crystallinity over the entire angular range of x-ray scattering was obtained.

The degree of crystallinity is defined as

$$X_{CR} = \frac{\int_{s_o}^{s_p} s^2 I_{CR}(s)ds}{\int_{s_o}^{s_p} s^2 I(s)\,ds} \cdot \frac{\int_{s_o}^{s_p} s^2 \overline{f^2}(s)ds}{\int_{s_o}^{s_p} s^2 \overline{f^2}(s)D(s)ds} \qquad (1)$$

where s is the reciprocal space coordinate and equals 2 sin θ/λ; I_{CR} and I are the crystalline and total intensities of coherent scattering respectively; $\overline{f^2}$ is the mean square average scattering factor; D (s) is the disorder function; and s_o and s_p are the lower and upper limits of integration in reciprocal space.

Ruland's method involves an iterative computation as discussed in Appendix C. This somewhat lengthy procedure has been deliberately adopted because it is the only one that seems capable of yielding a meaningful crystallinity parameter and has worked very well with some earlier studies on cotton cellulose (References 12-13).

It should be noted that according to this procedure it has been possible to arrive at identical results from two experiments carried out under different operating conditions and giving two totally dissimilar I vs 2θ profiles as may be seen from Figures 2 and 3.

Experiments for crystallinity would ideally be carried out on unoriented material or pulverized oriented material so as to randomize the crystallites. However, this has been found impractical in the present study since information on the "as-is" material is needed and the crystallite sizes may be altered by a mechanical pulverization process.

b. Preferred Orientation

Experiments for determining preferred orientation were carried out on the texture goniometer attachment to the Phillips x-ray diffractometer.

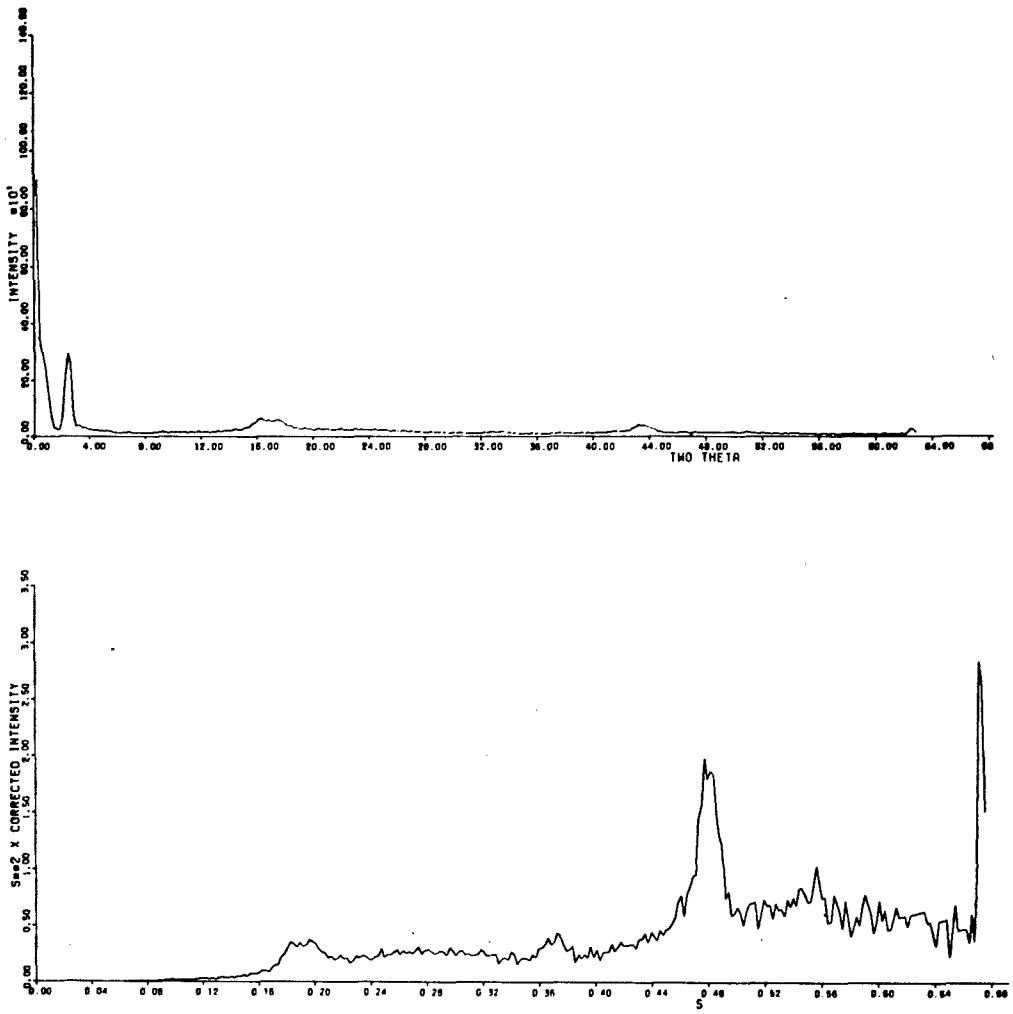

Figure 2. Illustrations of S^2I vs S Curves Under Different Operating Conditions

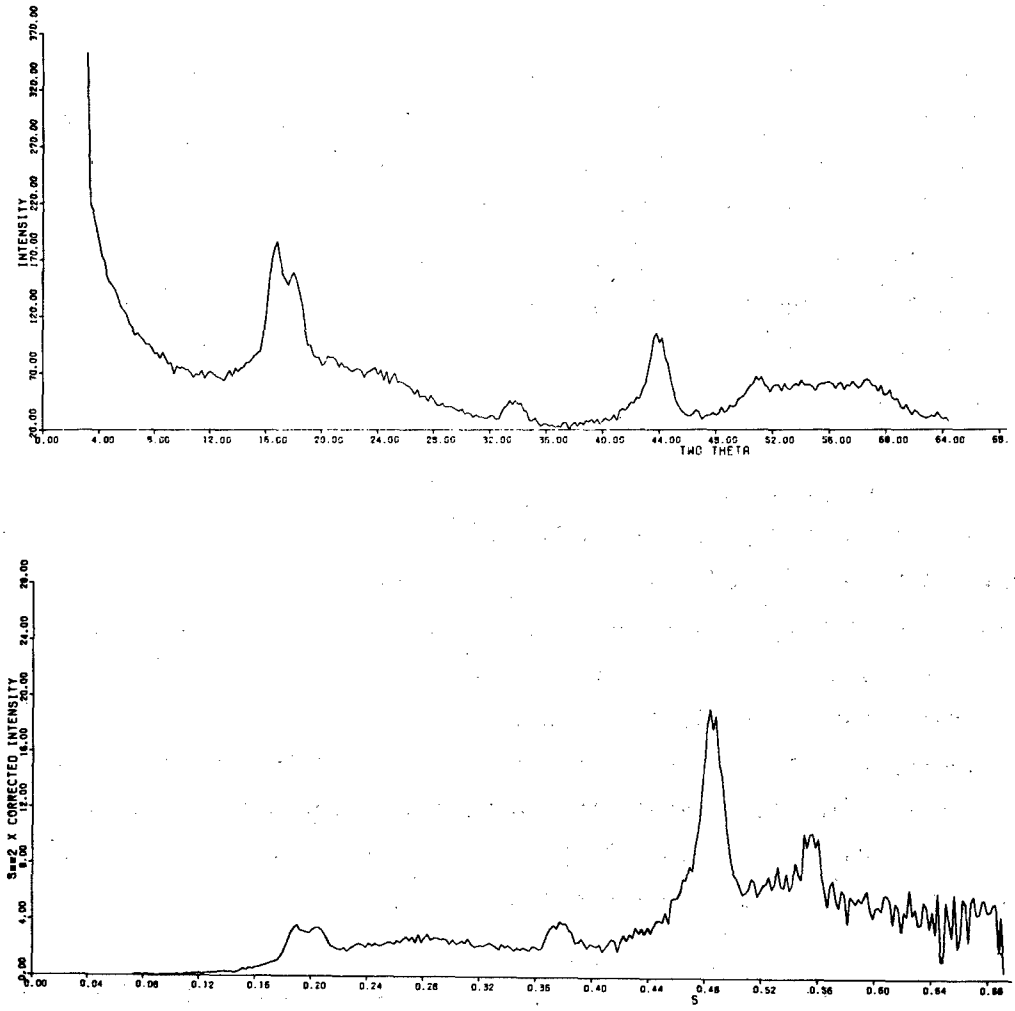

Figure 3. Illustrations of S^2I vs S Curves Under Different Operating Conditions

After locating the maximum intensity of the ($\bar{1}05$) reflection for each film, the specimen was rotated in its own plane (ϕ scan) to bring different planes into reflecting position. This reflection was chosen in preference to those with simpler (hkl) indices, because according to the widely accepted crystal structure of PET, the ($\bar{1}05$) plane is essentially normal to the c-axis and is therefore the best plane to use in correlating a distribution about the c-axis with mechanical properties (Reference 5).

Figure 4 gives the basis for the orientation experiments. ABCDPQRS represents the unit cell. EFGH is the ($\bar{1}05$) plane which is perpendicular to the film surface. As the specimen is rotated in its own plane different sets of ($\bar{1}05$) planes should come into the reflecting position satisfying Bragg's law. If, however, these planes are not randomly distributed in the film, the intensity measurement as a function of the angle of rotation would lead to a quantitative measure of preferred orientation.

Since no prior knowledge of the machine direction (draw direction) of the film during processing was available, the film's orientation axis could only be inferred from the symmetry evident in the azimuthal scanning over a full rotation of the specimen film in its own plane. In this way two complete peaks would appear in the orientation diagram from which the intensity distribution from $\phi = 0°$ (located at one of the two peaks) to $\phi = 90°$ was taken into account for the evaluation of orientation factor. In specimens which had suffered a two-way stretch four peaks would occur and the position of symmetry closer to the c-axis would in this case represent $\phi = 0°$.

Orientation factors were computed using Hermans' expression (Reference 8 and Appendix D):

$$\overline{\sin^2\phi} = \frac{\int_0^{\pi/2} I_{Coh}(\phi) \sin^3\phi \, d\phi}{\int_0^{\pi/2} I_{Coh}(\phi) \sin\phi \, d\phi} \qquad (2)$$

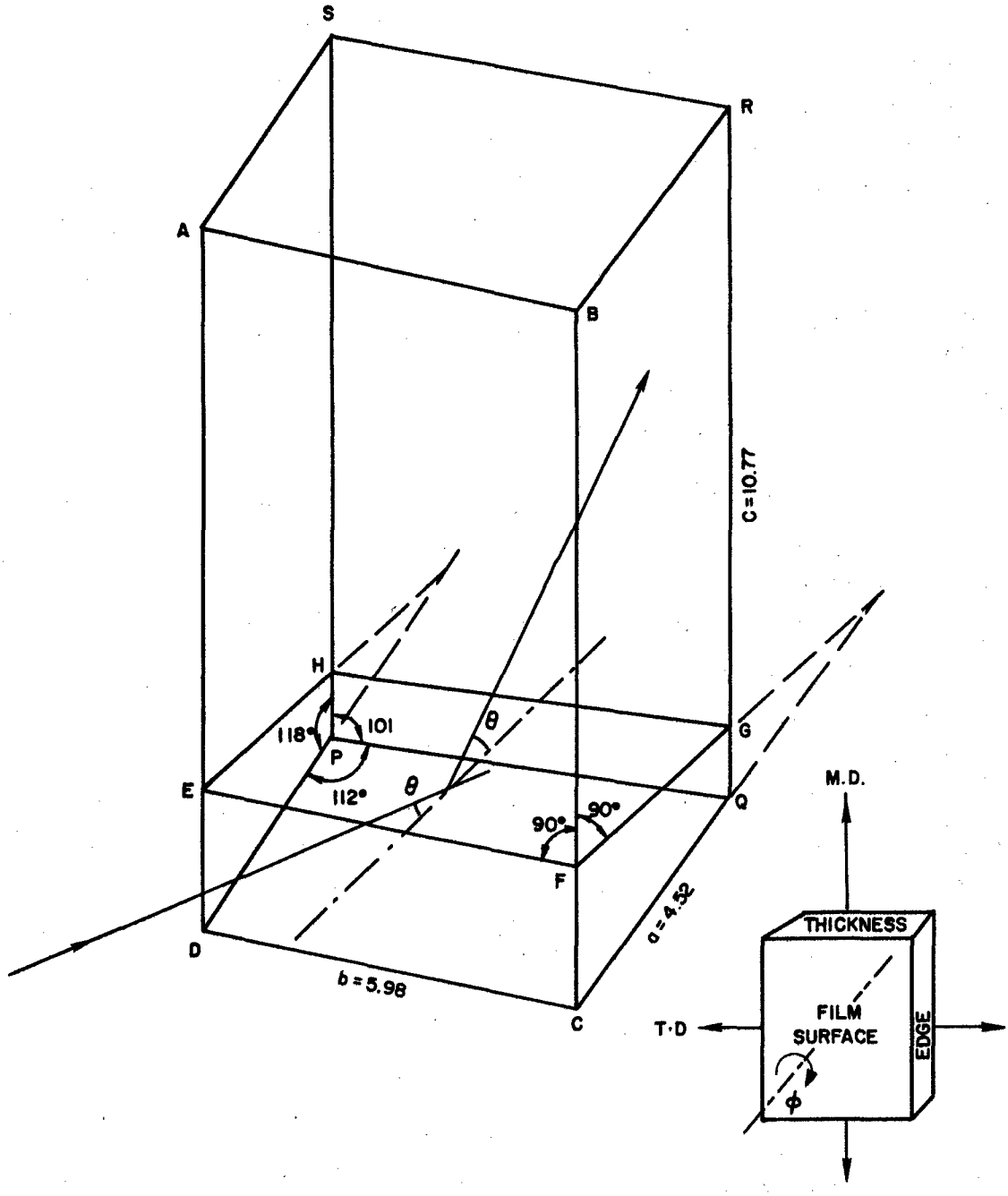

Figure 4. Experimental Basis of Orientation Determination

In the Phillips texture goniometer a complete rotation of the specimen in its own plane for transmission work takes 16 minutes. The orientation scan at this speed and five counting periods per minute corresponded to a measurement of intensity every 4.5° of ϕ. For greater accuracy when deemed more appropriate, the large degree ring of the pole figure device was moved in steps of 1° from ϕ = 0° to 360° or more and intensity measured at each step for fixed time.

Appendix D gives a brief outline of the method for computing the orientation factor from the observed intensity distribution as a function of azimuthal angle.

c. Crystallite Size Determination

Crystallite size is usually determined from the integral breadth of a diffraction line profile after making a correction for instrumental line broadening (Reference 14). The normal practice is to assume a Gaussian expression for the intensity distribution whereby the line breadth is given by

$$\beta_s^2 = \beta_b^2 - \beta_i^2 \tag{3}$$

where s, b, and i stand for sample diffraction, broadened sample profile, and instrumental line breadth, respectively. From the line breadth the crystallite size would be determined by Debye's relation:

$$D_{hk\ell} = \frac{0.9\lambda}{\beta_s \cos\theta_{hk\ell}} \tag{4}$$

This relation yields only an approximate value. For crystallite sizes of the order commonly found in polymeric materials, Debye's relation is not sensitive enough to distinguish between samples known to be processed differently. Wilson's variance-range analysis (References 15-17) has been found very helpful in investigating submicron crystallite dimensions. The experimental data required for this purpose are similar to those needed in other methods; viz., intensities at Bragg angle increments of 0.01° or 0.025° over the entire line breadth. Two estimates

for the crystallite dimensions are obtained from the variance-range curves (Appendix E):

$$\epsilon_k = \frac{\lambda}{\pi^2 k_s \cos\theta} ; \quad \epsilon_w = \frac{\lambda}{2\pi(-w_s)^{1/2}\cos\theta} \tag{5}$$

where ϵ_k and ϵ_w are the crystallite dimension; k_s and w_s are the slope and variance axis intercept from the variance range analysis curves, λ is the wavelength of the radiation, and θ is the Bragg angle.

The noteworthy features of this method are:

i) the correction procedure for instrumental line broadening is straightforward.

ii) one need not be unduly concerned with any particular intensity distribution function such as Gaussian or Cauchy type.

iii) useful interferences can be drawn from the two estimates for the crystalline sizes.

Hexamethylenetetramine powder well compacted served as the crystalline standard giving rise to k_i and w_i from the corresponding variance-range curves. The experimental diffraction profile for the sample was then corrected for instrumental line breadth by means of the expressions:

$$k_s = k_b - k_i$$
$$w_s = w_b - w_i \tag{6}$$

where s, b, and i have the same physical significance as before (Equation 3).

3. MEASUREMENT OF COMPLEX MODULUS OF ELASTICITY AND TAN δ

A "Rheovibron" model DDV-II was employed for the determination of modulus and tan δ as a function of temperature from about -150°C to +200°C, at 11 cycles per second. The length of the Mylar film strip was of the order of a few centimeters and breadth a few millimeters.

These sample sizes were chosen such that together with the film thickness, they satisfied the specifications required by the manufacturers for the useful range of measurement with the direct reading dynamic visco-elastometer (Reference 18).

A sinusoidal tensile strain of an amplitude of 0.005 cm was applied to one end of the sample and the sinusoidal stress generated at the other end was calculated by measuring the corresponding amplitude of the oscillating load. The instrument is based on the direct reading of the force and tan δ. Dispersion curves could be prepared over a wide range of temperature in a relatively short time. On consideration of attaining equilibrium state for each temperature, experiments on each test strip of film were spread over five to six hours. Each type of Mylar film was investigated with two strips cut at right angles to one another within the same sheet.

Liquid nitrogen was used for first cooling the specimen down to approximately -160°C and then measurements were conveniently made as temperature was increased. Around room temperature, a heating appliance was switched on and the current was adjusted from time to time so as to raise the temperature at a rate of about 1°C per minute.

The complex modulus is given by the formula

$$E^* = \frac{\text{Oscillating stress}}{\text{Oscillating strain}} = \frac{\Delta F/S}{\Delta L/L} \qquad (7)$$

where ΔF is the amplitude of oscillating load, S is the area of cross section, ΔL is the amplitude of sinusoidal extension, and L the specimen length. According to the design of the instrument,

and

$$L = 5.\times A \times N \times 10^{-2}\ \text{mm}$$
$$F = \frac{N}{D} \cdot 10^{7}\ \text{dyne} \qquad (8)$$

where A and N are certain instrument constants dependent upon the ranges of force and tan δ employed, as seen on the respective meters, and D is the displacement force. If S and L are measured in mm^2 and mm, respectively, E* would then be given by:

$$E^* = (L/S)_{mm} \times (A \times D - k) \times 2 \times 10^{10} \text{ dynes/cm}^2, \quad (9)$$

k being the correction factor needed to compensate for displacement error in the load measuring dial at zero load.

The instrument constant A was generally unity, but its value increased by a factor of $\sqrt{10}$ when lower ranges of force had to be used to account for the specimen softening at high temperatures. It may be mentioned in passing that A is the amplitude factor which would increase when the material becomes softer, but the actual amplitude remains unaffected in practice since the corresponding tan δ range is varied by a factor N such that AxN = 1. Thus, the amplitude of the sinusiodal strain is always of the order of 0.25% - 0.5% of the initial length of the film strip.

From the experimentally observed values of displacement force D, the complex modulus E* was calculated. Making use of the parameter tan δ read directly on the instrument, the elastic modulus E', and loss modulus E" were calculated from the relations:

$$E' = E^* \cos \delta \approx E^*, \text{when } \delta \text{ is small}$$
$$E'' = E^* \sin \delta \approx E^* \tan \delta, \text{when } \delta \text{ is small} \quad (10)$$

4. TENSILE PROPERTIES

The first and foremost criterion of the usefulness of any material would be its mechanical properties; whether the material will bear a load demanded by its end-use before breaking and a repeated application of that load before yielding. For the purpose of investigating these aspects, the Instron tensile strength tester was used and the stress strain diagram was obtained. A load cell of 1000 lbs capacity was employed. Strips of 5 x 1 cm were cut parallel and perpendicular to

machine directions from the Mylar sheets. In order to assess the strengths in other characteristic directions in the material, individual films were also examined under conoscopically polarized light. Positions of extinction were carefully observed and corresponding angles with the longer side of the strips, (measuring about 4 mm x 1 mm) were recorded. Then strips for the Instron tests were cut parallel and perpendicular to the trace of optic axial plane. Wherever the edges of the films coincided with the two optically determined directions, supplementary tests were made on film strips cut diagonally with respect to the original sheets, i.e., at 45° to the machine and transverse directions. The specimens were strained at the rate of 20% per minute of their initial length corresponding to the specimen length of 2 inches and crosshead speed of 0.4 inch per minute. All the experiments were carried out at room temperature, 70°F, and 40% relative humidity.

SECTION IV

RESULTS AND DISCUSSION

Figures 5 to 10 represent the x-ray diffraction patterns obtained from the six types of Mylar films. They give a general view of the qualitative differences. It is, however, most convenient and appropriate to present and discuss the results associated with each type of film examined rather than analyze all films at one time in terms of a specific crystalline parameter or tensile property.

1. MYLAR FILM TYPE A

From Table 2 it may be seen that the strength is largest in the direction normal to the trace of optic axial plane, i.e., a line joining the emergent points of the optic axes from the polymer film surface, as seen when using conoscopic polarized light. There is some systematic error between the mean values obtained from individual sheets, which are shown in different columns under the same heading. This may be attributed to the slight discrepancies arising while cutting the specimen strips. A simple statistical test shows that the difference between the means of the tensile strengths in the machine and transverse directions is not significant.

Table 3 gives the comparative values of all the mechanical properties tested on the Instron in the indicated different directions. The results are in accordance with the observations usually made on polymers, viz., the higher the strength, the lower the extensibility. From the x-ray studies on Mylar film of 10 mil type A, it is seen that the orientation factor (f_x = 0.276) is lower in film A than in the case of certain other types. The disorder parameter k = 0.3 can be considered in the case of 1000A film to hold true for the bulk of the material as though it is isotropic in character, in view of the poor orientation. The x-ray diffraction spectra used in determination of crystallinity and disorder parameter, orientation factor, and crystallite size are shown in Figures 6-9, respectively.

TABLE 2

TENSILE STRENGTHS FOR MYLAR FILMS 10 MIL TYPE A: STRIPS IN DIFFERENT DIRECTIONS (x 10^9 DYNES/CM^2)

M. D.[a]		T. D.[b]		N. O.[c]		P. O.[d]	
1.42	1.49	1.40	1.40	1.89	1.99	1.31	1.32
1.37	1.53	1.43	1.42	1.87	1.96	1.24	1.27
1.42	1.51	1.35		1.88	2.00	1.28	1.24
		1.43		1.86	1.99	1.24	
		1.43		1.85	2.00		
		1.42					
Mean	1.457	1.410		1.929		1.271	
S.D	.057	.025		.061		.027	
%S.D	3.9	1.8		3.2		2.1	

a. M. D: Strips cut parallel to machine direction.

b. T. D: Strips cut parallel to transverse direction (normal to a).

c. N. O: Strips cut normal to the trace of optic axial plane.

d. P. O: Strips cut parallel to the trace of optic axial plane.

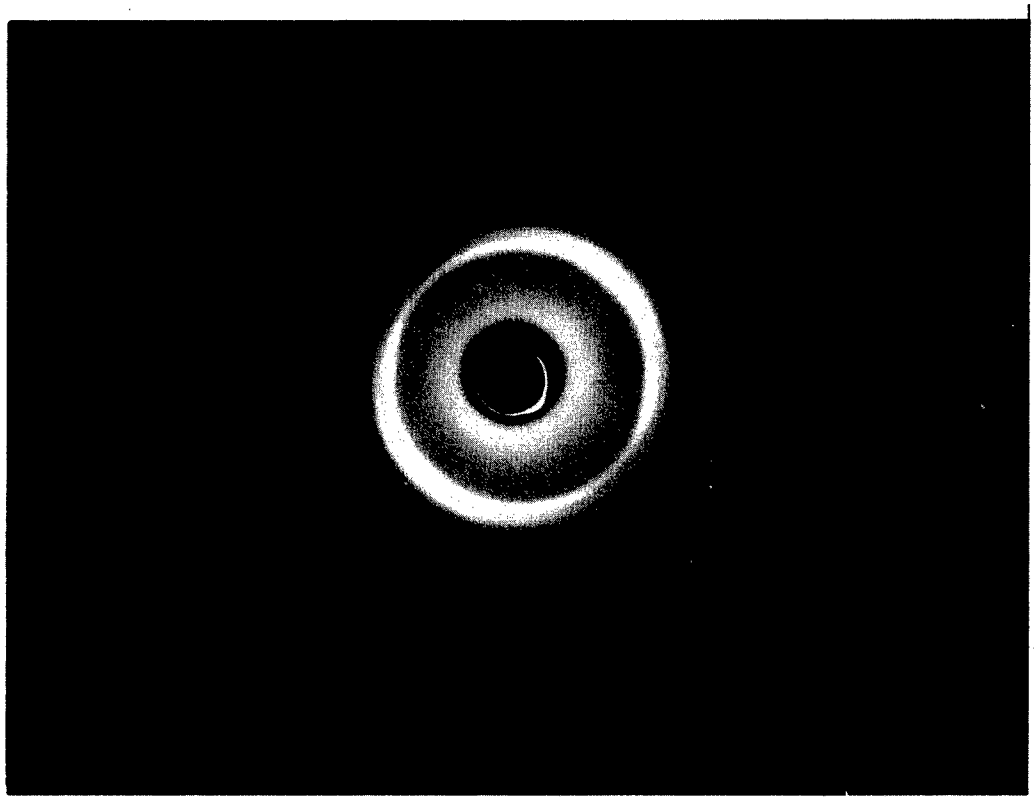

Figure 5. Flat Film X-Ray Diffraction Photograph for Type 1000A Mylar Film

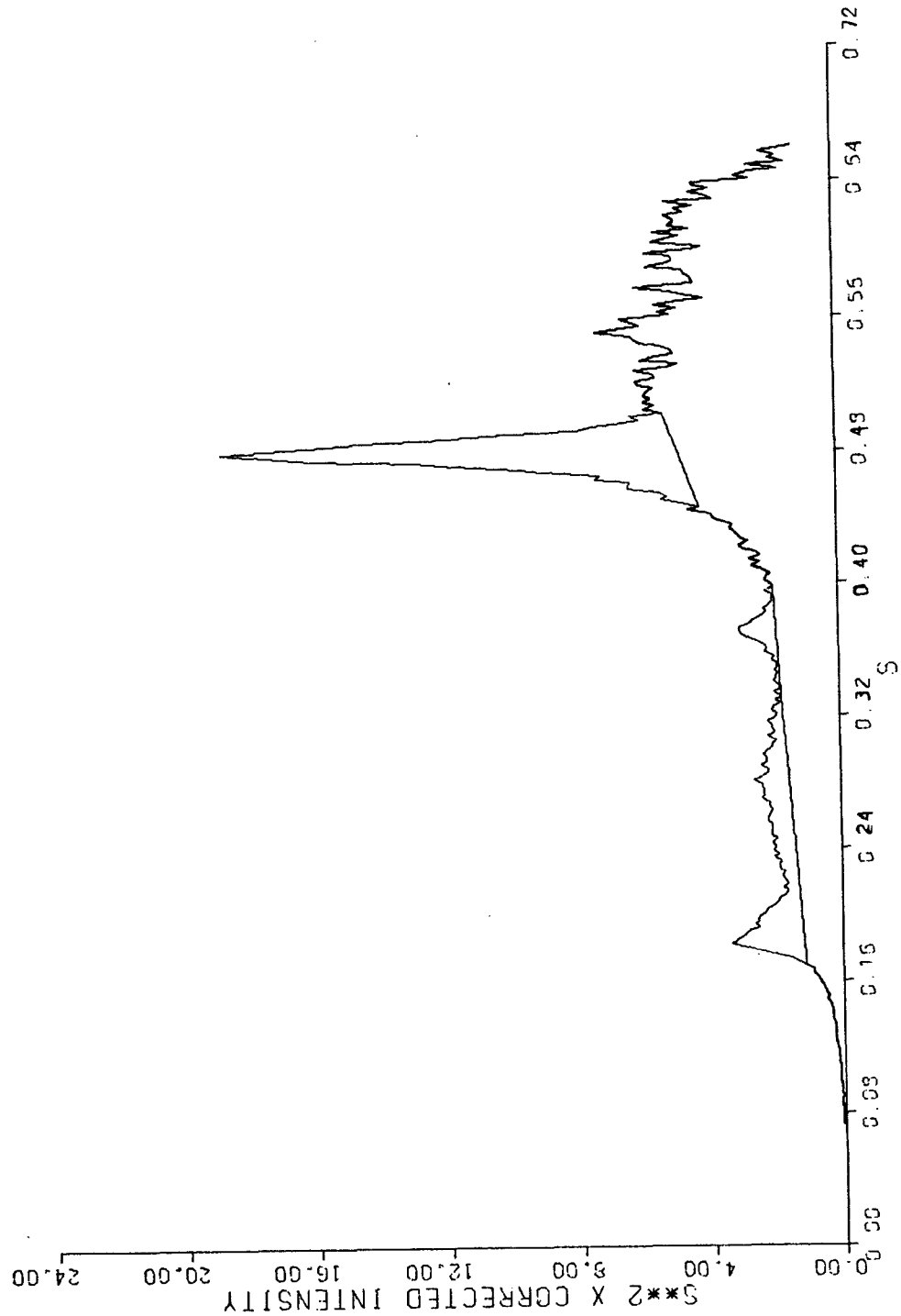

Figure 6. Crystalline and Amorphous Contribution to Total X-Ray Scattering Intensity. Used in the Calculation of Degree of Crystallinity and Disorder Parameter for Mylar Film Type 1000A (Table 15). S is the Magnitude of the Reciprocal Lattice Vector

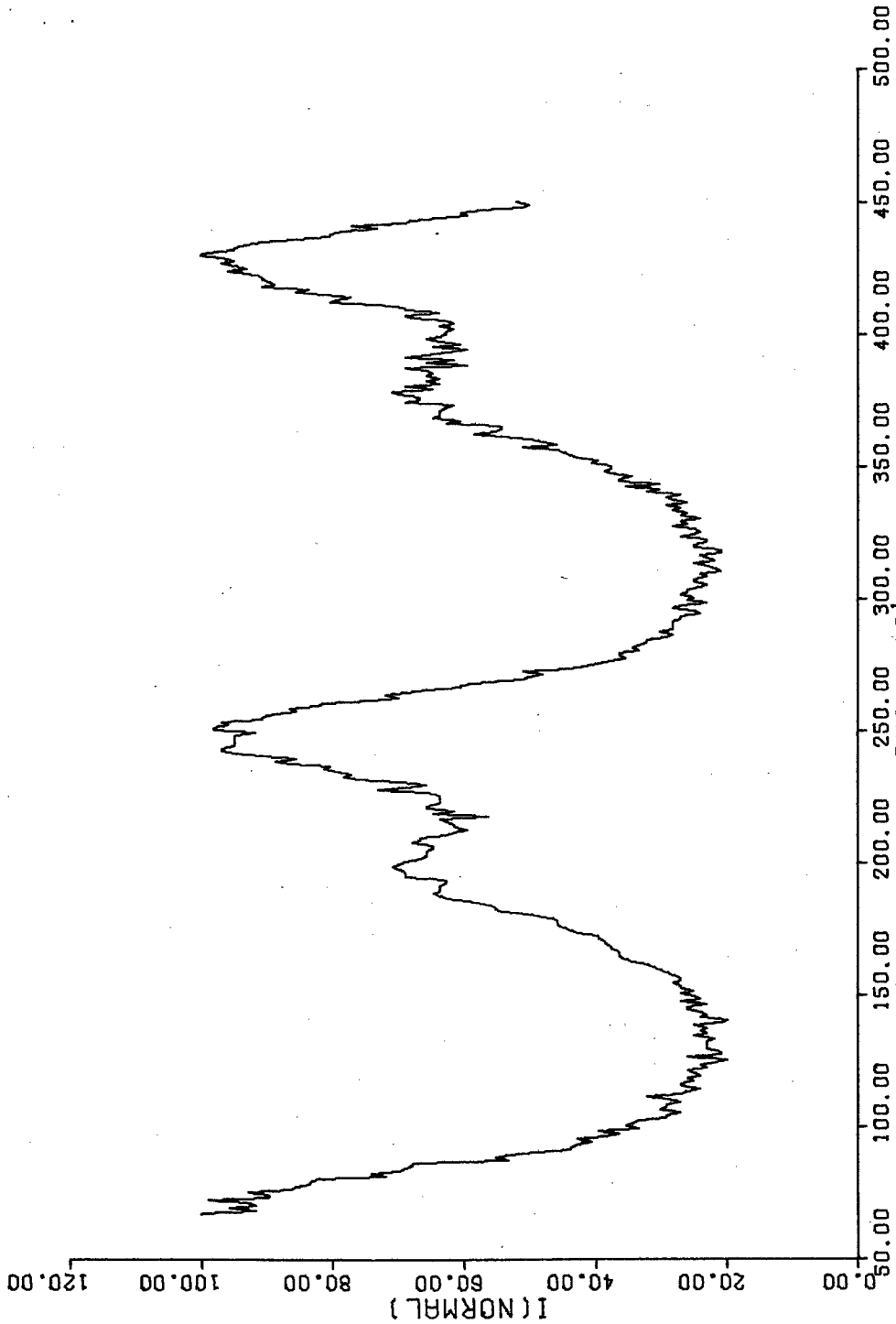

Figure 7. Orientation Scan for Mylar Film Type 1000A. Used in Calculation of Orientation Factor (Table 16). ϕ Scan for T05 Reflection, $2\theta = 42.5°$

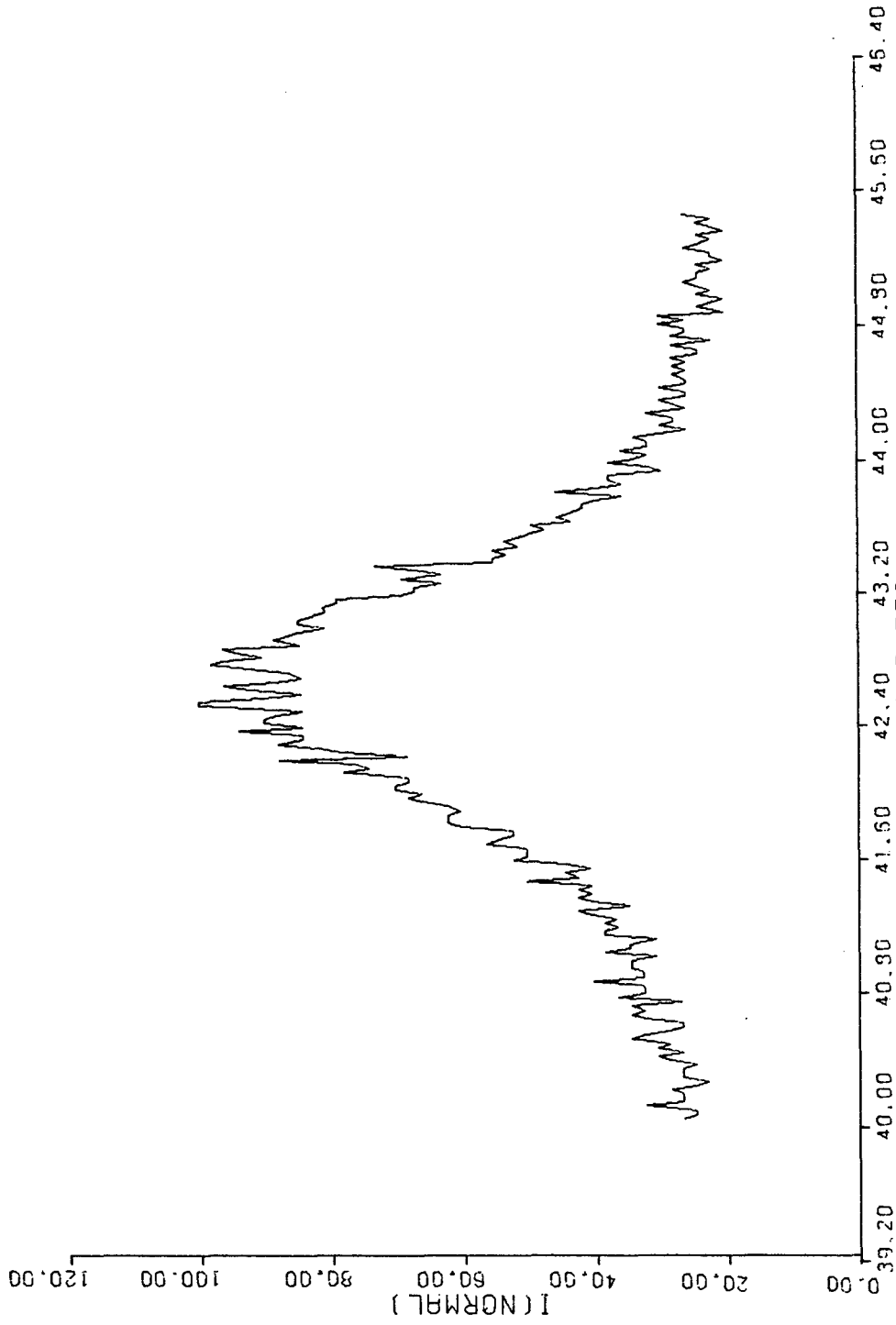

Figure 8. Radial (2θ) Intensity Distribution for $\bar{1}05$ Reflection for Mylar Film Type 1000A. Used in Calculation of Crystallite Size (Table 17 and Figure 9).

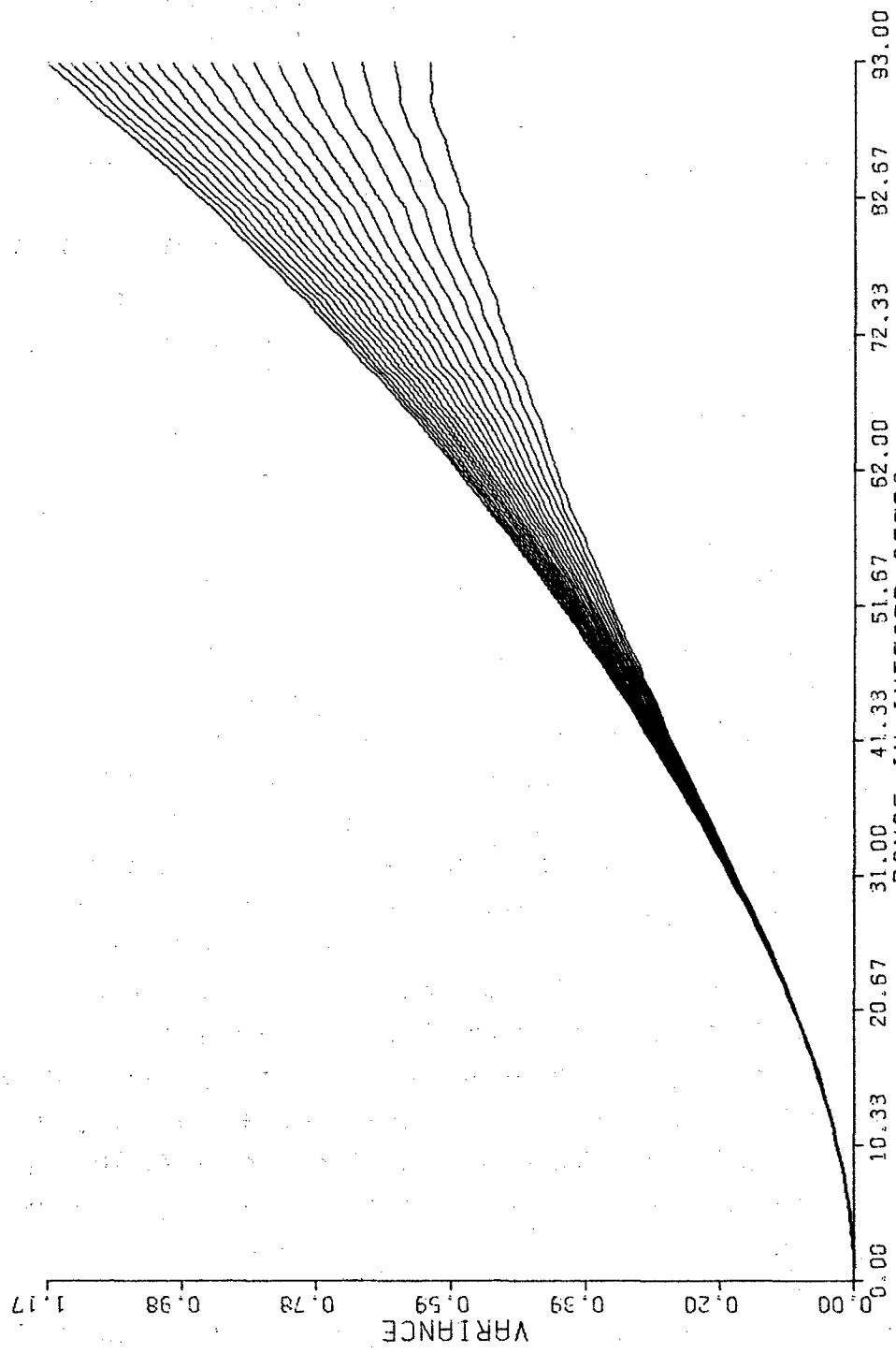

Figure 9. Wilson's Variance Range Analysis Applied to Intensity Distribution for Figure 8, Mylar Film Type 1000A (Table 17)

TABLE 3

MECHANICAL PROPERTIES OF MYLAR FILM TYPE A IN DIFFERENT DIRECTIONS

	M. D.	T. D.	M. O.	P. O.
Tensile Strength ($\times 10^9$ dynes/cm^2)	1.46	1.41	1.93	1.27
Elastic Modulus ($\times 10^{10}$ dynes/cm^2)	3.68	3.53	3.79	3.19
Extension at break (Strain %)	56.2	62.6	49.5	90.2

2. MYLAR FILM TYPES S

Table 4 summarizes the results for film 1000S. It may be shown that difference between the mean tensile strengths in directions a and c or between b and d is statistically nonsignificant. This is only to be expected, because the trace of optic axial plane was found in this film to be nearly parallel to the transverse direction, being inclined at an angle of only 12° as seen under polarized light. This is quite in contrast with the corresponding inclination of 51° in the film type 1000A. The latter is biaxially stretched i.e., strained both in the machine and transverse directions simultaneously during processing or successively during and after processing. This would naturally result in an orientation of the long chain molecules of PET at an angle to either of the two directions (M.D. and T.D.). If these stretches are nearly equal, the inclination might approximate 45° as in film type 1000A. Also on account of the greater orientation, film strips cut at this angle would have the greatest strength.

The film type S is more "balanced" with nearly equal strengths in all the four directions. Thus, the maximum strength of almost 2.0×10^9 dynes/cm^2 which is reached in the direction c-(normal to the

trace of optic axial plane) of 1000A remains unattainable in film type 1000S where there is apparently a poorer orientation. The orientation factor in this film is 0.037 as against 0.146 for film type 1000A. The apparently poor orientation in film S may also be interpreted differently in the light of strength data (Table 5). As for the significant differences in the values for tensile strengths between the film types 1000A and 1000S, (1.66×10^9 and 1.59×10^9 dynes/cm^2, respectively, in M.D. and T.D. for S type as against 1.46×10^9 and 1.41×10^9 dynes/cm^2, respectively, for A type), it seems more desirable to resolve the azimuthal scan into two intensity distributions, one arising from the orientation on extension in the machine direction and another due to orientation on stretching the film laterally. Unfortunately, the procedure for resolution could at best only be arbitrary and depending on the manner of resolution the two line profiles for orientation could lead to different results for orientation parameters.

Thus by two variations of "hand smoothing" of the same experimental azimuthal scan, two sets of values were obtained: (1) orientation factors of 0.72 and 0.66 for the peaks resolved in the M.D. and T.D. respectively; (2) orientation factors of 0.58 and 0.49 being the corresponding values in the second method.

In either case, it is important to note, the orientation was larger in the machine direction leading to significantly higher strengths in that direction.

The poor overall orientation ($f_x = 0.037$) might then be attributed to the overlapping of two relatively strong stretches in mutually perpendicular directions. A similar analysis of the azimuthal scan was not done for the film type 1000A because of the greater overlapping. In passing, it may be mentioned that the reflection from (024) planes, occurring at $2\theta = 41.8°$ partially overlaps the azimuthal line profile of ($\bar{1}05$) both in film types 1000S and 1000A. This is more marked in A due to the shift in the ($\bar{1}05$) reflection from the meridian.

It must be pointed out here that the maximum intensity of radial distribution occurs at the angle $2\theta = 43.4°$ with a second peak at $2\theta = 16.4°$ having only about 60% intensity of the former.

Thus the $(\bar{1}05)$ planes which are normal to the machine direction are already quite preferentially oriented in the reflecting position. Therefore, the disorder parameter from this experiment is no longer representative of the isotropic order in the bulk of material and is strictly not comparable with the value of 0.3 for the disorder, almost isotropic in nature, obtained for film type 1000A. However, one could speculate that film type 1000S would have attained the maximum strength of 2.0×10^9 dynes/sq. cm were it not for the greater disorder. The x-ray diffraction spectra used in determination of crystallinity and disorder parameter, orientation factor, and crystallite size are shown in Figures 11-14, respectively.

TABLE 4

TENSILE STRENGTH FOR MYLAR FILMS 10 MIL TYPE S: STRIPS IN DIFFERENT DIRECTIONS ($\times 10^9$ dynes/cm^2)

MD	a	T. D.	b	N. O.	c	P. O	d
1.70	1.63	1.59	1.56	1.63	1.67	1.53	1.50
1.65	1.64	1.58	1.60	1.60	1.68	1.56	1.51
1.67		1.66		1.60	1.65	1.56	1.65
1.66		1.54		1.53	1.71	1.63	
				1.59	1.72	1.61	
Mean	1.658	1.588		1.637		1.569	
S. D.	.023	0.038		.056		.052	
%S. D.	1.4	2.4		3.4		3.3	

TABLE 5

MECHANICAL PROPERTIES OF MYLAR FILM TYPE 1000S
IN DIFFERENT DIRECTIONS

	a M.D.	b T.D.	c N.O.	d P.O.
Tensile Strength (x 10^9 dynes/sq cm)	1.66	1.59	1.64	1.57
Elastic Modulus (x 10^{10} dynes/sq cm)	3.91	3.57	3.61	3.64
Extension at Break (Percent of initial length)	58.2	68.0	57.6	66.2

3. MYLAR FILM TYPE 700D

Table 6 gives a summary of results on the tensile strengths of film type 700D. The machine direction in this case was inclined at an angle of 87° to the trace of optic axial plane (the transverse direction and trace of optical axial plane are almost coincident). Therefore, the measurements in the machine and transverse directions would be almost identical with those that might be made normal and parallel to the trace of the optic axial in the film. The values quoted in columns three and four then arise from film strips cut at right angles to each other and at equal inclination to machine/transverse directions. As might be expected, the tensile strength is the highest in the machine direction and least in the transverse direction, the value being intermediate at 45° to either. From the coincidence of the machine direction with the normal to the trace of optic axial plane, it may be inferred that this film is uniaxially strained and the orientation factor for this film should be considerably greater than that obtained for either type 1000A or 1000S films. Results from three independent experiments with film type 700D show that the Hermans' orientation factors are: 0.56, 0.57 and 0.58, all within reasonable limits of experimental error.

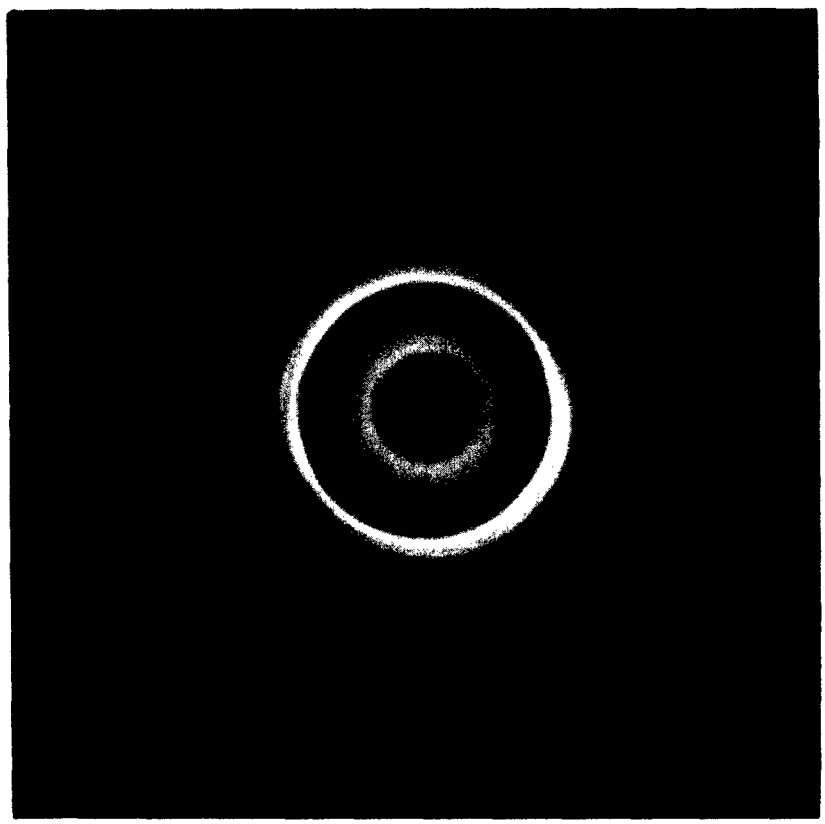

Figure 10. Flat Film X-Ray Diffraction Photograph for Type 1000S Mylar Film

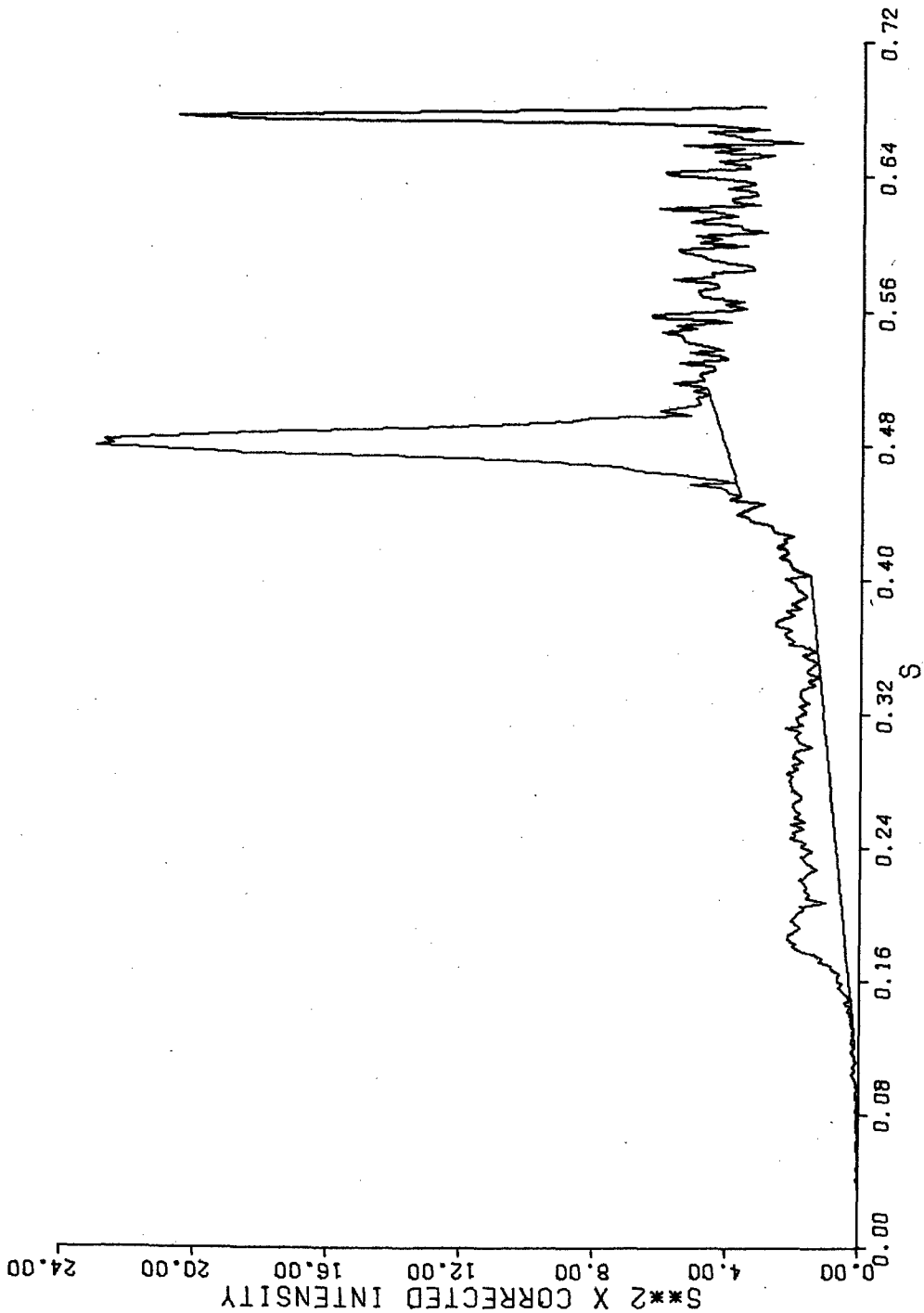

Figure 11. Crystalline and Amorphous Contribution to Total X-Ray Scattering Intensity. Used in the Calculation of Degree of Crystallinity and Disorder Parameter for Mylar Film Type 1000S (Table 15). S is the Magnitude of the Reciprocal Lattice Vector

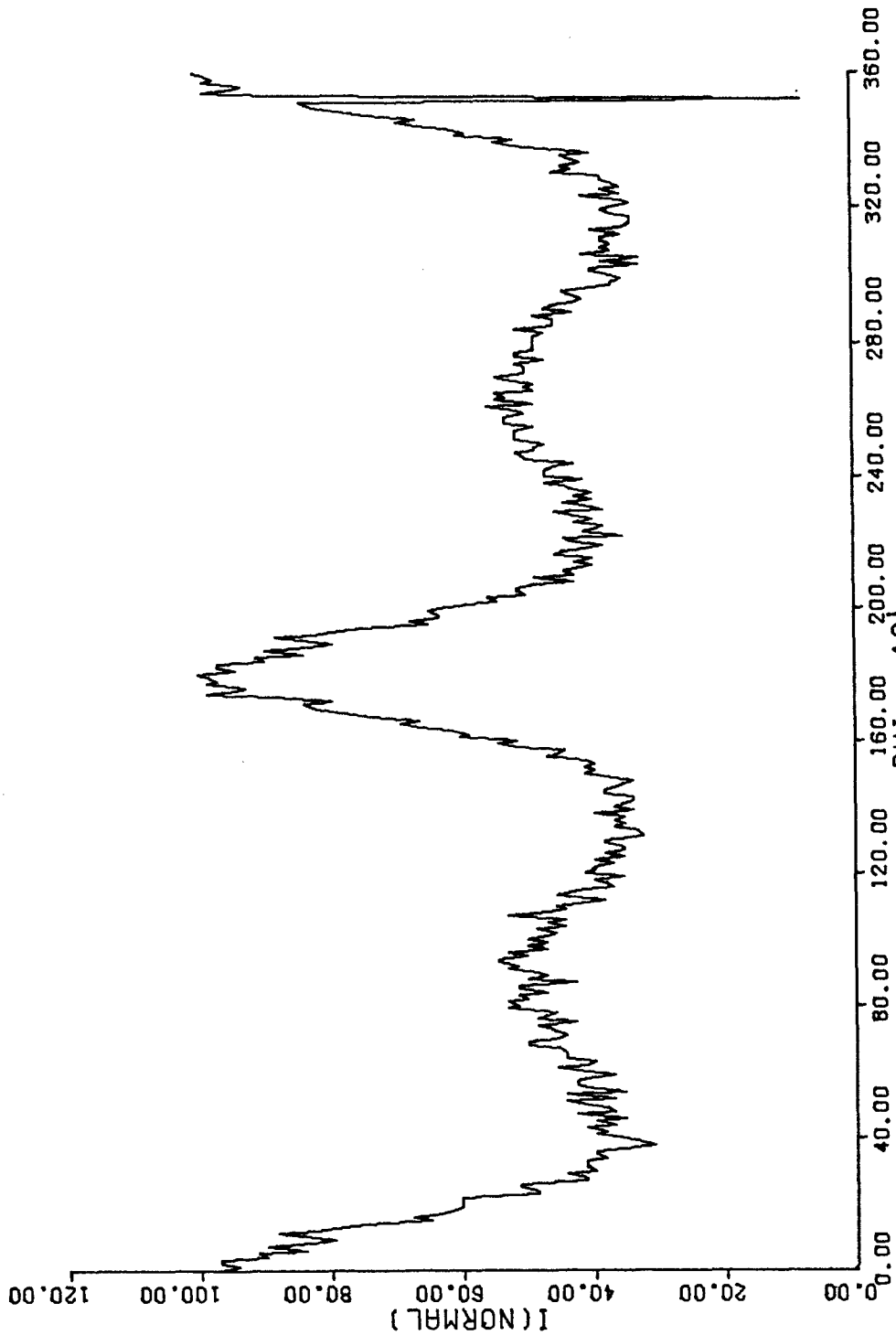

Figure 12. Orientation Scan for Mylar Film Type 1000S, Used in Calculation of Orientation Factor (Table 16). ϕ Scan for $\bar{1}05$ Reflection, $2\theta = 42.5°$

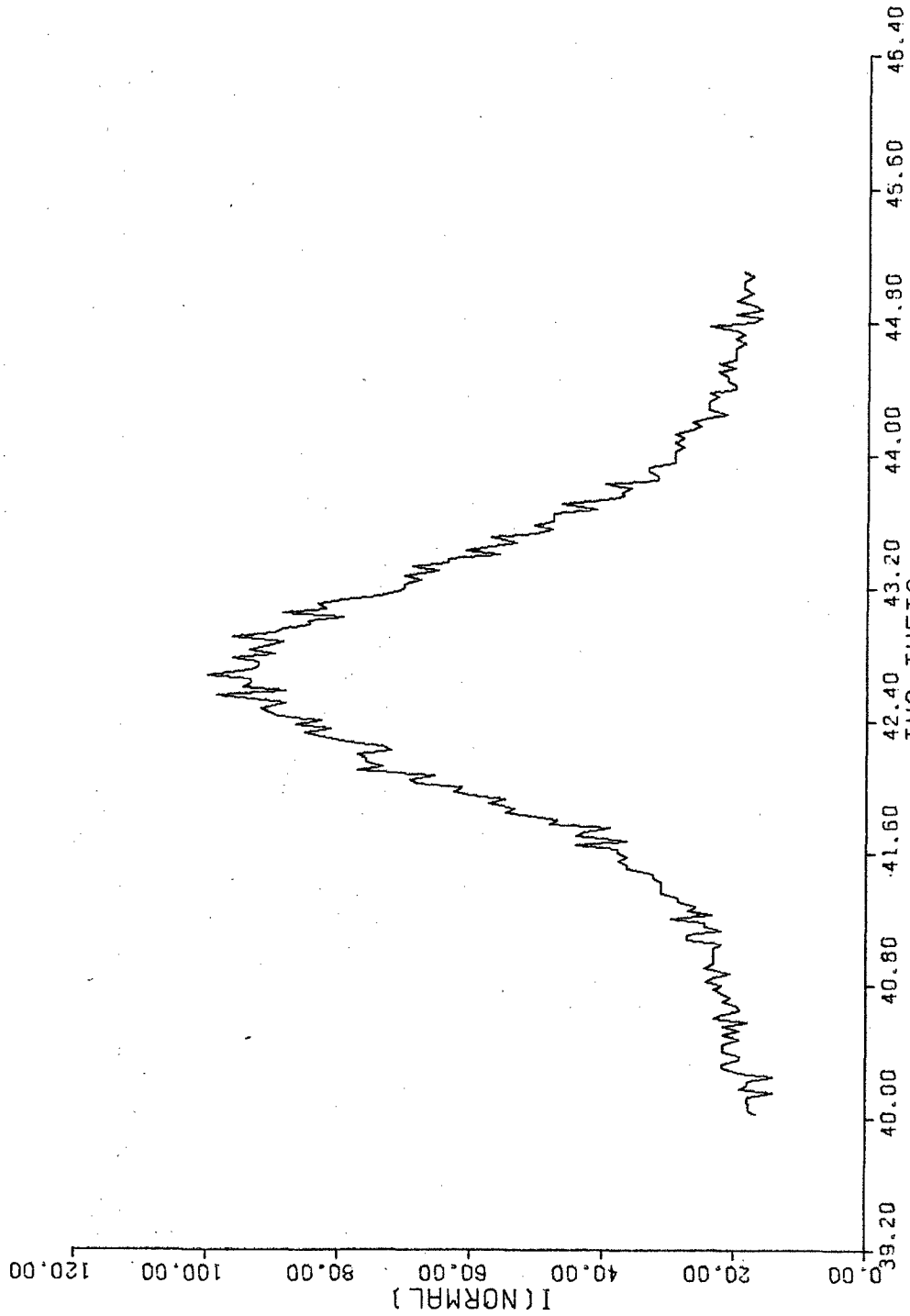

Figure 13. Radial (2θ) Intensity Distribution for T05 Reflection for Mylar Film Type 1000S. Used in Calculation of Crystallite Size (Table 17 and Figure 14)

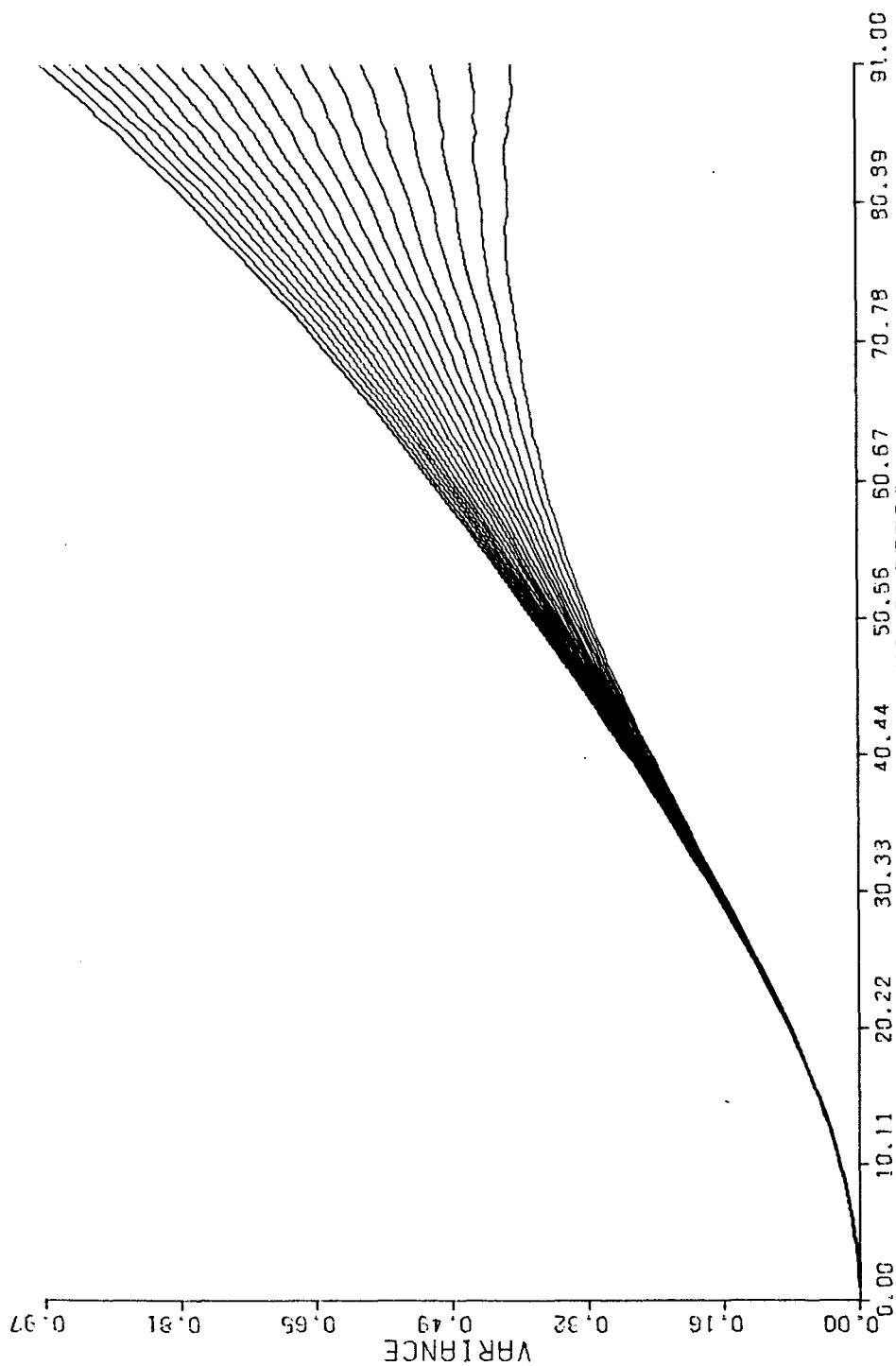

Figure 14. Wilson's Variance Range Analysis Applied to Intensity Distribution for Figure 13, Mylar Film Type 1000A (Table 17)

Because of the presence of a high degree of preferred orientation, the evaluation of crystallinity and disorder is now critically dependent on how the specimen is oriented with respect to the x-ray beam and the machine direction of the film. With the beam perpendicular to the film surface, as usual, and the machine direction horizontal, a scan of the x-ray scattering by the vertical goniometer leads to a disorder parameter of 1.0 and a degree of crystallinity of 0.34, other things remaining the same. If the machine direction were held vertical, the values of disorder parameter and crystallinity are respectively 0.8 and 0.52.

TABLE 6

TENSILE STRENGTHS OF MYLAR FILM TYPE 700D IN DIFFERENT DIRECTIONS (x 10^9 DYNES/SQ CM)

	M. D.	T. D.	at 45° to MD/TD	
	1.73	1.07	1.35	1.19
	1.87	1.05	1.33	1.30
	1.72	1.06	1.43	1.25
	1.72	1.07	1.34	1.33
	1.83	1.03	1.38	1.32
	1.75	1.04	1.29	1.22
Mean	1.770	1.053	1.311	
S.D.	.059	.015	.064	
% S.D.	3.3	1.4	4.9	

TABLE 7

MECHANICAL PROPERTIES OF MYLAR FILM TYPE 700D FILMS
IN DIFFERENT DIRECTIONS

	M. D.	T. D.	at 45° to MD/TD
Tensile Strength ($\times 10^9$ dynes/cm^2)	1.77	1.05	1.31
Elastic Modulus ($\times 10^{10}$ dynes/cm^2)	3.95	3.17	3.45
Extension at Break (Percent of initial length)	32.0	47.4	46.2

Naturally, it becomes hazardous to attempt any correlation of these parameters and it becomes more desirable to randomize the crystallites by pulverizing the films (with the attendant uncertainties of the effects of such a treatment) before crystallinity is evaluated.

A resume´ of the results from the tests on type 700D film with the Instron is given in Table 7. The extensibilities for this film are lower than for either S or A. In the machine direction it is almost 30%, approximately half the value obtained in the film type A or S. The x-ray diffraction spectra used for morphological characterization are found in Figures 16 - 19.

4. MYLAR FILM TYPE 142T

Table 8 gives the details of results obtained on the tensile strength tests. Here again as in the case of type 700D film the normal to the trace of the optic axial plane coincided with the machine direction, in which a strength of 2.392×10^9 dynes/cm^2, the highest ever, was observed. This agrees very well with Heffelfinger's remark (Reference 1) that type T has an exceptional tensile strength in the longitudinal direction. As one might expect the strength in the transverse direction is the least, while at 45° to either, it is intermediate.

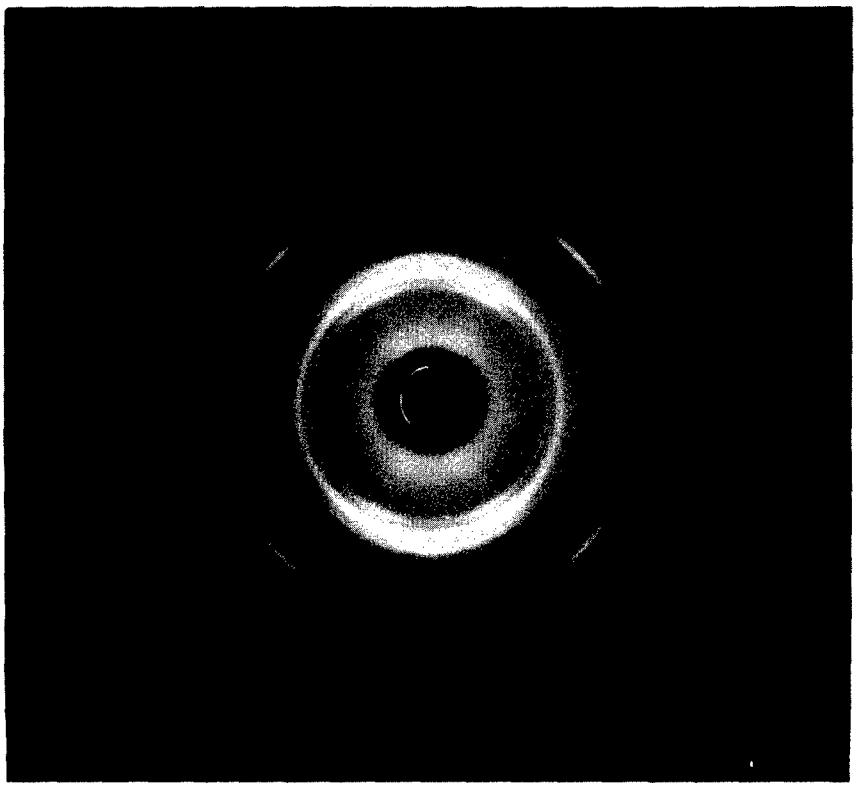

Figure 15. Flat Film X-Ray Diffraction Photograph for Type 700D Mylar Film

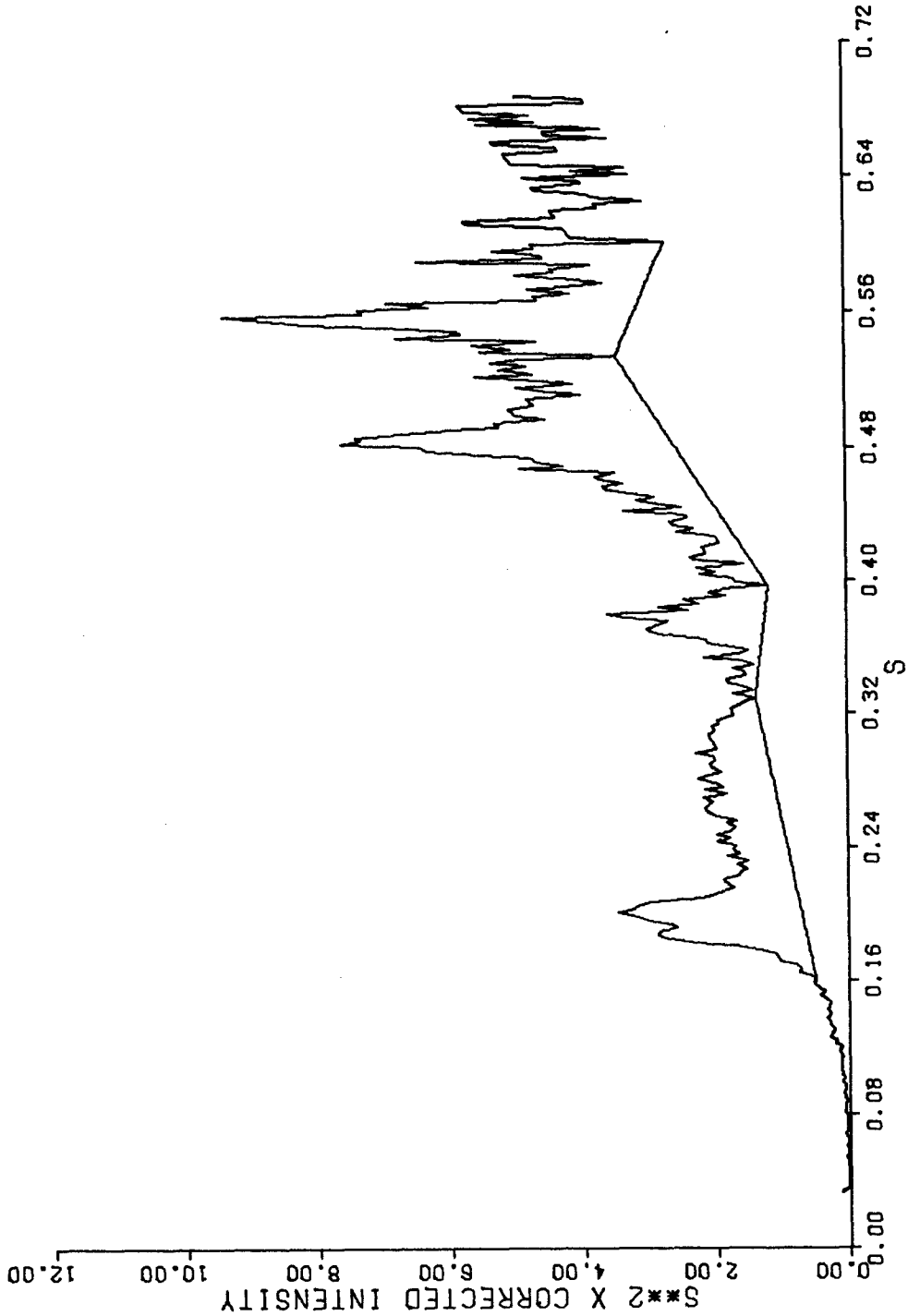

Figure 16. Crystalline and Amorphous Contribution to Total X-Ray Scattering Intensity. Used in the Calculation of Degree of Crystallinity and Disorder Parameter for Mylar Film Type 700D (Table 15). S is the Magnitude of the Reciprocal Lattice Vector

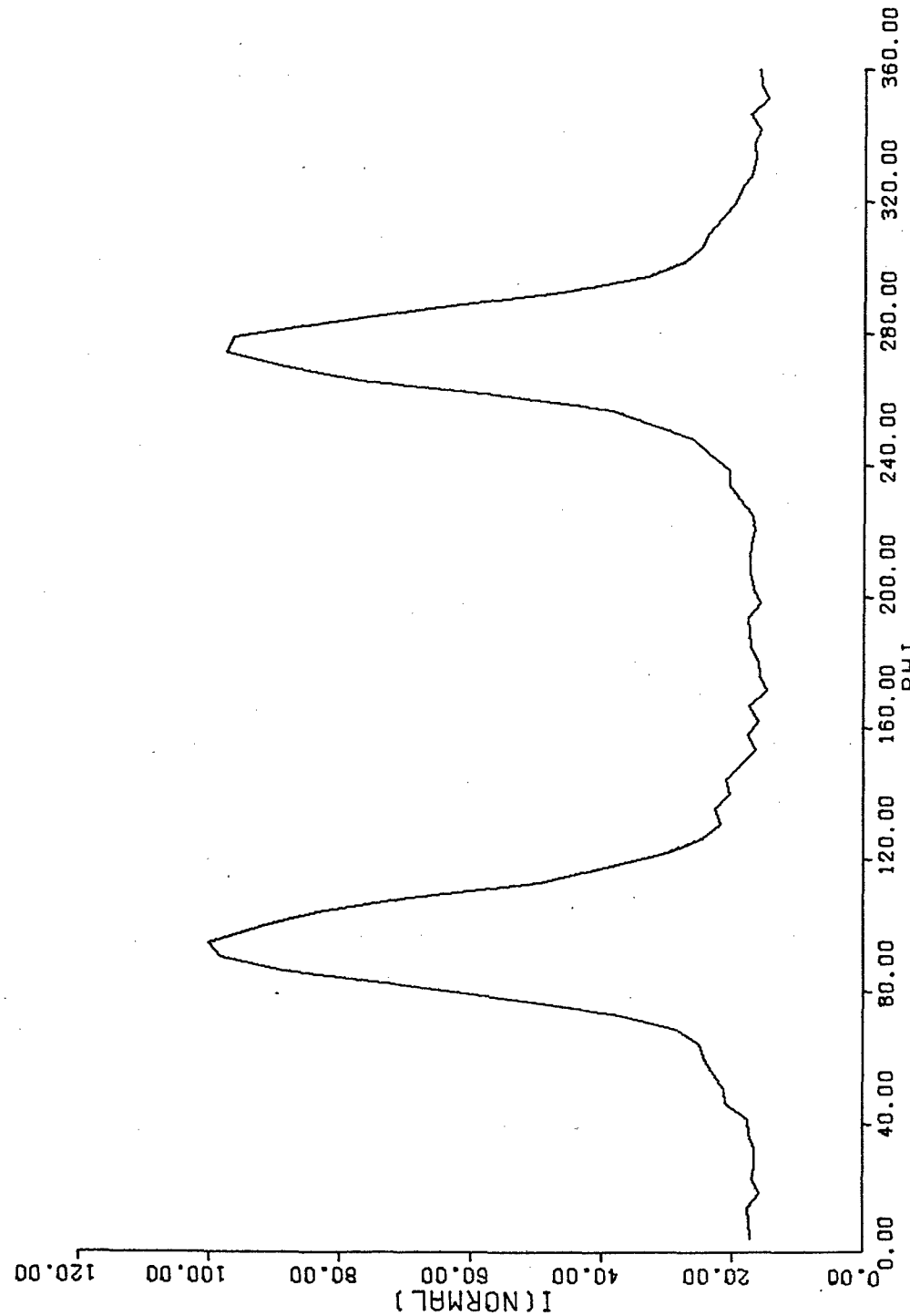

Figure 17. Orientation Scan for Mylar Film Type 700D. Used in Calculation of Orientation Factor (Table 16). ϕ Scan for $\bar{1}05$ Reflection, $2\theta = 42.5°$

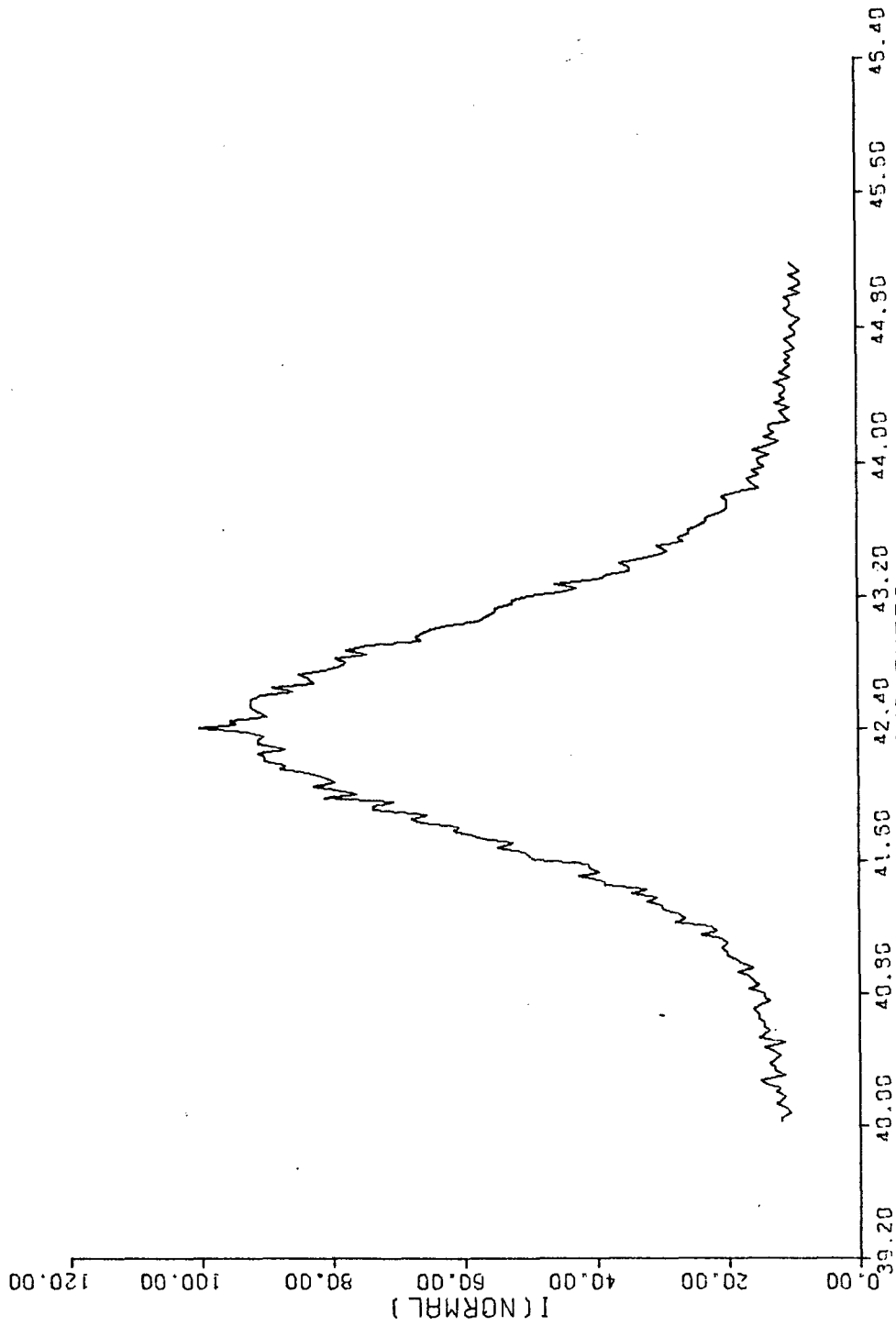

Figure 18. Radial (2θ) Intensity Distribution for $\bar{1}05$ Reflection for Mylar Film Type 700D. Used in Calculation of Crystallite Size (Table 17 and Figure 19)

Figure 19. Wilson's Variance Range Analysis Applied to Intensity Distribution from Figure 18, Mylar Film Type 700D (Table 17)

Two azimuthal scans were made for this film, the first a continuous one with cumulative counting at intervals of $\phi = 4.5°$ and the second a step scan with measurements taken for a fixed time at intervals of $\phi = 1°$. The orientation factors computed from the intensity data were quite comparable, being 0.491 and 0.464, respectively. However, these values are numerically lower than those observed in 700D. The considerably higher strength (2.39×10^9 dynes/cm^2) observed in the machine direction in film type 142T compared to 1.82×10^9 dynes/cm^2 for 700D (in the same direction) cannot be explained solely on the basis of orientation factor. The disorder parameter ($k = 0.9$) obtained for 142T is lower than the value ($k = 1.3$) for 700D suggesting higher intrinsic strength for the film type 142T. However, from the limited studies it would be difficult to affirm this, because in the first place, the definite existence of anisotropic order both in type 142T and type 700D films must be properly taken into account and in the second place the lower intensities in the radial and azimuthal scans of type 142T films (Figures 21-24) would imply a most probable modification of the morphological structure about which not much is known.

The extremely low extensibility coupled with the high tensile strength in the machine direction would indicate that the film type 142T is probably tensilized, i.e., it has been given a post-stretch, subsequent to two way stretching. Table 9 gives a resume' of all mechanical properties for type 142T film. The toughness of this film is particularly seen from its low extensibility in the machine direction (about 11% in contrast with 28% for 700D, 48% for type 1000S and 63% for type 1000A films).

TABLE 8

TENSILE STRENGTH FOR MYLAR FILMS 1.42 MIL TYPE T
($\times 10^9$ DYNES/CM^2)

	M. D.	T. D.	at 45° to MD/TD	
			1.40	1.79
	2.41	1.35	1.40	1.66
	2.12	1.32	1.61	1.66
	2.41	1.37	1.79	1.71
	2.59	1.32	1.84	1.84
	2.41	1.54	1.74	
	2.41	1.42	1.48	
Mean	2.392	1.387	1.660	
S. D.	.138	.075	.152	
% S. D.	5.7	5.4	9.2	

TABLE 9

MECHANICAL PROPERTIES OF 142T MYLAR FILMS
IN DIFFERENT DIRECTIONS

	M. D.	T. D.	at 45° to MD/TD
Tensile Strength ($\times 10^9$ dynes/sq. cm)	2.39	1.39	1.66
Elastic Modulus ($\times 10^{10}$ dynes/sq. cm)	5.74	3.76	4.24
Extention at Break (Percent Strain)	10.9	30.5	21.0

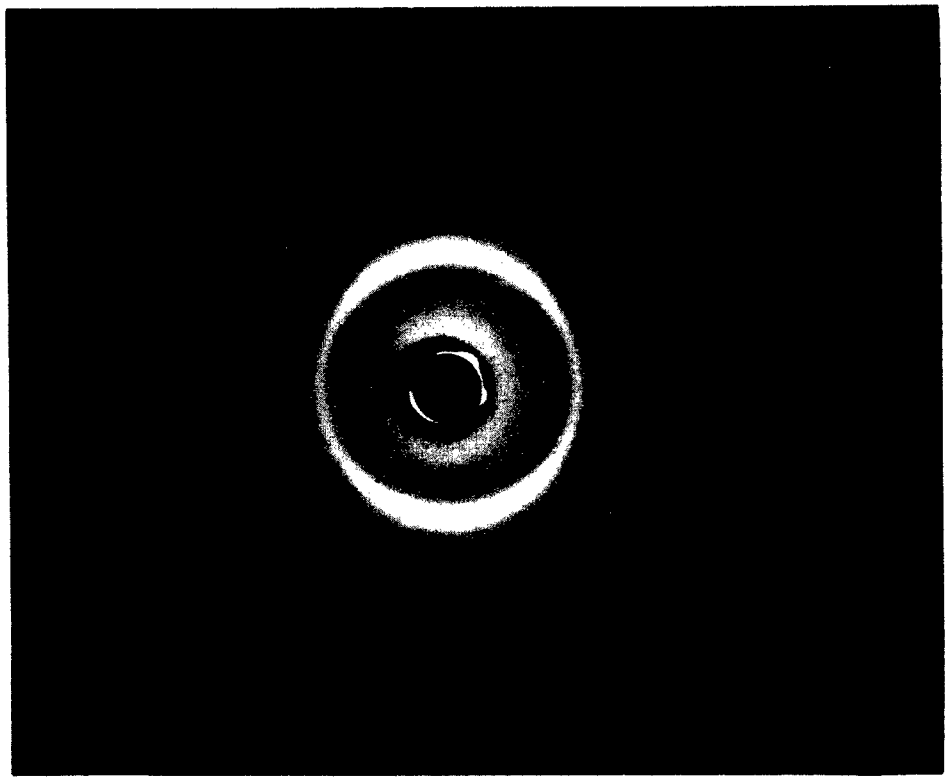

Figure 20. Flat Film X-Ray Diffraction Photograph for Type 142T Mylar Film

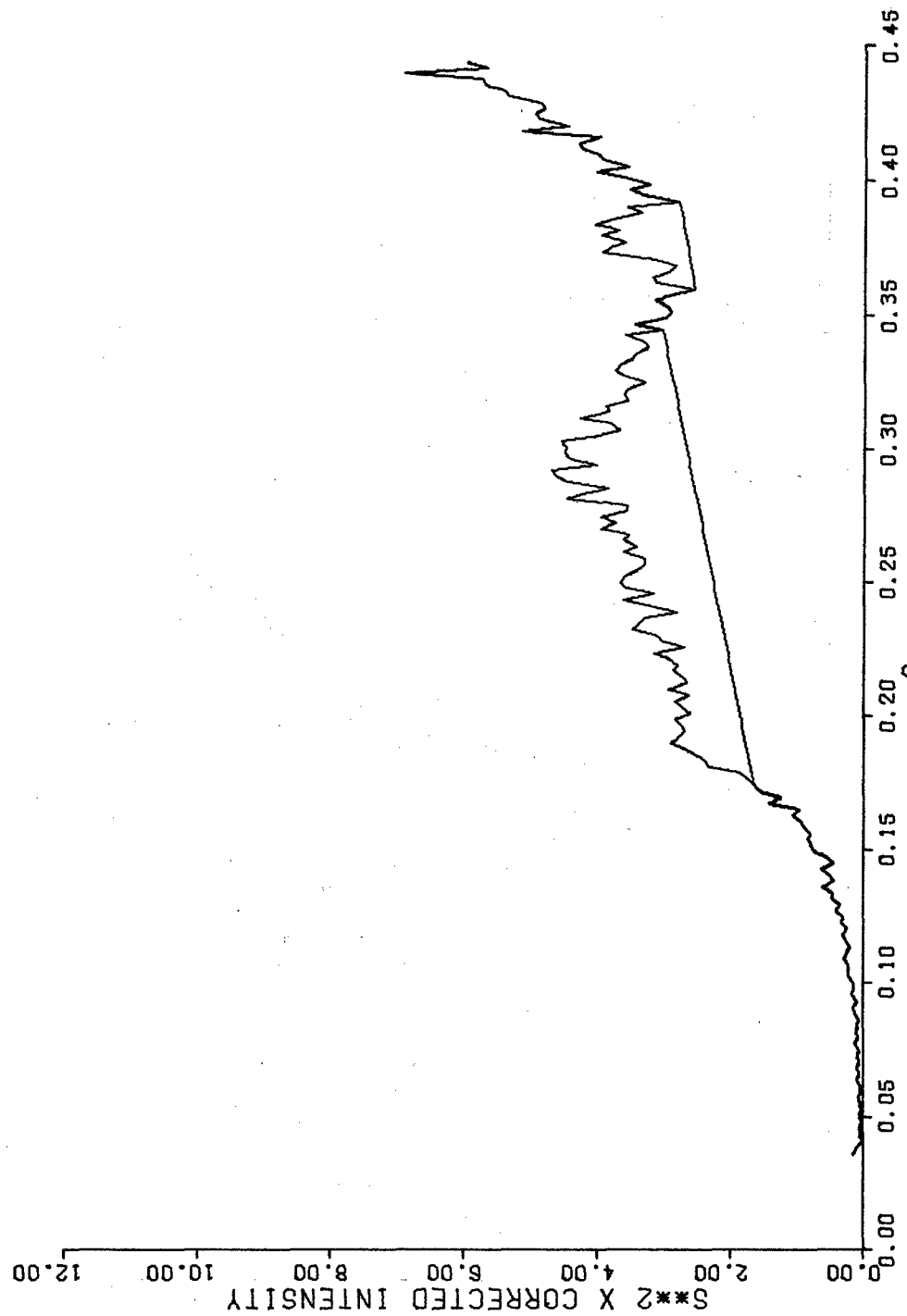

Figure 21. Crystalline and Amorphous Contribution to Total X-Ray Scattering Intensity. Used in the Calculation of Degree of Crystallinity and Disorder Parameter for Mylar Film Type 142T (Table 15). S is the Magnitude of the Reciprocal Lattice Vector

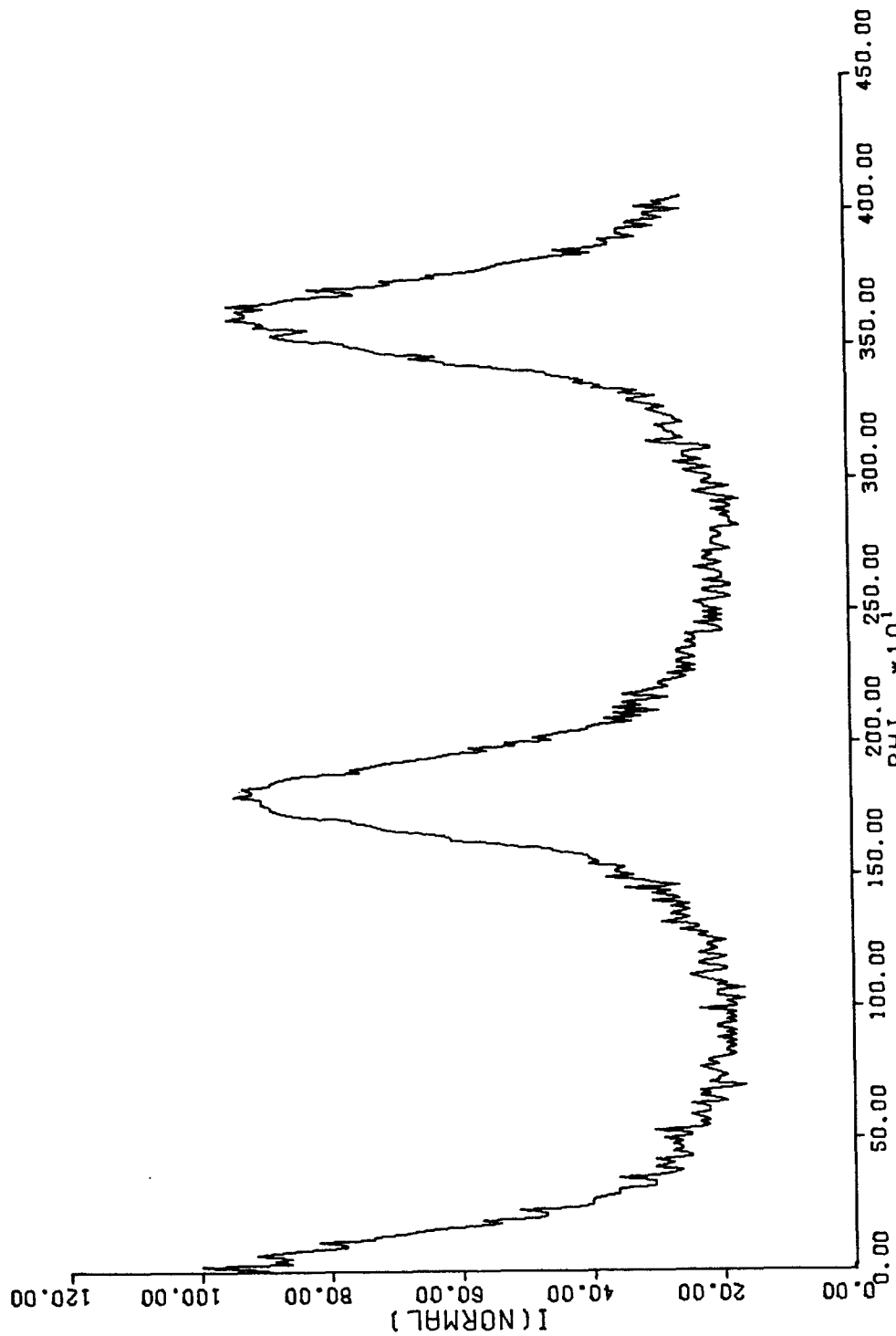

Figure 22. Orientation Scan for Mylar Film Type 142T, Used in Calculation of Orientation Factor (Table 16). ϕ Scan for T05 Reflection, $2\theta = 42.5°$

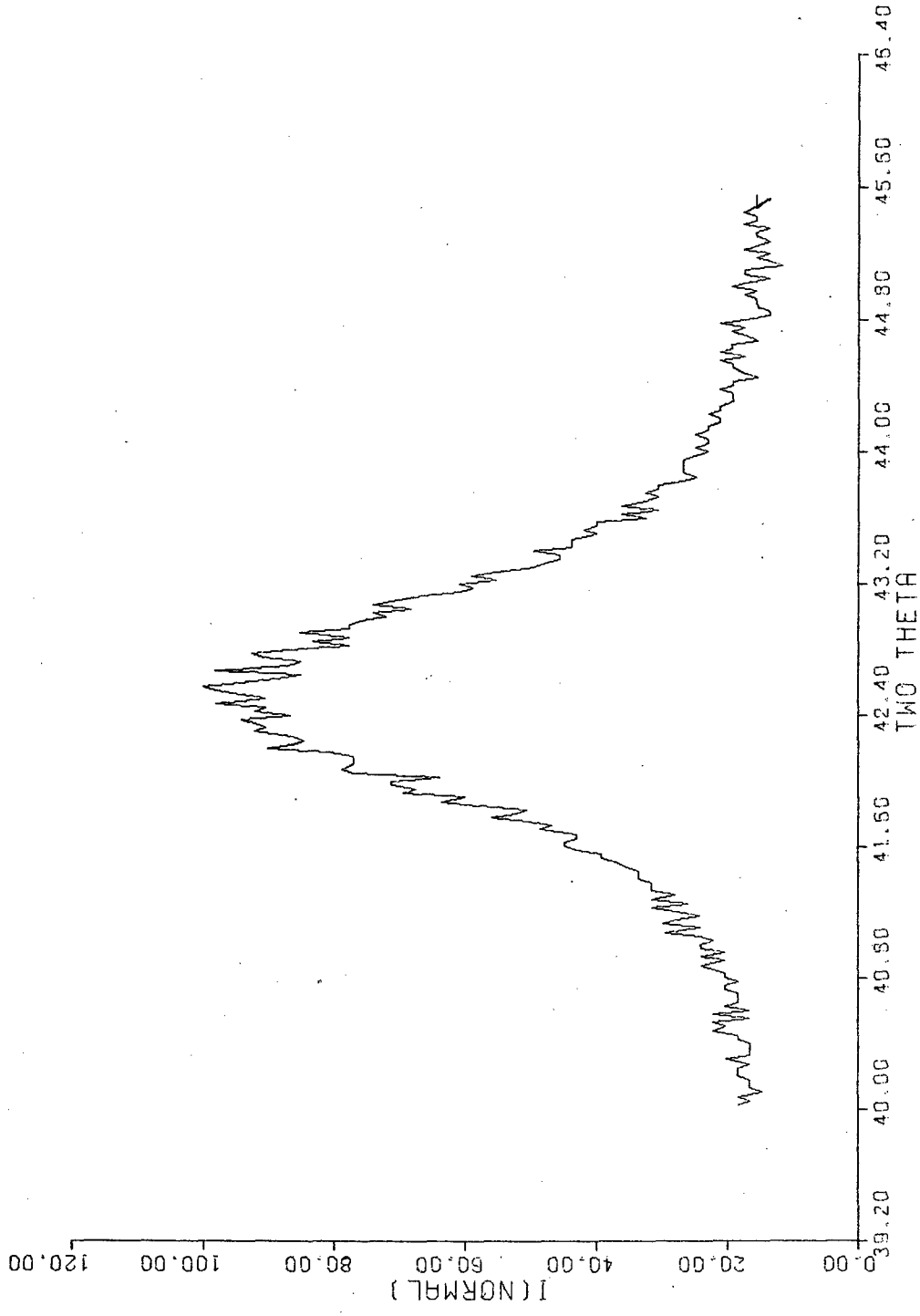

Figure 23. Radial (2θ) Intensity Distribution for $\bar{1}05$ Reflection for Mylar Film Type 142T. Used in Calculation of Crystallite Size (Table 17 and Figure 24)

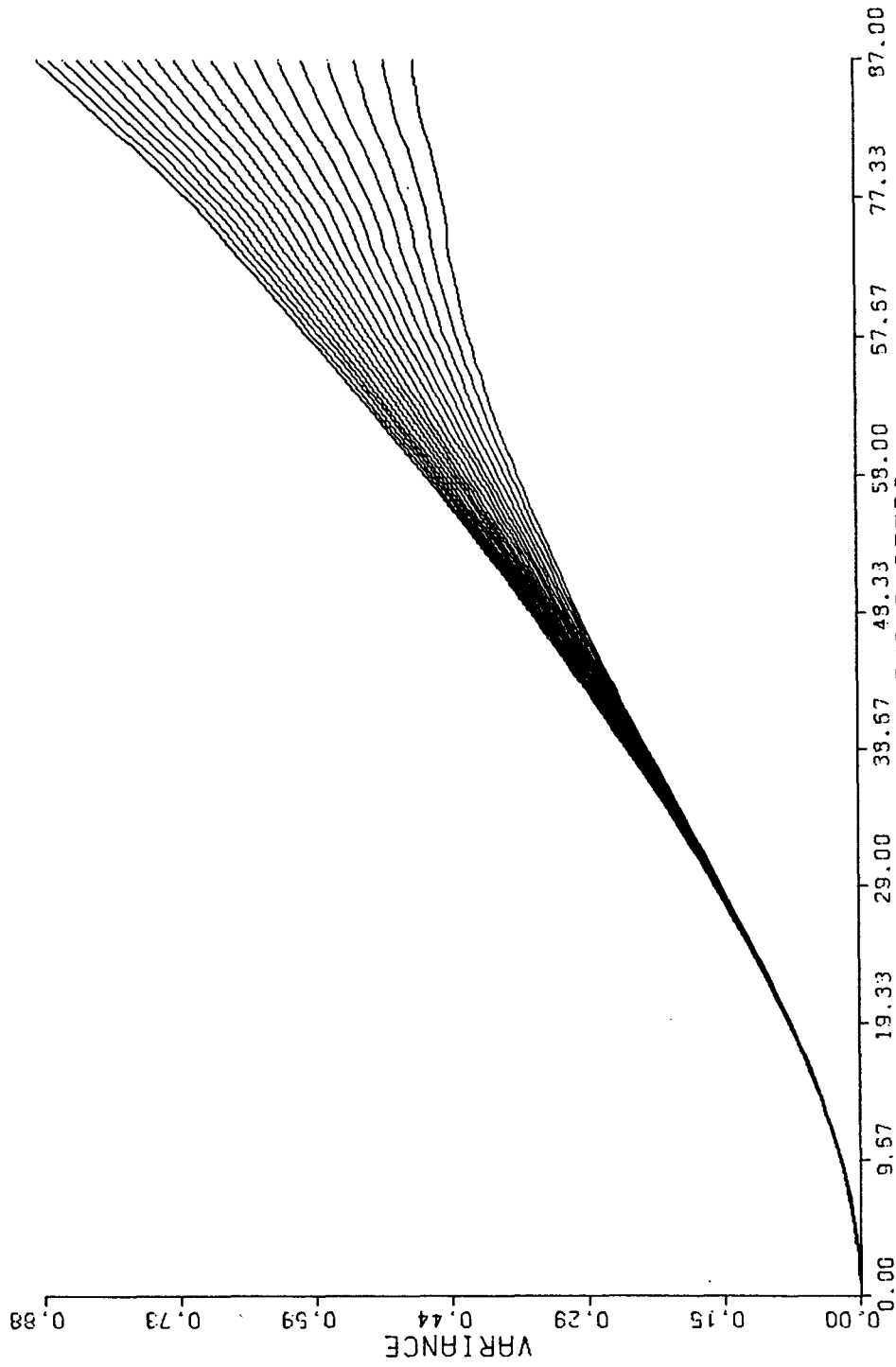

Figure 24. Wilson's Variance Range Analysis Applied to Intensity Distribution from Figure 23, Mylar Film Type 142T (Table 17)

5. MYLAR FILM TYPE 75M25

Table 10 summarizes the results on tensile strength tests on Mylar film type 75M25 in different directions. It is easily seen that there is no significant difference in the values obtained for the machine and transverse directions and the highest strength is exhibited, as always, in a direction normal to the intersection of the film and the optic axial plane. It is worth noting here that the strength in the machine direction is lower for this type of Mylar film than all others investigated. The association of strength with crystallite orientation is very hard to assess in the Mylar film type 75M25 for three reasons: (1) the intensity of diffracted x-rays is considerably lower than in other types of films, resulting in a heavy general background scatter; (2) the profile of the azimuthal scan is very flat with barely perceptible broad peaks rising above the background; and (3) the bulk of the material itself does not seem to be crystalline, as judged from the radial scan (Figures 26-29).

Table 11 gives a resume´ of the mechanical properties for Mylar film type 75M25. This film is used for packaging purposes which explains the equal strengths in the machine and transverse directions. The poor intensity of scattered x-rays is due to the special coatings which serve as barriers to moisture or gases. Film type 75M25 is in some respects similar to film type 1000A, though the strength is in all directions somewhat lower for M type than for A type. They have a comparable extension at break and crystallite orientation. The orientation factor for 75M25 is 0.260 as against 0.276 for 1000A.

TABLE 10

TENSILE STRENGTHS OF MYLAR FILMS TYPE 75M25 IN DIFFERENT DIRECTIONS (x 10^9 DYNES/CM^2)

	M.D.	T.D.	N.O.	P.O.	
	1.22	1.18	1.40	1.13	1.22
	1.37	1.32	1.37	1.42	1.13
	1.08	1.30	1.62	1.08	1.05
	1.22	1.37	1.45	0.93	
	1.32	1.08	1.67	1.13	
	1.27	1.03	1.52	0.93	
Mean	1.247	1.213	1.505	1.113	
S.D.	0.091	0.126	.110	.141	
% S.D.	7.3	10.4	7.3	12.7	

TABLE 11

MECHANICAL PROPERTIES OF MYLAR FILMS TYPE 75M25 IN DIFFERENT DIRECTIONS

	M.D.	T.D.	N.O.	P.O.
Tensile Strength (x 10^9 dynes/sq cm)	1.25	1.21	1.51	1.11
Elastic Modulus (x 10^{10} dynes/sq cm)	4.96	5.00	5.00	4.15
Extension at Break (Percent Strain)	55.3	49.6	54.2	54.0

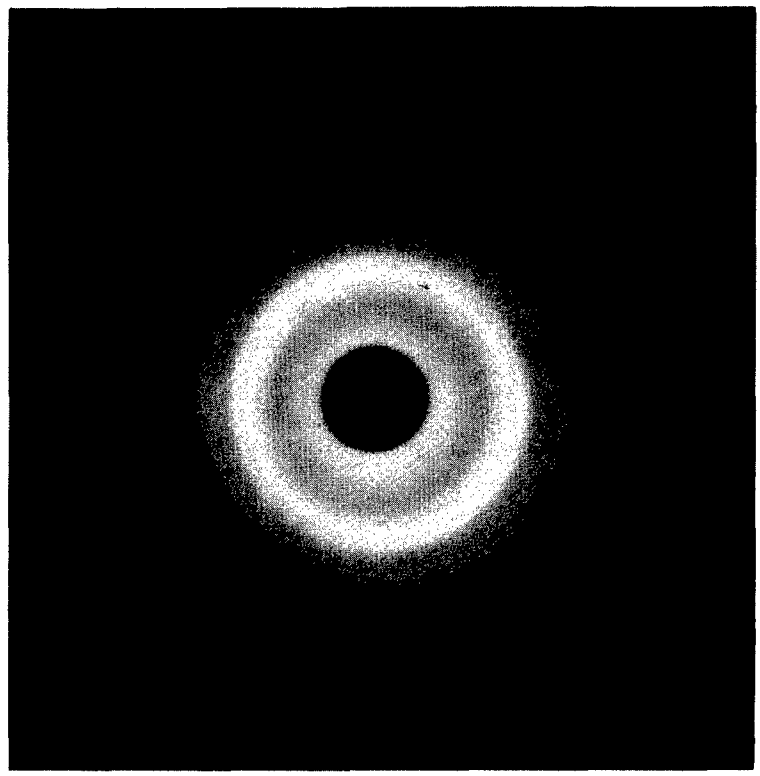

Figure 25. Flat Film X-Ray Diffraction Photograph for Type 75M25 Mylar Film

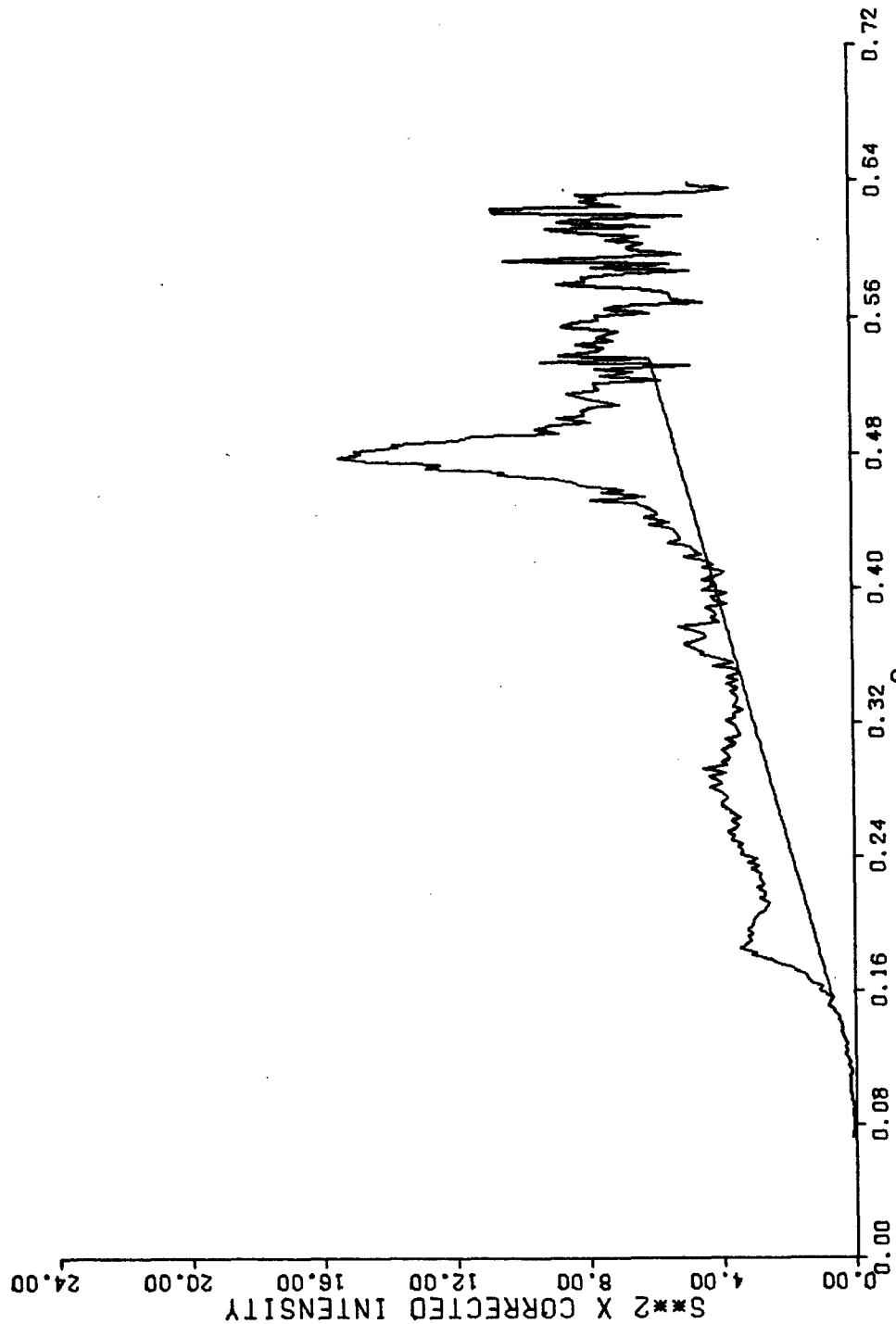

Figure 26. Crystalline and Amorphous Contribution to Total X-Ray Scattering Intensity. Used in the Calculation of Degree of Crystallinity and Disorder Parameter for Mylar Film Type 75M25 (Table 15). S is the Magnitude of the Reciprocal Lattice Vector

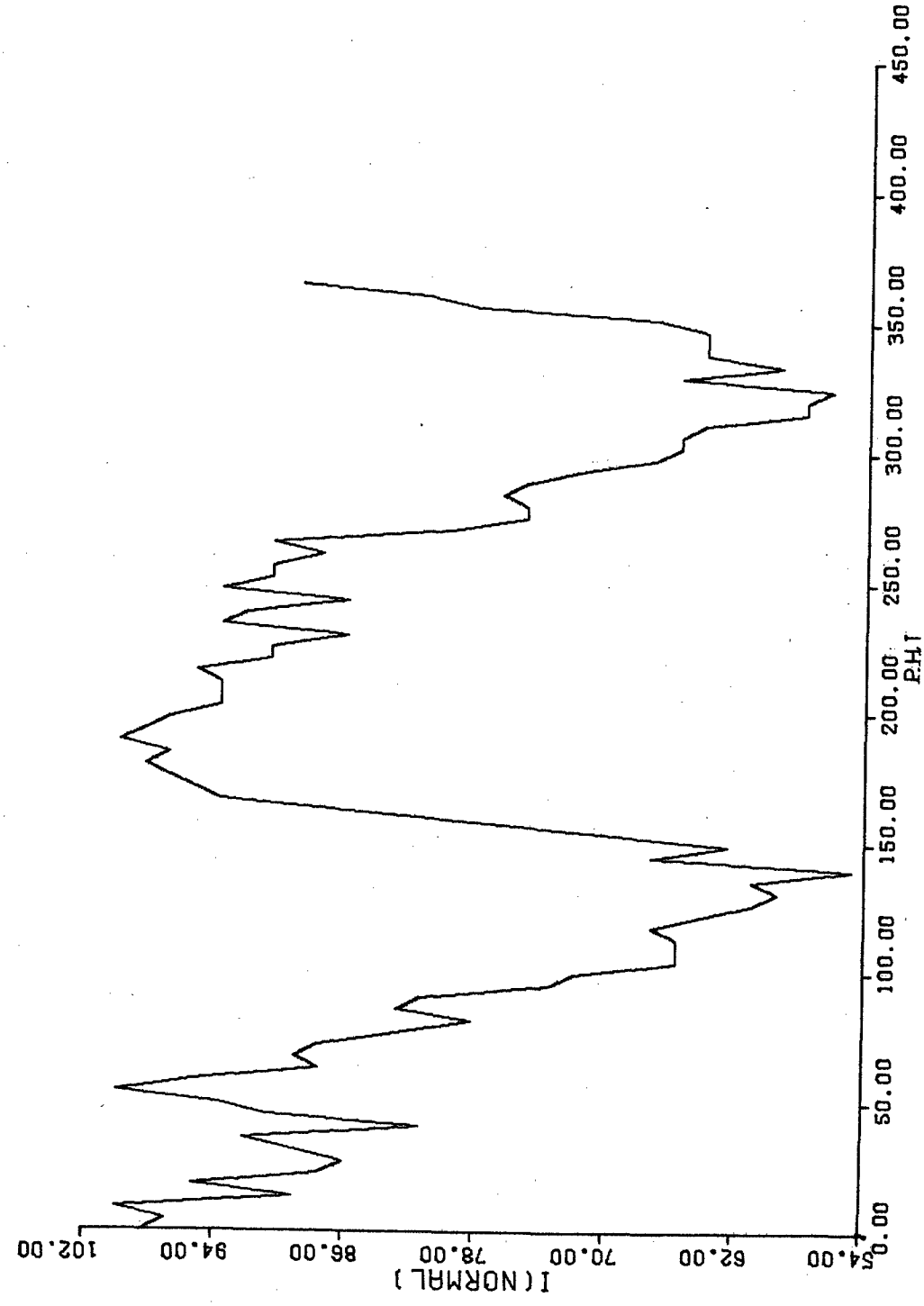

Figure 27. Orientation Scan for Mylar Film Type 75M25. Used in Calculation of Orientation Factor (Table 16). ϕ Scan for $\bar{1}05$ Reflection, $2\theta = 42.5°$

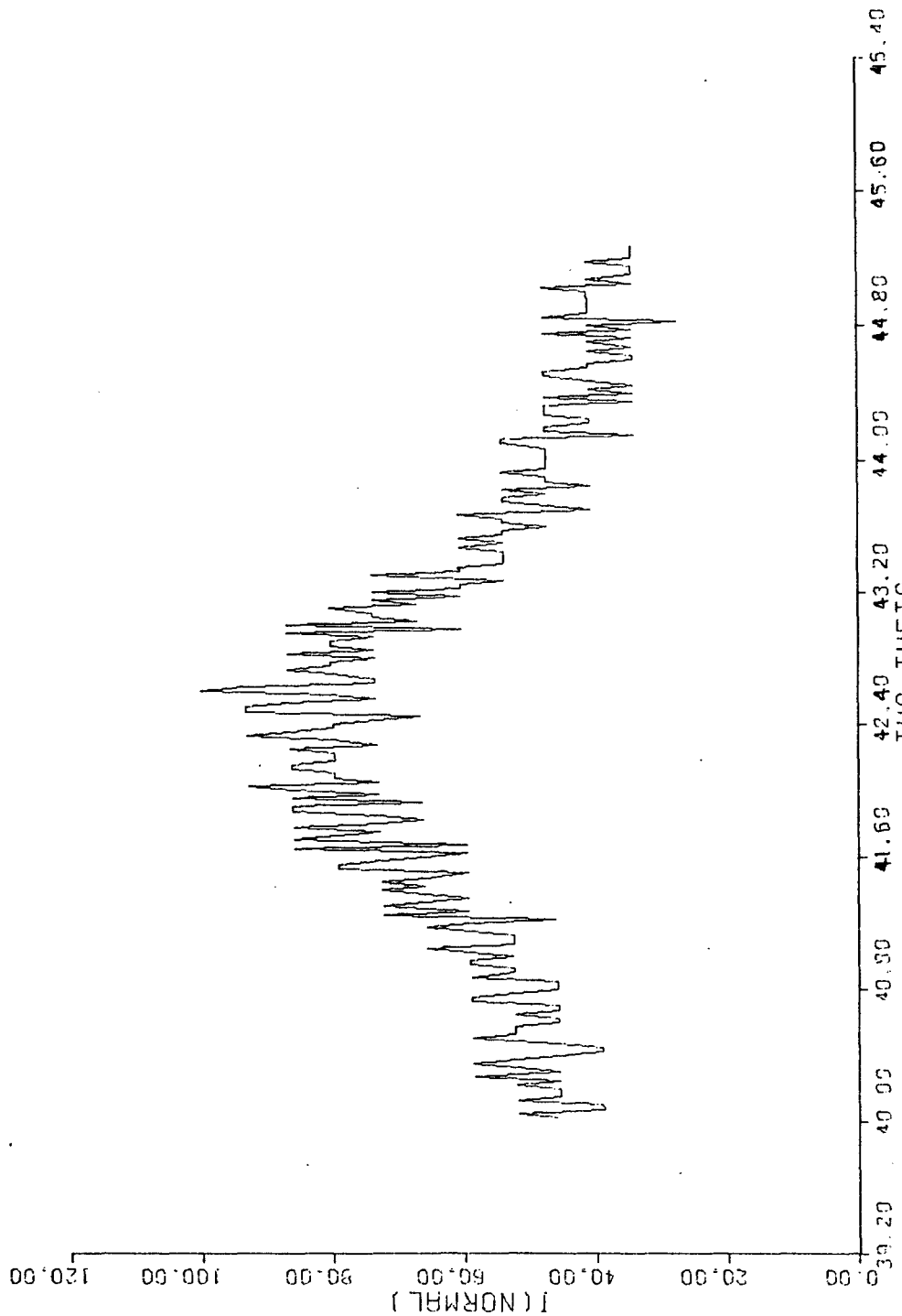

Figure 28. Radial (2θ) Intensity Distribution for $\bar{1}05$ Reflection for Mylar Film Type 75M25. Used in Calculation of Crystallite Size (Table 17 and Figure 29)

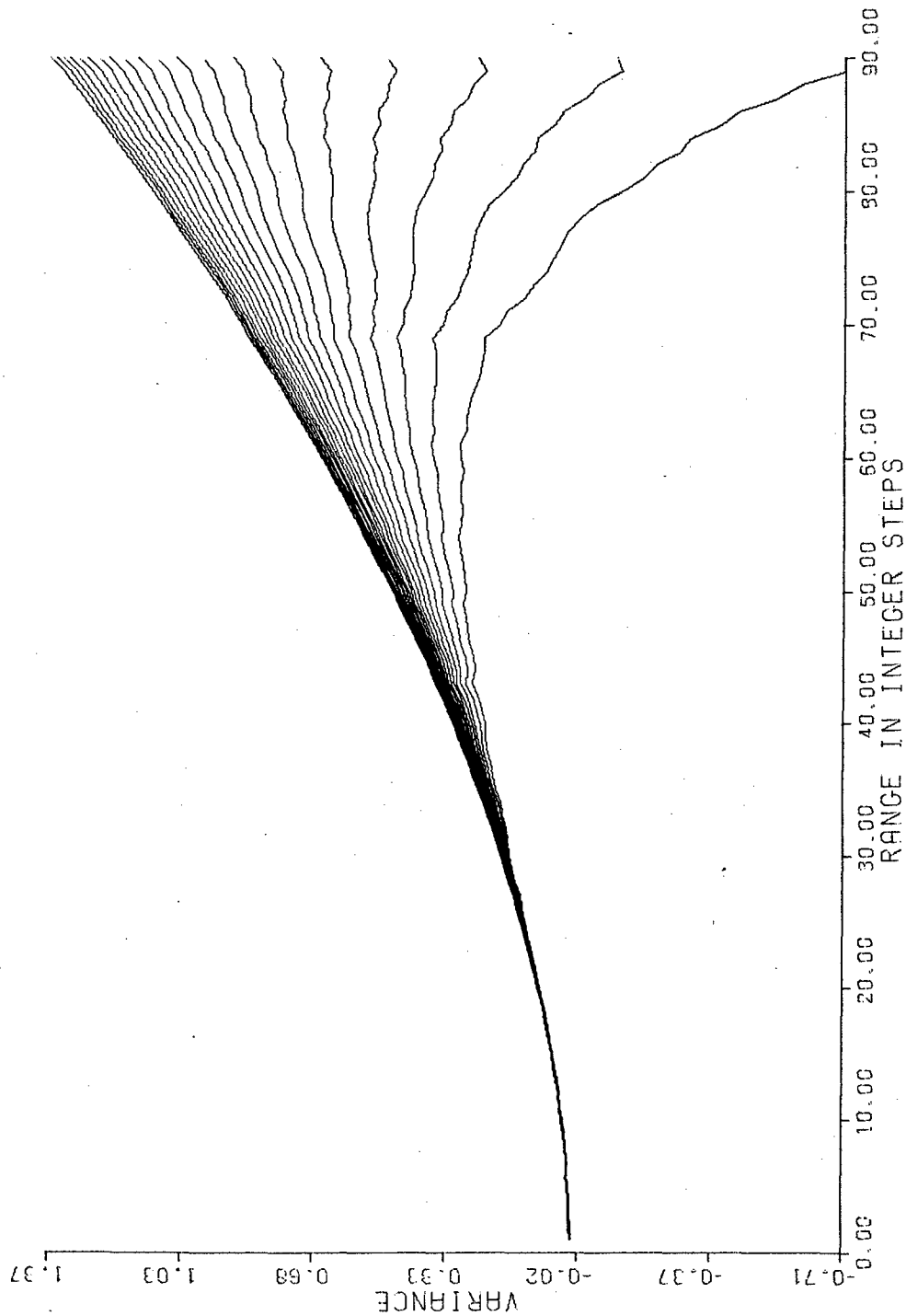

Figure 29. Wilson's Variance Range Analysis Applied to Intensity Distribution from Figure 28, Mylar Film Type 75M25 (Table 17)

6. MYLAR FILM TYPE 40C

Tables 12 and 13 summarize the results obtained on this film from experiments with the Instron tensile tester. As in the case of Mylar film types 700D and 142T, investigations under polarized light showed that for type 40C, the machine direction in the film coincided with the normal to the trace of optic axial plane. The significantly higher strength in the machine direction would suggest a relatively high orientation of the crystallites. The determination of Hermans' orientation factor for this particular film is a hard task. The film being hardly one hundredth of a millimeter thick, at least 100 strips would be needed to make up a stack of films sufficiently thick to give x-ray scattering of the same order of intensity as four sheets of 1000A or 1000S or six of type 700D films (specimens for x-ray diffraction analysis require usually a thickness of 1 mm to give satisfactory results). There is no great difficulty in cutting films of 7 or 10 mil to the specified size, parallel to one of the edges of a sheet or in arranging them appropriately for an orientation experiment. This assumes a primary importance in the case of thin films like 40C which explains the variability in values for the orientation factor obtained in two independent experiments, viz. $f_x = 0.50$ and $f_x = 0.34$. For obvious reasons the higher value of f_x would be nearer the truth in this case. The x-ray diffraction spectra used in the morphological characterization of this type film are presented in Figures 31-34.

7. OVERVIEW OF THE CORRELATION OF MECHANICAL PROPERTIES WITH STRUCTURE

In the preceding section individual types of Mylar films were analyzed particularly with respect to their tensile properties. We shall now discuss in broad terms how they may be related to the structural parameters such as crystallite size and orientation.

TABLE 12

TENSILE STRENGTH FOR MYLAR FILM TYPE 40C
IN DIFFERENT DIRECTIONS (x 10^9 DYNES/CM^2)

	M. D.	T. D.	At 45° to M. D. / T. D.	
	1.52	1.01	1.25	1.40
	1.47	1.10	1.40	1.40
	1.61	1.20	1.40	1.40
	1.47	1.01	1.40	1.40
	1.61	1.01	1.40	1.40
	1.56	1.10	1.40	
Mean	1.540	1.072	1.386	
S. D.	.070	.058	.043	
% S. D.	4.5	5.4	3.1	

TABLE 13

MECHANICAL PROPERTIES OF MYLAR FILM TYPE 40C
IN DIFFERENT DIRECTIONS

	M. D.	T. D.	At 45° to MD/TD
Tensile Strength (x 10^9 dynes/sq cm)	1.54	1.072	1.39
Elastic Modulus (x 10^9 dynes/sq cm)	5.99	4.18	4.70
Extension at break (Percent Strain)	16.6	30.8	27.7

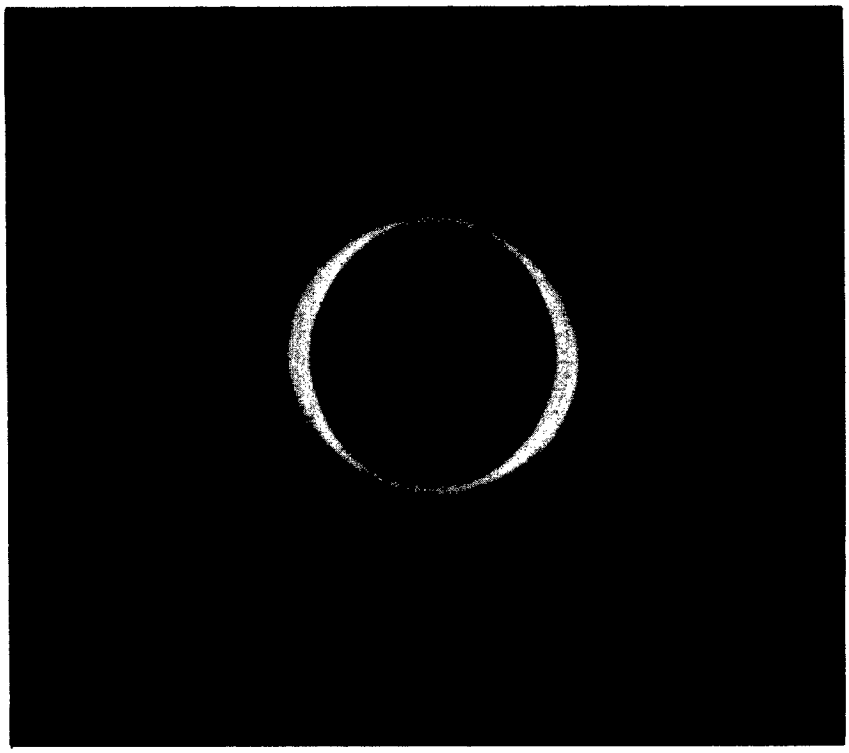

Figure 30. Flat Film X-Ray Diffraction Photograph for Type 40C Mylar Film

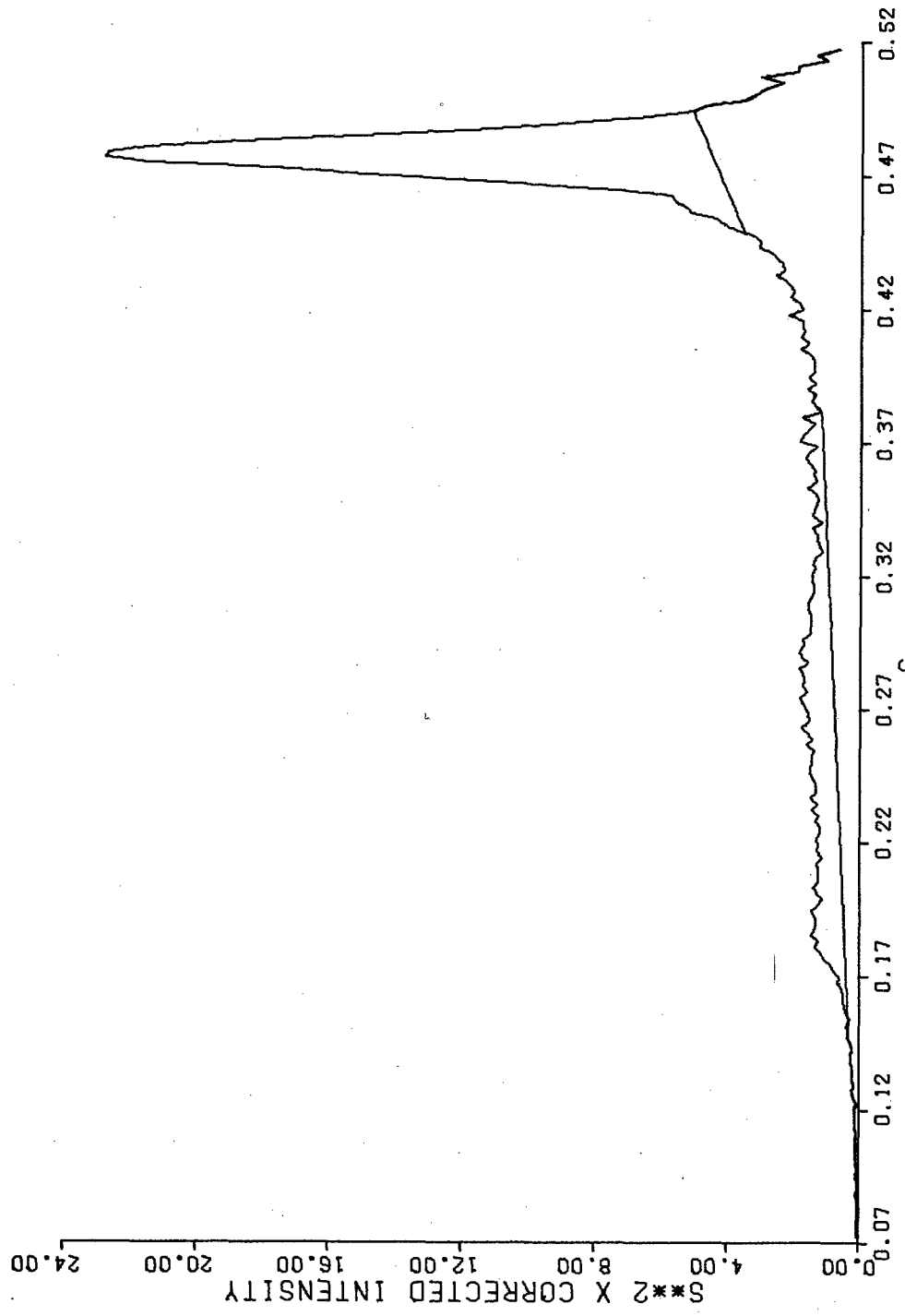

Figure 31. Crystalline and Amorphous Contribution to Total X-Ray Scattering Intensity. Used in the Calculation of Degree of Crystallinity and Disorder Parameter for Mylar Film Type 40C (Table 15). S is the Magnitude of the Reciprocal Lattice Vector

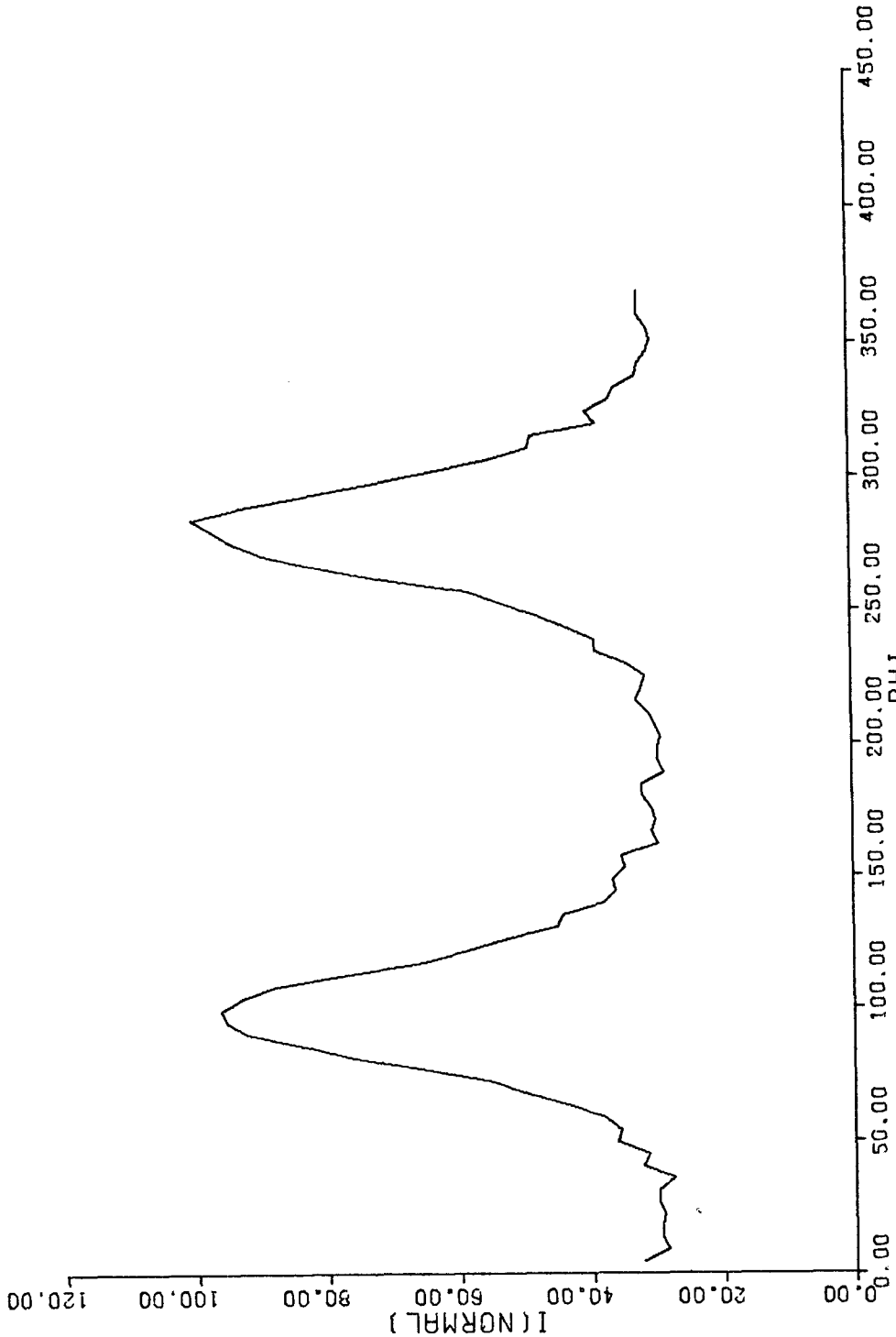

Figure 32. Orientation Scan for Mylar Film Type 40C. Used in Calculation of Orientation Factor (Table 16). ϕ Scan for $\bar{T}05$ Reflection, $2\theta = 42.5°$

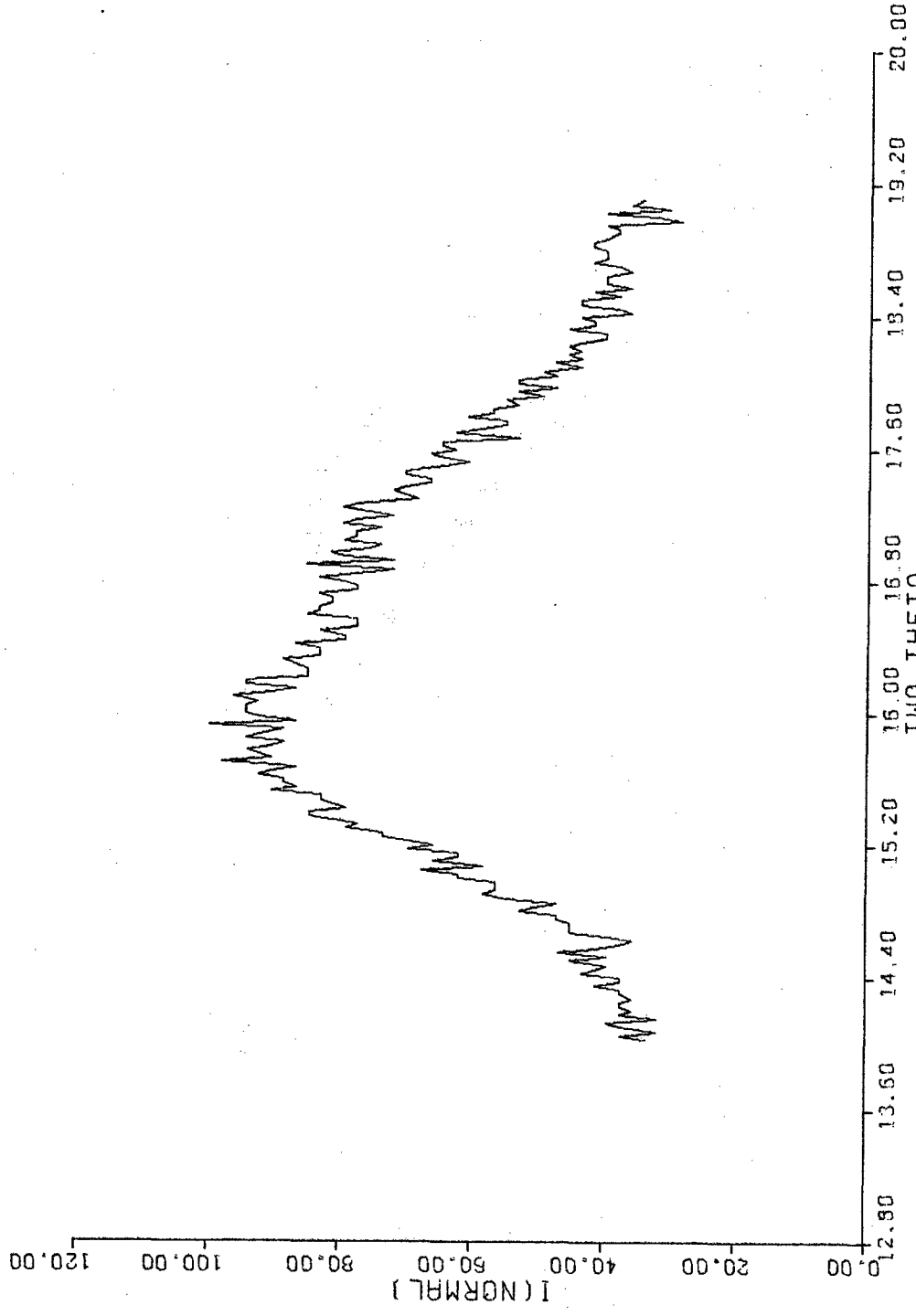

Figure 33. Radial (2θ) Intensity Distribution for $\bar{1}05$ Reflection for Mylar Film Type 40C. Used in Calculation of Crystallite Size (Table 17 and Figure 34).

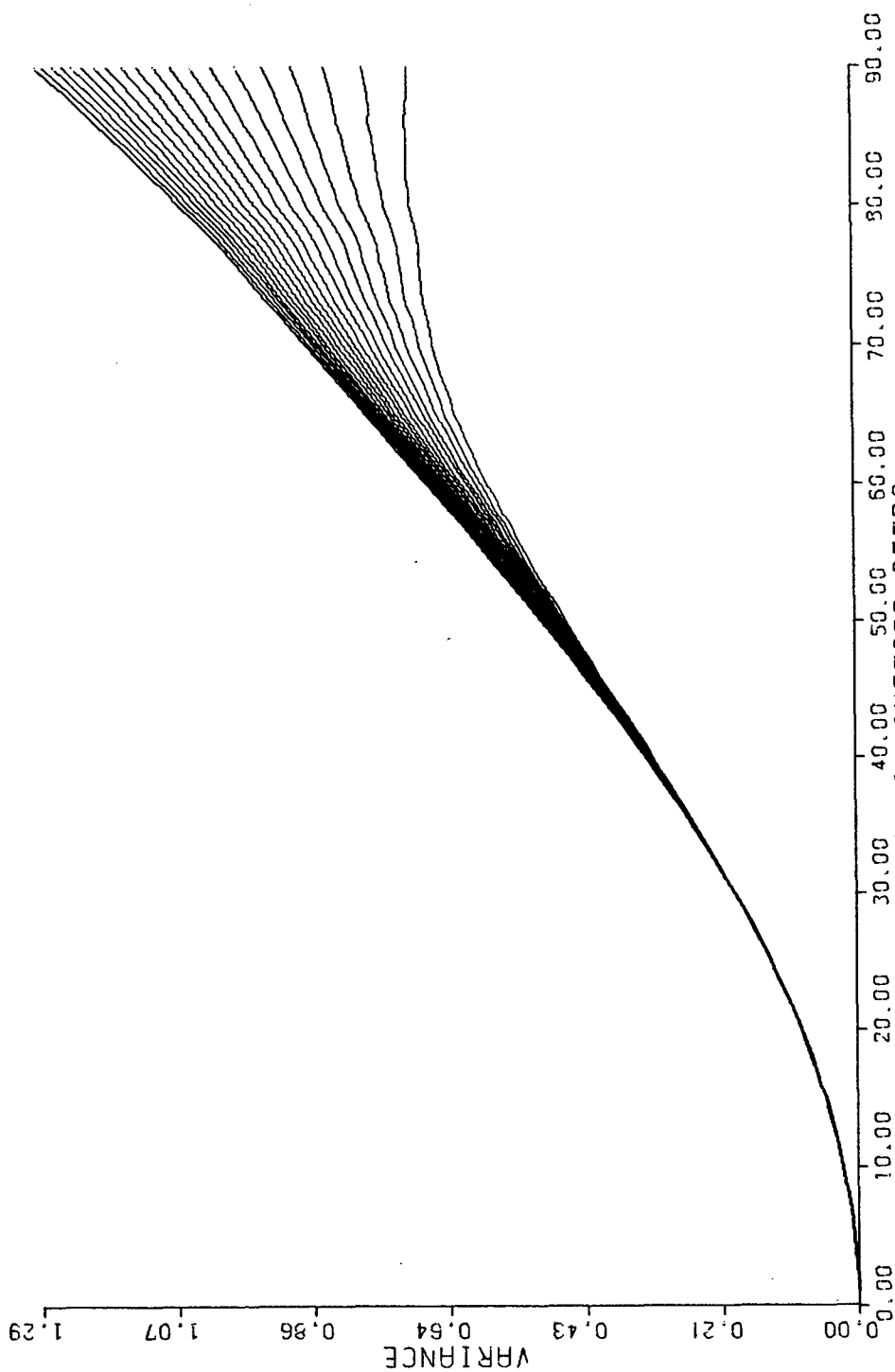

Figure 34. Wilson's Variance Range Analysis Applied to Intensity Distribution from Figure 33, Mylar Film Type 40C (Table 17)

Table 14 gives a resume' of the rheovibron data, and Tables 15 - 17 the results from x-ray investigation.

The six types of films may, in the light of our experimental observations, be classified into two categories: (1) unoriented, or poorly oriented, A, S, and M; and (2) highly oriented, C, D, and T. Among the poorly oriented films, M type is distinct in the sense that in addition to PET, some other material is present as a surface coating possibly consisting of a metal atom, which accounts for a higher x-ray absorption than could be solely attributed to the atoms of carbon, hydrogen, and oxygen constituting the PET molecules. The coating as noted earlier serves as a barrier to moisture and gases. Type M film is thus useful especially for packaging which does not require exceptionally high or unidirectional strength.

Film types A and S which exhibit biaxial stretching to different degrees are useful for general purposes. Film type A is noted to be valuable in electrical applications, such as insulation between turns in a transformer coil, laminations, etc. In the present investigation no attempt was made to distinguish between types A and S. The usefulness of film type A in insulators is apparently based on certain additional patented processes during and subsequent to two-way stretching. Type S is likewise to possess superior surface characteristics. All the three types of films in the first category have approximately the same order of extension at break, 50 - 60% of the initial length.

Films of types C, D, and T fall into the second category exhibiting a higher degree of orientation. Of the three, film type T has an exceptional tensile strength in the machine (longitudinal) direction. At a level of 2.4×10^9 dynes/cm^2 it is nearly twice as strong as the Mylar film used in packaging. It finds applications similar to those of film type A, with the additional requirement of very high unidirectional strength as is required for magnetic recording tape having high speed and faithful acoustic reproduction capability. Film type T also has the lowest extensibility, barely 10%, in the machine direction.

This combination (very high strength and very low extensibility) has been possible through a two-way stretch during film formation, followed by an additional stretch longitudinally, a process described as "tensilizing". Heat-setting plays an important role in these patented techniques which have not been simulated in this study of limited objectives. Types D and C have progressively lower strengths in the machine direction than type T. Of these two, film type C is usually made in thinner thicknesses which find application in electronic capacitors where low electric fault count and good high temperature insulation resistance are the more desired characteristics. Films of type D are made in larger thicknesses which are suitable for use in engineering reproduction and stationery supplies. Film type C is made in thicknesses below 1 mil and film type D in thicknesses above 3 mil.

As far as crystallite orientation is concerned, Hermans' x-ray orientation factor ranges from 0.45 to 0.60 for the film types C, D, and T. For types M and A it is about 0.3 while for type S the apparent value is close to zero, but in all three cases, a precise determination is not possible for different reasons: in type M there is the additional material incorporated along with polyester resin proper, in type A another reflection largely overlaps with the one selected for evaluation of orientation, and in type S orientation is balanced in the machine and transverse directions.

Nevertheless, more detailed analyses of azimuthal line profile with the x-ray beam not only normal, but also parallel (edgewise and endwise) to the film surface will give a clearer understanding of the orientation phenomena. Two such studies have been published by Heffelfinger (References 5 and 6) but no indication is given on the type of Mylar film used in this investigation.

From the rheovibron experiments, it was seen that in the film types 142T, 75M25, and 40C, the loss modulus (or phase angle) is very small at room temperature (tan δ equals 0.01 approximately) but it increases at a faster rate as the temperature is increased, reaching

values close to 0.2. Film type M, however, reaches the maximum at a much lower temperature (80°C) than all the others (around 115°C). Film types A, S, and D exhibit a value of tan δ almost five to eight times for the other three films.

Crystallite size may be affected by the degree of orientation present in the film. Kaji (Reference 19) has noticed that as the molecular chains are pulled in one direction, causing closer packing, the extent of crystallization increases. Film type 700D has higher values for both orientation factor and crystallite size (0.57 and 108A) than film type 142T (0.48 and 65A, respectively). The higher strength and lower extensibility in the machine direction of type 142T are undoubtedly attributable to the "tensilizing" process. This, along with the dynamic viscoelastic data above, will need further investigation when known processing techniques are available.

TABLE 14 (a)

MAXIMUM VALUES OBTAINED FOR TAN δ AND THE TEMPERATURES AT WHICH THEY OCCUR IN DIFFERENT MYLAR FILMS

	1000A	1000S	700D	142T	75M25	40C
Tan δ (M.D.) Max	.125	.141	.160	.187	.237	.180
Temp.(M.D.)	113°C	120°C	116°C	125°C	80°C	113°C
Tan δ (T.D.) Max	.133	.123	.107	.156	.227	.151
Temp(T.D.)	115°C.	120°C	110°C	125°C	84°C	117°C

TABLE 14 (b)

TAN δ AND DYNAMIC ELASTIC MODULI ($E^* \times 10^{10}$ DYNES/CM^2) FOR DIFFERENT FILMS AT ROOM TEMPERATURE (20°C) MEASURED IN THE MACHINE AND TRANSVERSE DIRECTIONS

		1000A	1000S	700D	142T	75M25	40°C
M.D.	tan δ	.070	.078	.050	.009	.018	.007
	E*	4.0	6.2	6.4	8.1	3.2	5.4
T.D.	tan δ	.043	.070	.004	.010	.015	.015
	E*	3.0	2.2	3.8	4.1	2.8	3.4

TABLE 15

STRUCTURAL PARAMETERS FROM (2θ) SCANS OF DIFFERENT MYLAR FILMS

Experiment Reference Number	Sample	Strong Peak at 2θ	Second Strong Peak	Relative Intensity (%)	Orientation of $\bar{1}05$ planes	k	X_{CR}	CV (%)
65.74**	1000A	16.20°	43.20°	80	nearly random	1.20	0.29	0.08
66.74**	1000A	16.20°	43.20°	60	"	0.3	0.48	9.9
4.75*	1000S	43.40°	16.00°	60	normal to MD	0.6	0.49	0.04
41.74**	700D	17.80°	43.8°	40	"	1.0	0.34	
44.75**	700D	17.80°	43.6°	40	"	1.3	0.55	0.04
29.74**	142T	16.80°	43.6°	40	"	0.9	0.35	1.55
45.74**	75M25	16.40°	43.2°	70	"	0.9	0.30	0.06
36.74*	40C	43.20°	16.00°	40	"	0.3	0.44	0.06

*Data Collected Along M.D.
**Data Collected Along T.D.

TABLE 16

CRYSTALLITE ORIENTATION IN DIFFERENT MYLAR FILMS

Sample	Half Max. Orientation Angle	Hermans' Orientation Factor, f_x	Average β	(2θ) Peak Position	Experiment Reference Number
1000A	--	.276	44.0°	42.4°	67.74
1000A	--	.146	49.0°	42.5°	50.75
1000S	--	.037	53.2°	42.5°	1.75
(Resolved)		.72 .66	25.4° 28.3°	42.5°	1.75
		.58 .49	31.8° 35.8°	42.5°	1.75
700D	15.6°	.56	32.7°	42.5°	42.74
	17.2°	.57	32.4°	43.0°	46.75
	16.3°	.58	31.8°	42.85°	56.75
142T	17.5°	.46	36.7°	42.5°	51.75
75M25		.26	44.6°	42.5°	46.74
				42.7°	65.75
40C	21.3°	.50	35.2°	42.5°	37.74
	21.3°	.34	41.6°	42.7°	64.75

TABLE 17

CRYSTALLITE SIZES COMPUTED FROM ($\bar{1}05$) REFLECTIONS FOR DIFFERENT MYLAR FILMS

Specimen & Reference Number	Slope $(2\theta°)^2 \times 10^2$	Intercept $(2\theta°)^2 \times 10^4$	ε_K (Å)	ε_{W_o} (Å)	Integral Breadth	Peak Position
Hexamine Standard	1.5	22[a]			.1325°	
1000A (26.75)	18.9	1252	55.2	42.2	.725°	42.52°
(49.75)	21.6	2188	47.8	32.1	.675°	42.50°
1000S	15.2	345	66.6	78.7	.75°	42.673°
700D (47.75)	13.5	0	80.0	321	.75°	42.400°
(43.74)	14.2	156	75.7	113	.725°	42.65°
142T	15.9	547	66.7	63.2	.725°	42.57°
75M25	32.5	3750	31.0	24.6	1°	42.60°
40C**	32.7	3450	29.0	24.1	1.325°	15.925°

**Data Collected Along T.D.

SECTION V

CONCLUSIONS

Crystallite orientation is one of the most important factors in determining physical properties, especially tensile characteristics. Heat treatment, not used in the present investigation, would play a significant role in determining whether the long chains of PET are in extended or folded form. Stress-strain curves of PET films as a function of temperature would yield valuable information in this respect. Degree of crystallinity is acknowledged as another important factor in the mechanical properties of materials. If the degree of crystallinity is low, the material is known to exhibit a greater flexibility, but poor strength and, in general, isotropic properties. Associated with this will be the crystallite sizes and how well the crystals are formed. In polymeric materials the boundaries of the crystalline regions are diffuse since various parts of a single polymer molecule might be in either the crystalline or amorphous phase of the bulk material. This diffuse region can be characterized by the disorder parameter (Reference 20). However, the temperature contribution to this disorder parameter (Reference 20) would first have to be extracted, leading to a true correlation of crystallite size, disorder, and degree of crystallinity with mechanical properties. Such an investigation would be easily performed for a thermoplastic resin which had not undergone extensive orientation (randomly oriented crystallites). In the present case, pulverization of the highly oriented films would have possibly changed the morphology. Thus, it was discarded as a means of achieving randomization of the crystallites. Instead of randomizing the material, one could computationally compensate for the anisotropy (Reference 20). Another possibility remains; namely, if the material cannot be randomized, or if computationally much time is involved in accounting for anisotropy, then collect the x-ray diffraction data in a randomization mode on a fully automated four circle diffractometer. Such a randomization operation mode for use with a Picker FACS-1 fully Automated Diffractometer is presently operational in our laboratory. The authors plan to proceed with this analysis.

Very applicable to this type of correlation between microstructure of polymeric materials and their mechanical properties will be this laboratory's newly fabricated Dynamic Imaging System (to be described in a future Technical Report). This system will enable the scientist to observe microstructural changes, as evidenced by x-ray diffraction patterns, while simultaneously applying known stresses to the films at a prescribed rate. Such high speed detection should give better correlation between structure and properties of a material because all events can be recorded before relaxation phenomena can occur.

REFERENCES

1. C. J. Heffelfinger and K. L. Knox, "The Science and Technology of Polymer Films", Volume II Editor: O. J. Sweeting, Chapter XIV, Polyester Films, Wiley-Interscience, New York, 1971.

2. W. T. Astbury and C. J. Brown, "Structure of Terylene", Nature 158, (4024), p. 871, Dec. 14 (1946).

3. R. de P. Daubeny, C. W. Bunn, and C. J. Brown, "The Crystal Structure of Polyethylene Terephthalate", Proc. Royal Soc., London A-226 (1167), 531-542 (1954).

4. Yu. Ya. Tomashpolskii and G. S. Matkova, "An Electron Diffraction Study of the Crystalline Structure of Polyethylene Terephthalate", Vysokomol. Soyed., 6, (2), 274-280 (1964).

5. C. J. Heffelfinger and R. L. Burton, "X-ray Determination of the Crystallite Orientation Distributions of Polyethylene Terephthalate Films", J. Polymer Sci., 17, 289-306 (1960).

6. C. J. Heffelfinger and P. G. Schmidt, "Structure and Properties of Oriented Polyethylene Terephthalate Films," J. Appl. Polymer Sci., 9, 2661-2680 (1965).

7. J. H. Dumbleton and B. B. Bowles, "X-ray Determination of Crystallinity and Orientation in Polyethylene Terephthalate (Fibers and Films)", J. Polymer Sci., Part A-2, 4, 951-958, (1966).

8. J. J. Hermans, P. H. Hermans, D. Vermaas, and A. Weidinger,, "Quantitative Evaluation of Orientation in Cellulose Fibers from the X-ray Diagram", Recueil des Travaux Chimie de Pays-Bas, 65, 427-447 (1946).

9. R. H. Blessing, P. Coppens, and P. Becker, "Computer Analysis of Step-Scanned X-ray Data, J. Appl. Cryst., 7 (5) 488-492 (1974).

10. H. Ruck and H. Krassig, "The Adaptation of the Norelco Diffractometer to a Multipurpose Fiber and Powder Camera", Norelco Reporter, 7, 71-74, 93, (1960).

11. W. Ruland, "X-ray Determination of Crystallinity and Diffuse Disorder Scattering", Acta Cryst., 14, 1180-1185 (1961).

12. A. Viswanathan and V. Venkatakrishnan, "Disorder in Cellulosic Fibers", J. Appl. Polymer Sci., 13, 785-795 (1969).

13. S. G. Shenouda and A. Viswanathan, "Crystalline Character of Native and Chemically Treated Egyptian Cottons, (Parts I and II)", J. Appl. Polymer Sci., 15, 2259-2275 (1971) and 16, 395-406 (1972).

REFERENCES (Contd)

14. L. E. Alexander, "X-ray Diffracton Methods in Polymer Science", Wiley-Interscience, New York 1969, Chapter 7, pp 423-453.

15. E. R. Pike and A. J. C. Wilson, "Theory of the Use of Centroids of Diffraction Profiles", British Journal of Applied Physics, 10, 57-68 (1959).

16. A. J. C. Wilson, "On Variance as a Measure of Line Broadening in Diffractometry: General Theory and Small Particle Size", Proc. Physical Soc., (London), 80, 286-294, (1962).

17. J. I. Langford and A. J. C. Wilson, "On Variance as a Measure of Line Broadening in Diffractometry: Some Preliminary Measurements on Annealed Aluminum and Nickel and on Cold-Worked Nickel", Crystallography and Crystal Perfection, G. N. Ramachandran, Ed., Academic Press; London, 1963, p. 207.

18. Rheovibron, Model DDV, II Instruction Manual 17, August 1969, Toyo Baldwin Co., Ltd., Tokyo, Japan.

19. K. Kaji, "Increase of the Crystallite Size by Application of Tensile Stress for Highly Oriented Polymer", Die Makromol. Chemi., 175 311-325 (1974).

20. W. Ruland, "X-ray Determination of Temperature Dependence of the State of Order in Polyethylene (in German)", Faserforschungund Textil Tecknik, 18 (2), 59-63 (1967).

21. A. Viswanathan, "Fiber Structures: A Fresh Look from Metallography", J. Appl. Polymer Sci. 11, 1027-1032 (1967).

22. R. Bonart, R. Hoseman, F. Motzkus, and H. Ruck, "X-Ray Determination of Crystallinity in High Polymeric Substances", Norelco Report 7, 81-87, 96-97 (1960).

23. C. R. Desper, "A Computer-Controlled X-ray Diffractometer for Texture Studies of Polycrystalline Materials", Advances in X-ray Analysis, Vol. 12, p 404, Plennum Press, New York, N. Y. (1969).

24. M. Polanyi, Z. Physik. 7, 149 (1921).

25. J. H. Dumbelton and B. B. Bowles, "X-ray Determination of Crystallinity and Orientation in Polyethylene Terephthalate (Fibers and Films)", J. Polymer Sci., 4, 951-958 (1966).

26. J. I. Langford, "The Variance and Other Measures of Line Broadening in Powder Diffractometry", J. Appl. Cryst. 1, 48-59 and 131-138 (1968).

APPENDIX A

POLYETHYLENE TEREPHTHALATE FILM MANUFACTURERS

COUNTRY	MANUFACTURER	PRODUCT TM
Belgium	Gevaert	Gevar
France	Kodak-Pathe	Estar
France	La Cellophane SA	Terphane
Germany	Kalle	Hostaphan
Great Britain	I.C.I.	Melinex
Great Britain	Kodak Ltd.	Estar
Italy	Montecatini Edison	Montivel
Japan	Fuju	Fuji film
Japan	Mitsubishi	Diafoil
Japan	Teijin-Konishiroku	Sakura, Koni
Japan	Teijin-Konishiroku	Teteron
Japan	Toyo Rayon	Luminar
Luxembourg	duPont S.A.	Mylar
Netherlands	I.C.I.N.V.	Melinex
Switzerland	Celfa AG	Folex
United States	Celanese Plastics	Celanar
United States	duPont	Mylar, Cronar
United States	Eastman Kodak	Estar
United States	American Viscoe FMC	Avistar
United States	Goodyear	Videne
United States	Minnesota Mining	Scotchpar

APPENDIX B

PROPERTIES OF MYLAR[a] POLYESTER FILM AT 23°C TESTED ACCORDING TO ASTM STANDARDS[b]

Property	Typical Values for 1 mil	
	"balanced" film	"tensilized" film
Ultimate Strength (MD)[c], psi	25,000	40,000
Ultimate Elongation (MD), %	120	50
Tensile Modulus (MD), psi	550,000	800,000
Impact Strength, kg-cm	6.0	6.0
Density, g/cc	1.395	1.377
Coefficient of Friction (Kinetic, Film to Film)	0.45	0.38
Bursting Strength, psi	66	55
Folding Endurance Cycles	300,000	

Dielectric Strength	7500	V/mil	at 60 Hz
Dielectric Constant	3.30	"	at 60 Hz
Dielectric Constant	3.25	"	at 1 KHz
Dielectric Constant	3.0	"	at 1 MHz
Dielectric Constant	2.8	"	at 1000 MHz

Permeability

CO_2	16	cc/100 $in.^2$ 25 hr-atmo.
H_2	100	"
N	1	"
O_2	6	"
H_2O	1.8	"

a. Mylar Trade Mark of duPont
b. Values for Properties Quoted from Reference 1
c. M.D. Machine Direction

APPENDIX C

X-RAY DETERMINATION OF THE STATE OF ORDER AND CRYSTALLINITY IN HIGH POLYMERS

The degree of crystallinity is a term especially coined for studies on high polymers (Reference 20) because unlike for other substances, there is considerable overlapping of the few reflections present in an x-ray diffraction pattern of a polymeric material. Ruland's theory (Reference 11) is the only one that accounts for the loss in intensity of the diffraction peaks due to various effects emphasized by Hosemann (Reference 21).

Ruland defines the weight fraction of crystalline material, obtained from x-ray diffraction as:

$$x_{CR} = \frac{\int_0^\infty s^2 \, I_{CR}(s) \, ds}{\int_0^\infty s^2 \, \overline{f^2(s)} \, D(s) \, ds} \qquad (11)$$

where I_{CR} is the coherent intensity from the crystalline fraction; $\overline{f^2}$ is the mean square atomic scattering ($\overline{f^2} = \Sigma N_i f_i^2 / \Sigma N_i$), N_i being the number of atoms of type i with an atomic scattering factor f_i; and D(s) is Ruland's disorder function which takes into account the loss of intensity concentrated at the reciprocal lattice position s. Total intensity integrated over the entire reciprocal space would be given by

$$I_{total} = 4\pi \int_0^\infty s^2 \, I(s) \, ds = 4\pi \int_0^\infty s^2 \, \overline{f^2(s)} \, ds \qquad (12)$$

From Equations 11 and 12 Ruland obtained an expression for the degree of crystallinity:

$$x_{CR} = \frac{\int_0^\infty s^2 \, I_{CR}(s) \, ds}{\int_0^\infty s^2 \, I(s) \, ds_{total}} \cdot \frac{\int_0^\infty s^2 \, \overline{f^2(s)} \, ds}{\int_0^\infty s^2 \, \overline{f^2(s)} \, D(s) \, ds} \qquad (13)$$

For this to have physical significance, the numerical value for the degree of crystallinity should be a constant, independent of the range of integration. The first approximation isotropic disorder function is assumed to be

$$D(s) = e^{-ks^2} \tag{14}$$

and the value of k is varied until consistent values for degree of crystallinity are obtained over different ranges of s. The computation is performed in two stages: first, the ratio

$$K = \int_{s_o}^{s_p} s^2 \overline{f^2(s)}\, ds \Big/ \int_{s_o}^{s_p} s^2 \overline{f^2(s)}\, D(s)\, ds \tag{15}$$

is determined for each value of k and each upper limit s_p. It is computationally and physically expedient not to change s_o during a given integration sequence $\left[\{s_p\},\ p = 1, 2, 3 \ldots\ldots\right]^{o}$.

Second, the degree of crystallinity is calculated from the expression:

$$X_{CR} = K \int_{s_o}^{s_p} s^2 I_{CR}(s)\, ds \Big/ \int_{s_o}^{s_p} s^2 I_{total}(s)\, ds \tag{16}$$

using the observed intensities I_{CR} and I_{total} (after corrections for air scatter, specimen-absorption, and polarization). The value of the disorder parameter relevant to the polymer sample being investigated is the one in correspondence with the minimum coefficient of variation in X_{CR} (Note: X_{CR} is obtained for each s_p). Usually three or four upper integration limits are possible.

In performing this type of computation for highly amorphous polymer material, it is sometimes questionable as to what part of the total intensity is attributable to amorphous scattering. That is,

$$I_{CR}(s) = I_{total}(s) - I_{amorphous}(s) \tag{17}$$

For this reason various amorphous intensity curves were chosen and the most representative for each case was in correspondence with the inferior of the above mentioned minimum coefficient of variation in X_{CR}.

Ruland extended his theory subsequently to take into account an anisotropic disorder function in the crystallinity determination (Reference 22). This led to a somewhat higher crystallinity value for polyethylene than that obtained by assuming an isotropic disorder function. However, in the present investigation, although the material is anisotropic, the computation used the isotropic disorder function but the experimental data was collected anisotropically. The material could have been randomized as was done with cotton cellulose (Reference 12). This procedure was not followed in the case of Mylar as it was apprehended that the state of order and crystallization (morphology) of the material would be affected by mechanically pulverizing the samples. In addition the x-ray diffractometer was not of the four circle fully automated type which could easily average by a randomization algorithm (Reference 23).

APPENDIX D

X-RAY DETERMINATION OF THE DEGREE OF ORIENTATION IN POLYMERIC SUBSTANCES

The theory of fiber diagrams as given by Polanyi (Reference 24) enables one to derive the orientation in a fiber from the intensity distribution in the diatropic interferences. The planes $(\bar{1}05)$ give rise to a reflection almost on the meridian and therefore the expressions derived by Polanyi for orientation parameters may be applied directly to azimuthal intensity profiles from $(\bar{1}05)$ reflections of Mylar. These are relatively intense and free from overlapping by adjacent reflections. If the angle along a diffraction arc from a given reference position is indicated by ϕ and the intensity distribution by $I(\phi)$, the orientation factor, as defined by Hermans (Reference 8) becomes:

$$f_x = 1 - \frac{3}{2}\overline{\sin^2\phi} \tag{18}$$

where

$$\overline{\sin^2\phi} = \int_0^{\pi/2} \sin^3\phi \, d\phi \Big/ \int_0^{\pi/2} \sin\phi \, d\phi \tag{19}$$

In ideally oriented fibers the $(\bar{1}05)$ reflection intensity profile would be symmetrical about the reference direction, as was noted by Dumbleton and Bowles (Reference 25). The number of crystallites oriented so as to give a reflection in reciprocal space is proportional to $2\pi \sin\phi \, d\phi$, i.e., the area of a ring on the scattering sphere with co-latitudes ϕ and $\phi + d\phi$. Integration $(o \leq \phi \leq \frac{\pi}{2})$ yields the total number of crystallites with reference to the planes concerned $(\bar{1}05)$. From $\sin^2\phi$ computed from the two integrals involving the intensity distribution as a function of ϕ, an average value $\beta = \text{arc sin}\sqrt{\sin^2\phi}$ for the inclination of the normal to $(\bar{1}05)$ planes to the reference direction may be estimated.

From the expression for f_x above it is easily seen that the orientation factor is unity when $\beta = 0°$, i.e., there is a perfect alignment of the normals to $(\bar{1}05)$ with respect to the reference direction. Random orientation may be inferred from $f_x = 0$ which

occurs when $\sin^2 \phi = 2/3$ or $\phi = 54.7°$. The value $f_x = -1/2$ is obtained when $\beta = 90°$, i.e., when the normals to $(\bar{1}05)$ planes are all oriented perpendicular to the reference direction, which in the present case is the direction of stretch (machine direction). The Mylar films herein investigated were subsequently stretched in a transverse direction, i.e., at right angles to the machine direction. In the absence of a more exact formula for evaluating such a biaxial orientation, computation was done as though there was only a unidirectional stretch and the result was interpreted in terms of biaxial orientation.

APPENDIX E

DETERMINATION OF THE CRYSTALLITE SIZE USING WILSON'S VARIANCE-RANGE ANALYSIS

Pike and Wilson (Reference 15) first presented the theory of using centroids of diffraction line profiles in order to achieve high accuracy in the measurement of diffraction angles. This was especially useful where the profile is observed by counting x-ray quanta for a fixed time with a detector at a series of equidistant steps along the profile. Wilson (Reference 16) later developed a theory of the variance of line broadening in relation to small particle size determination. He proposed the expression:

$$W = \frac{\frac{1}{2}(\sigma_1 + \sigma_2)K}{\pi^2 p} - \frac{L}{4\pi^2 p^2} \qquad (20)$$

where K is the Scherrer constant, p the particle size, σ_1 and σ_2 are the range of 2θ on either side of the peak position and L was defined by Wilson as a taper parameter, a measure of the angularity or initial rate of taper.

The theory was next used by Langford and Wilson for the evaluation of line broadening in annealed aluminum and nickel (References 17, 26). The variance range analysis is found to be extremely useful for very broad reflections as occur in polymers. It provides two estimates for the particle (or crystallite) size based on the variance intercept W_o and the slope, k, for the variance-range curve:

$$\epsilon_{W_o} = \frac{\lambda}{2\pi(-w_o)\cos\theta} \qquad (21)$$

and

$$\epsilon_k = \frac{\lambda}{4\pi^2 k \cos\theta} \qquad (22)$$

Wilson subsequently derived a mathematical expression relating the two size estimates, ε_{W_o} and ε_k (Reference 16).

The noteworthy features in this method are: the correction for instrumental line broadening is straightforward; no particular distribution function e.g., Gaussian or Cauchy need be assumed; and useful inferences can be drawn from the two estimates for the crystallite sizes. In the present investigation well compacted hexamethylenetetramine powder served as a standard, giving rise to k_i and W_i from the variance-range curves. The experimental diffraction profile for the sample could then be corrected with the help of expressions.

$$k_s = k_b - k_i$$

$$W_s = W_b - W_i$$

where s, b, and i have the same physical significance as before, namely s - specimen, b - broadened, and i - instrumental.

APPENDIX F

IDENTIFICATION OF COMPUTER PROGRAM CONTROL CARDS

This computer program was assembled in a fashion such that control cards read by the MAIN program facilitates usage. The control cards are:

CRSFRA - This calls Subroutine SAREA after which KPLOT = 4, allowing control card PLOTCV to be used as desired. SAREA reads in theta values and corresponding coherent intensities, which have already been corrected for polarization, absorption, and air scattering, via the format 4(2F10.3). Reading of data is terminated when the angle read is 999999.999.

CRYSIZ - This calls Subroutine VARENS, which is programed after the Variance Method, ala, J. I. Langford and A. J. C. Wilson (Reference 17).

DSORPA - This calls Subroutine DISORD after which KPLOT = 6 allowing control card PLOTCV to be used as desired. Prior to using DSORPA, control card CRSFRA should have been used so that from Subroutine SAREA, the appropriate square of the reciprocal lattice vector times intensity is stored in array X(I). This subroutine logic is based on Ruland's method of determining the degree of crystallinity and the disorder parameter associated with lattice imperfections of the first kind. Straight-line segments are drawn between points IFIRST and ILAST with the number of such segments being NUMINT. Exclusive of these straight-line approximations to the amorphous background intensity multiplied by the square of the reciprocal lattice vector, all other regions have the total intensity equal to the amorphous contribution. For each assumed amorphous contribution, the program scans a set of disorder

parameters NKPTS(I). For each value of the disorder parameter integrations are performed from a set lower limit of the reciprocal lattice vector to successively higher prescribed upper limits. This set of integration ranges (usually three to five) have associated with each of them a number XCR. These are averaged and the root mean square deviation is computed. The "best fit" criterion is achieved when a minimum coefficient of variation is determined (CV) in correspondence with a unique amorphous contribution, a given value of the disorder parameter, and the specified set of integration ranges. This subroutine is based on a paper by W. Ruland (Reference 11).

ENDPLT - This calls subroutine PLOTE which is used to signal the CALCOMP plotting package that the plotting is finished.

ENDRUN - Terminates the computations, program goes to STOP.

HELICL - This calls Subroutine HELIXX which was never used in the present investigation but is included since it was previously used by one of the authors in another study dealing with helical conformation polymers.

ORNTAT - This calls Subroutine ORIENT after which KPLOT = 5, allowing control card PLOTCV to be used as desired. PHISCN should have been called before using this control card. That is, it is necessary that the phi angles and their corresponding normalized intensities be available in arrays X(I) and YSN(I), respectively. Subroutine ORIENT computes Hermans' orientation factor and the corresponding angle (Reference 8).

PHISCN - This calls Subroutine INPHI, where phi angles and intensities are read via format 2I7. Again as in

INTHETA, the data read statement is terminated with 9's, (i.e., 17, 9999999). The intensities are normalized and then ready for orientation computation. After this KPLOT = 3, allowing the control card PLOTCV to be used as desired.

PLOTCV - This calls Subroutine PTCURV. Whenever a computation is performed by a subroutine where a CALCOMP plot is desired a control parameter KPLOT is designated so that when the card PLOTCV is used the appropriate portion of PTCURV will be designated.

STRPLT - This initiates the plotting sequence used in the CALCOMP plotting package.

THETAS - This calls Subroutine INTHETA, where the two values and intensities are read. The intensities are corrected for polarization and normalized. Here KPLOT = 2, allowing control card PLOTCV to be used if desired. The input format is integer 2I6, first the angles and second the intensities which have previously been corrected for air scatter, absorption, etc. The program stops reading data when it reads an I6 format 999999.

APPENDIX G

COMPUTER PROGRAM FOR ANALYZING X-RAY DIFFRACTION DATA YIELDING CRYSTALLITE SIZE, ORIENTATION FACTOR, DISORDER PARAMETER, AND DEGREE OF CRYSTALLINITY

```
      PROGRAM MAIN(INPUT,OUTPUT,PUNCH,TAPE5=INPUT,TAPE6=OUTPUT,TAPE7=PUN
     1CH,PLOT)
      REAL X(2000),Y(2000),YS(2000),YC(2000)
      REAL YSN(2000),XO(2000),LAMBDA,VARN(20,200)
      INTEGER MESG(8),ICOND(8)
      COMMON/ZZZ/YSN,XO,NP,MESG,ICOND,LAMBDA,VARN
      COMMON/ZZ/X,Y,YS,YC
      DATA R1,R2,R3,R4,R5,R6,R7,R8,R9,R10,R11,R12/6HPLOTCV,6HCRYSIZ,6H
     1     ,6HENDRUN,6HTHETAS,6HPHISCN,6HCRSFRA,6HORNTAT,6HDSORPA,6HENDPL
     2T,6HSTRPLT,6HHELICL/
    2 READ(5,11) RECORD
   11 FORMAT(A6)
      IF(RECORD - R1) 30,50,30
   30 IF(RECORD - R2) 31,51,31
   31 IF(RECORD - R3) 32,2,32
   32 IF(RECORD - R4) 33,52,33
   33 IF(RECORD - R5) 34,53,34
   34 IF(RECORD - R6) 35,54,35
   35 IF(RECORD - R7) 36,55,36
   36 IF(RECORD - R8) 37,56,37
   37 IF(RECORD - R9) 38,57,38
   38 IF(RECORD - R10) 39,58,39
   39 IF(RECORD - R11) 40,59,40
   40 IF(RECORD - R12) 999,60,999
   50 CALL PTCURV(IM,IJ,KPLOT)
      GO TO 2
   51 CALL VARENS(DLTHET,IM,IJ)
      KPLOT=1
      GO TO 2
   52 WRITE(6,199)
  199 FORMAT(//10(12H   ENDRUN   ))
      GO TO 99
   53 CALL INTHETA
      KPLOT=2
      GO TO 2
   54 CALL INPHI
      KPLOT=3
      GO TO 2
   55 CALL SAREA
      KPLOT=4
      GO TO 2
   56 CALL ORIENT
      KPLOT=5
      GO TO 2
   57 CALL DISORD
      KPLOT=6
      GO TO 2
   58 CALL PLOTE
  100 CALL PLOT(10.0,0.0,-3)
      GO TO 2
   59 CALL PLOT(1.,1.,-3)
      GO TO 2
   60 CALL HELIXX
      GO TO 2
  999 WRITE(6,113)
  113 FORMAT(1H1,5X,10HXXXXXXXXXX,5X,A6,5X,25HIS NOT A PROPER DATA CARD)
   99 CONTINUE

      STOP
      END
```

```
      SUBROUTINE INTHETA
      REAL X(2000),Y(2000),YS(2000),YC(2000)
      REAL YSN(2000),XO(2000),LAMBDA,VARN(20,200)
      INTEGER MESG(8),ICOND(8)
      COMMON/ZZZ/YSN,XO,NP,MESG,ICOND,LAMBDA,VARN
      COMMON/ZZ/X,Y,YS,YC
      RAD=3.14159/180.
C
C     MESG IS USED FOR IDENTIFICATION
C
 1    READ (5,10) MESG
 10   FORMAT(8A10)
C
C     ICOND IS USED TO LABEL CONDITIONS OF EXPERIMENT
C
      READ (5,10) ICOND
C
C     LAMBDA IS THE WAVELENGTH OF RADIATION USED
C
      READ (5,11) LAMBDA
 11   FORMAT(F7.5)
      I=0
  6   I=I+1
      IF(I.GT.1990) GO TO 101
      READ (5,12) IX,IY
C
C     IX = ANGLES MULTIPLIED BY 100  AND IY = EXPERIMENTAL INTENSITIES
C
   12 FORMAT(2I6)
      IF(IX.EQ.999999.OR.IY.EQ.999999) GO TO 3
      X(I) = IX/100.
C
C     XO(I) ARRAY ARE THE TRUE TWO THETA ANGLES
C
      XO(I)=X(I)
C
C     X(I) ARRAY ARE THE TRUE THETA ANGLES
C
      X(I)=X(I)/2.
C
C     Y(I) ARRAY ARE DECIMAL FORMAT INTENSITIES
C
      Y(I)=FLOAT(IY)
      GO TO 6
C
C     NP = NUMBER OF DATA POINTS
C
  3   NP=I-1
      CONST=LAMBDA/2.
C
      DO 7 I=1,NP
      P= (1+ ((COS(RAD*XO(I)))**2))/2
C
C     P = POLARIZATION CORRECTION
C
      YC(I) = Y(I)
C
```

```
C      YS(I) = INTENSITIES CORRECTED FOR POLARIZATION
C
       YS(I)=YC(I)/P
C
C      X(I) ARRAY NOW BECOMES D-SPACINGS
C
       X(I)=X(I)*RAD
   7   X(I)=CONST/SIN(X(I))
C
C
C      BEGIN NORMALIZATION OF INTENSITIES
C
       AMAX=0.0
       DO 8 I=1,NP
 8     AMAX = AMAX1(AMAX,YS(I))
       DO 9 I=1,NP
 9     YSN(I) = 100.*YS(I)/AMAX
       WRITE (6,110) MESG
  110   FORMAT(1H1,5X,8A10)
       WRITE (6,112) ICOND
  112   FORMAT(5X,8A10)
       WRITE (6,111) LAMBDA,NP
  111  FORMAT(5X,*LAMBDA=*,F7.5,5X,*NUMBER OF DATA POINTS=*,I5,//)
       WRITE (6,15)
    15 FORMAT(10X,*TWO THETA*,3X,*D(A)*,4X,*I*,6X,*NUMBER *,3X,*I(PC)*,3X
      1,*I(NM)*,//)
       WRITE(6,14) ((XO(I),X(I),Y(I),I,YS(I),YSN(I)),I = 1,NP)
 14    FORMAT(10X,F7.3,3X,F6.3,2X,F6.0,4X,I4,2X,F7.2,2X,F6.2)
       GO TO 99
  101   WRITE(6,13)
  13   FORMAT(5X,*NUMBER OF DATA POINTS EXCEEDS 1980*)
    99 RETURN
       END
```

```
      SUBROUTINE PTCURV(IM,IJ,KPLOT)
      REAL X(2000),Y(2000),YS(2000),YC(2000)
      REAL YSN(2000),XO(2000),LAMBDA,VARN(20,200)
      INTEGER MESG(8),ICOND(8)
      COMMON/ZZZ/YSN,XO,NP,MESG,ICOND,LAMBDA,VARN
      COMMON/ZZ/X,Y,YS,YC
      N=NP
      PRINT 777
  777 FORMAT(* PLOT CURVE *)
      IF(KPLOT - 1) 30,910,30
   30 IF(KPLOT - 2) 31,920,31
   31 IF(KPLOT - 3) 32,930,32
   32 IF(KPLOT - 4) 33,940,33
   33 IF(KPLOT - 5) 34,950,34
   34 IF(KPLOT - 6) 99,960,99
C
C     VARENS PLOTTING BEGINS
C
  910 CONTINUE
      PMIN = 1.E 24
      PMAX = 0.
      DO1I=1,IM
      DO1J=1,IJ
      P1=VARN(I,J)
      PMAX = AMAX1(PMAX,P1)
    1 PMIN = AMIN1(PMIN,P1)
      DA = FLOAT(IJ)/10.
      DB=(PMAX-PMIN)/7.
      Y(IJ+1)=PMIN
      Y(IJ+2)=DB
      X(IJ+1) = 0.
      X(IJ+2)=DA
      DO2I=1,IJ
      K=IJ-I+1
    2 X(I) = FLOAT(K)
      CALL AXIS(0.0,0.0,22HRANGE IN INTEGER STEPS,-22,10.0,0.0,0.,DA)
      CALL AXIS(0.0,0.0,8HVARIANCE,8,7.0,90.0,PMIN,DB)
      DO3I=1,IM
      DO4J=1,IJ
    4 Y(J)=VARN(I,J)
      CALL LINE(X,Y,IJ,1,0,0)
    3 CONTINUE
      CALL SYMBOL(4.0,8.5,.175,MESG,0.0,80)
      CALL SYMBOL(6.0,7.5,.175,ICOND,0.0,80)
      CALL PLOT(14.,0.,-3)
      GO TO 99
C
C      INTHETA PLOTTING BEGINS
C
  920 CONTINUE
      CALL SCALE(XO,22.0,N,1)
      CALL SCALE (Y,7.0,N,1)
      CALL AXIS (0.0,0.0,9HTWO THETA,-9,24.0,0.0,XO(N+1),XO(N+2))
      CALL AXIS (0.0,0.0,9HINTENSITY,9,7.0,90.0,Y(N+1),Y(N+2))
      CALL LINE (XO,Y,N,1,0,2)
      CALL SYMBOL (7.0,8.5,.175,MESG,0.0,80)
      CALL SYMBOL ( 9.0,7.5,.175,ICOND,0.0,80)
```

```
      CALL PLOT (28.0,0.0,-3)
      CALL SCALE (XO,22.0,N,1)
      CALL SCALE (YSN,7.0,N,1)
      CALL AXIS (0.0,0.0,9HTWO THETA,-9,24.0,0.0,XO(N+1),XO(N+2))
      CALL AXIS (0.0,0.0,9HI(NORMAL),9,7.0,90.0,YSN(N+1),YSN(N+2))
      CALL LINE (XO,YSN,N,1,0,2)
      CALL SYMBOL (7.0,8.5,.175,MESG,0.0,80)
      CALL SYMBOL ( 9.0,7.5,.175,ICOND,0.0,80)
      CALL PLOT(28.,0.,-3)
      GO TO 99
C
C       INPHI PLOTTING BEGINS
C
  930 CONTINUE
      CALL SCALE(X,22.0,N,1)
      CALL SCALE (Y,7.0,N,1)
      CALL AXIS (0.0,0.0,3HPHI,-3,24.0,0.0,X(N+1),X(N+2))
      CALL AXIS (0.0,0.0,9HINTENSITY,9,7.0,90.0,Y(N+1),Y(N+2))
      CALL LINE (X,Y,N,1,0,2)
      CALL SYMBOL (7.0,8.5,.175,MESG,0.0,80)
      CALL SYMBOL ( 9.0,7.5,.175,ICOND,0.0,80)
      CALL PLOT (28.0,0.0,-3)
      CALL SCALE (X,22.0,N,1)
      CALL SCALE(YSN,7.,N,1)
      CALL AXIS (0.0,0.0,3HPHI,-3,24.0,0.0,X(N+1),X(N+2))
      CALL AXIS(0.,0.,9HI(NORMAL),9,7.,90.,YSN(N+1),YSN(N+2))
      CALL LINE (X,YSN,N,1,0,2)
      CALL SYMBOL (7.0,8.5,.175,MESG,0.0,80)
      CALL SYMBOL ( 9.0,7.5,.175,ICOND,0.0,80)
      CALL PLOT (28.0,0.0,-3)
      GO TO 99
C
C       SAREA PLOTTING BEGINS
C
  940 CONTINUE
      CALL SCALE (X,22.0,N,1)
      CALL SCALE (YC,7.0,N,1)
      CALL AXIS (0.0,0.0,1HS,-3,24.0,0.0,X(N+1),X(N+2))
      CALL AXIS (0.0,0.0,26HS**2 X CORRECTED INTENSITY,26,7.0,90.0,YC(N+
     11),YC(N+2))
      CALL LINE (X,YC,N,1,0,2)
      CALL SYMBOL (7.0,8.5,.175,MESG,0.0,80)
      CALL SYMBOL (9.0,7.5,.175,ICOND,0.0,80)
      CALL PLOT (28.,0.,-3)
      GO TO 99
C
C       ORIENT PLOTTING BEGINS
C
  950 CONTINUE
      GO TO 99
C
C       DISORD PLOTTING BEGINS
C
  960 CONTINUE
      CALL SCALE (X,22.0,N,1)
      CALL SCALE (YC,7.0,N,1)
      CALL AXIS (0.0,0.0,1HS,-3,24.0,0.0,X(N+1),X(N+2))
```

```
      CALL AXIS (0.0,0.0,26HS**2 X CORRECTED INTENSITY,26,7.0,90.0,YC(N+
     11),YC(N+2))
      CALL LINE (X,YC,N,1,0,2)
      Y(N+1) = YC(N+1)
      Y(N+2) = YC(N+2)
      CALL LINE (X,Y,N,1,0,2)
      CALL SYMBOL (7.0,8.5,.175,MESG,0.0,80)
      CALL SYMBOL (9.0,7.5,.175,ICOND,0.0,88)
      CALL PLOT (28.,0.,-3)
   99 RETURN
      END
```

```
      SUBROUTINE VARENS(CLASS,IM,IJ)
      REAL YSN(2000),XO(2000),LAMBDA,VARN(20,200)
      INTEGER MESG(8),ICOND(8)
      DIMENSIONX(200),Y(200)
      COMMON/ZZZ/YSN,XO,NP,MESG,ICOND,LAMBDA,VARN
      PRINT 777
  777 FORMAT(//,* ENTER CRSTAL *)
      READ(5,40) NFIRST,NLAST
      WRITE (6,41) NFIRST,NLAST
   41 FORMAT(/,* THE RANGE EXTENDS FROM *,I4,* TO *,I4,/)
   40 FORMAT(2I4)
      NCOUNT = 0
      DO 1 I = NFIRST,NLAST
      J = I - NFIRST + 1
      NCOUNT = NCOUNT + 1
      Y(J) = YSN(I)
    1 X(J) = XO(I)
      N = NCOUNT
   21 READ(5,11) CLASS,Z
      WRITE(6,778) CLASS,Z
  778 FORMAT(* DELTA TWO THETA (CLASS) = *,F5.3,/,* DELTA BACKGROUND (Z)
     1= *,F5.2,//)
   11 FORMAT(F6.3,F5.2)
      SY=SUM=0.
      D=ABS(Y(N)-Y(1))
      B=(Y(N)+Y(1))/2.
      DO5I=1,N
      L=N-I+1
      XN=N
      SY=SY+Y(I)
      XI=I
      XI=I
    5 SUM=SUM+XI*Y(L)
      SUM=SUM-SY
      TT=SY*CLASS
      R=B*XN/SY
      S=SUM/SY-(XN-1.)/2.+(XN+1.)*D/(12.*B)
      XBA = (SUM/SY + (R/(1.-R))*S)*CLASS
      J1=N/2
      J=N
      M=K=1
      MM=1
      BN=B
      WRITE(6,102) BN
  102 FORMAT(/,* INCREMENTED BACKGROUND = *,F10.4)
      GOTO9
    8 BN=BN-Z
      IF(BN - B + 20.*Z) 33,33,10
   10 CONTINUE
      WRITE(6,102) BN
      J=N
      M=K=1
    9 CONTINUE
      M2=J-M
      IF(M2)31,31,131
  131 CONTINUE
      XPHY=SNY=SM=0.
```

```
      DO30I=M,J
      L=J-I+M
      XJ=J
      W=J-M
      DN=W*(Y(N)-Y(1))/(XN-1.)
      XI=I-M+1
      XPHY=XPHY+Y(I)*(W-XI+1.)*(W-XI+1.)
      SM=SM+XI*Y(L)
   30 SNY=SNY+Y(I)
      SM=SM-SNY
      SN1=SM/SNY-W/2.+(W+2.)*DN/(12.*BN)
      SN2=XPHY/SNY-W*(2.*W+1.)/6.+W*(W+2.)*DN/(12.*BN)
      RN=W*BN/SNY
      ONE=(XPHY/SNY+(RN/(1.-RN))*SN2)*CLASS*CLASS
      TWO=(SM/SNY+(RN/(1.-RN))*SN1)*CLASS
      VARN(MM,K)=ONE-TWO*TWO
      J=J-1
      M=M+1
      K=K+1
      GO TO 9
   31 WRITE(6,101) (VARN(MM,K),K=1,J1)
  101 FORMAT(20F6.4)
      VARN(MM,J1+1)=BN
      MM=MM+1
      GOTO8
   33 CONTINUE
      IM=MM-1
      IJ=J1
      RETURN
      END
```

```
      SUBROUTINE INPHI
      REAL X(2000),Y(2000),YS(2000),YC(2000)
      REAL YSN(2000),XO(2000),LAMBDA,VARN(20,200)
      INTEGER MESG(8),ICOND(8)
      COMMON/ZZZ/YSN,XO,NP,MESG,ICOND,LAMBDA,VARN
      COMMON/ZZ/X,Y,YS,YC
 1    READ (5,10) MESG
 10   FORMAT(8A10)
      READ (5,10) ICOND
      I=0
  6   I=I+1
      IF(I.GT.1990) GO TO 101
      READ (5,12) IX,IY
   12 FORMAT(2I7)
      IF(IX.EQ.9999999) GO TO 3
      X(I) = IX/100.
      Y(I)=FLOAT(IY)
      GO TO 6
  3   NP=I-1
      AMAX=0.0
      DO 8 I=1,NP
8     AMAX=AMAX1(AMAX,Y(I))
      DO 9 I=1,NP
    9 YSN(I) = 100.*Y(I)/AMAX
      WRITE (6,110) MESG
 110   FORMAT(1H1,5X,8A10)
      WRITE (6,112) ICOND
 112   FORMAT(5X,8A10)
      WRITE (6,111) NP
 111  FORMAT(5X,*NUMBER OF DATA POINTS = *,I5,//)
      WRITE (6,15)
   15 FORMAT(3X,*NO.*,6X*PHI*,5X,*I*,6X,*I(NORM)*,//)
      WRITE(6,14) ((I,X(I),Y(I),YSN(I)),I=1,NP)
   14 FORMAT(2X,I4,4X,F7.2,2X,F5.0,2X,F7.2)
      GO TO 99
 101   WRITE(6,13)
 13   FORMAT(5X,*NUMBER OF DATA POINTS EXCEEDS 1980*)
   99 RETURN
      END
```

```
      SUBROUTINE SAREA
      REAL X(2000),Y(2000),YS(2000),YC(2000)
      REAL YSN(2000),XO(2000),LAMBDA,VARN(20,200)
      INTEGER MESG(8), ICOND (8)
      COMMON/ZZZ/YSN,XO,NP,MESG,ICOND,LAMBDA,VARN
      COMMON/ZZ/X,Y,YS,YC
      PIOV = 3.14159/180.
      PRINT 777
  777 FORMAT(* ENTER SAREA *)
      READ (5,101) MESG
  101 FORMAT (8A10)
      READ (5,101) ICOND
      WRITE(6,110) MESG
  110 FORMAT(/,5X,8A10)
      WRITE(6,112) ICOND
  112 FORMAT(20X,8A10)
      READ (5,102) LAMBDA
  102 FORMAT(F7.5)
      NP = 4
C
C     XO(I) ARE THE THETA VALUES
C     YSN(I) ARE THE COHERENT SCATTERING INTENSITIES ALREADY CORRECTED
C     FOR POLARIZATION AND AIR SCATTERING
C
      NBEGIN = 1
    1 READ(5,100)(XO(I),YSN(I),I=NBEGIN,NP)
  100 FORMAT (4(2F10.3))
      DO 2  K = NBEGIN,NP
      IF(XO(K).EQ.999999.999) GO TO 3
    2 CONTINUE
      NBEGIN = NP + 1
      NP = NBEGIN + 3
      GO TO 1
    3 NP = K-1
      DO 4 I = 1,NP
      A1 = PIOV*XO(I)
      A2 = SIN(A1)
      A3 = 2.*A2/LAMBDA
C
C     X(I) ARE THE SET OF S VALUES
C
      X(I) = A3
      A4 = A3**2
C
C     YC(I) IS THE COHERENT SCATTERING MULTIPLIED BY S**2.
C
    4 YC(I) = A4*YSN(I)
      WRITE (6,103)
  103 FORMAT (10X,6HNUMBER,4X,5HTHETA,5X,1HS,6X,7HI(NORM),3X,8HS**2 X I,
     I/)
      DO 5 I = 1,NP
      WRITE (6,104) I,XO(I),X(I),YSN(I),YC(I)
    5 CONTINUE
  104 FORMAT (10X,I4,F10.3,F10.5,F10.3,2X,1PE9.2)
      RETURN
      END
```

```
      SUBROUTINE DISORD
      REAL X(2000),Y(2000),YS(2000),YC(2000)
      REAL YSN(2000),XO(2000),LAMBDA,VARN(20,200)
      INTEGER MESG(8), ICOND (8)
      COMMON/ZZZ/YSN,XO,NP,MESG,ICOND,LAMBDA,VARN
      COMMON/ZZ/X,Y,YS,YC
      DIMENSION INT(300),XK(20),S(20),NATOMS(10),SFACT(2,20)
      DIMENSION DEGXCR(10)
      READ(5,110) NUMINT
  110 FORMAT(I4)
      ICOUNT = 0
      DO 30 II = 1,NUMINT
      ICOUNT = ICOUNT + 1
      READ(5,111) IFIRST,ILAST
  111 FORMAT(2I4)
      IF(ICOUNT.EQ.IFIRST) GO TO 53
      NLAST = IFIRST - 1
      DO 54 I = ICOUNT,NLAST
C
C     Y(I) IS THE AMORPHOUS BACKGROUND MULTIPLIED BY S**2.
C     YS(I) IS THE CRYSTALLINE CONTRIBUTION MULTIPLIED BY S**2.
C
      Y(I) = YC(I)
   54 YS(I) = 0.
      ICOUNT = NLAST
C
   53 A1 = X(IFIRST) + X(ILAST)
      A2 = X(IFIRST)**2. + X(ILAST)**2.
      B1 = YC(IFIRST) + YC(ILAST)
      B2 = X(IFIRST)*YC(IFIRST) + X(ILAST)*YC(ILAST)
      DENOM = 2.*A2 - A1**2.
      COEF1 = B1*A2 - B2*A1
      COEF2 = 2.*B2 - A1*B1
      COEF1 = COEF1/DENOM
      COEF2 = COEF2/DENOM
      DO 6 I = IFIRST,ILAST
      ICOUNT = ICOUNT + 1
      Y(I) = COEF1 + COEF2*X(I)
    6 YS(I) = YC(I) - Y(I)
   30 CONTINUE
C
      IF(ICOUNT.EQ.NP) GO TO 55
      ICOUNT = ICOUNT + 1
      DO 7 I = ICOUNT,NP
      Y(I) = YC(I)
    7 YS(I) = 0.
   55 CONTINUE
C
C     NOW READ IN THE LIMITS OF INTEGRATION BY SPECIFYING THE NUMBERS OF
C      THE S-VALUES IN THE ARRAY X(I).
C
      READ (5,105) NINT,(INT(I),I=1,NINT)
  105 FORMAT(I2,26I3)
      READ (5,106) NKPTS,(XK(I),I=1,NKPTS)
  106 FORMAT (I2,19F4.2)
C
C     FOR THE K-VALUE OF THIS SET,WE WILL NOW COMPUTE THE CORRESPONDING
```

```
C     FIRST APPROXIMATION DISORDER FUNCTION EXP(-K*S**2) AND USE THIS
C     ALONG WITH THE PREVIOUSLY NUMBERED DATA POINTS TO EVALUATE THE
C     DEGREE OF CRYSTALLINITY.
C
C     FIRST ENTER SCATTERING FACTORS.
C
      READ (5,107) NSVALS,DLSC,ITYPES,(NATOMS(I),I=1,ITYPES)
  107 FORMAT (I4,F5.2,I4,30I2)
      DO 8 I=1,NSVALS
    8 S(I) = FLOAT(I)*DLSC
      READ (5,108) (SFACT(1,I),I=1,NSVALS)
C
C     START READING THE SCATTERING FACTORS FOR EACH TYPE OF ATOM IN THE
C     UNIT CELL AND COMPUTE THE MEAN SQUARE VALUES AT EACH S-VALUE. USE
C     INTERNATIONAL TABLES VOLUME III PAGE 202.
C
  108 FORMAT (13F6.3)
      DO 9 I=1,NSVALS
    9 SFACT(1,I) = NATOMS(1)*SFACT(1,I)**2.
      DO 10 I=2,ITYPES
      READ (5,108) (SFACT(2,K),K=1,NSVALS)
      DO 11 J=1,NSVALS
   11 SFACT(1,J) = SFACT(1,J) + NATOMS(I)*SFACT(2,J)**2.
   10 CONTINUE
      AAA = 0.
      DO 12 I=1,ITYPES
   12 AAA = AAA + NATOMS(I)
C
C     AAA IS THE TOTAL NUMBER OF ATOMS IN THE REPEAT UNIT.
C
      DO 13 I=1,NSVALS
   13 SFACT(1,I) = SFACT(1,I)/AAA
C
C     LET US NOW DO A LEAST SQUARES FIT TO THESE MEAN SQUARE SCATTERING
C     FACTORS. DO AS ABOVE (Y = A + BX + CX**2)
C
      A1 = 0.
      A2 = 0.
      A3 = 0.
      A4 = 0.
      A5 = 0.
      A6 = 0.
      A7 = 0.
      XSVALS = FLOAT(NSVALS)
      DO14 I = 1,NSVALS
      A1 = A1 + SFACT(1,I)
      A2 = A2 + S(I)
      A3 = A3 + S(I)**2.
      A4 = A4 + S(I)**3.
      A5 = A5 + S(I)**4.
      A6 = A6 + SFACT(1,I)*S(I)
      A7 = A7 + SFACT(1,I)*S(I)**2.
   14 CONTINUE
      DENOM = XSVALS*(A3*A5 - A4**2.) - A2*(A2*A5 - A3*A4) + A3*(A2*A4
     $-A3**2.)
      XNUM0 = A1*(A3*A5 - A4**2.) - A2*(A6*A5 - A7*A4) + A3*(A6*A4 - A7*
     $A3)
```

```
      XNUM1 = XSVALS*(A6*A5 - A7*A4) - A1*(A2*A5 - A3*A4) + A3*(A2*A7 -
     $A3*A6)
      XNUM2 = XSVALS*(A3*A7 - A4*A6) - A2*(A2*A7 - A3*A6) + A1*(A2*A4 -
     $A3**2.)
C
C     SCOF0,SCOF1, AND SCOF2 ARE THE COEFICIENTS TO THE LEAST SQUARES
C     FIT OF F SQUARE AVERAGE TO A QUADRATIC FORM.
C
      SCOF0 = XNUM0/DENOM
      SCOF1 = XNUM1/DENOM
      SCOF2 = XNUM2/DENOM
C
C     WE NOW BEGIN OUR SEQUENCE OF INTEGRATIONS. FROM RULAND'S THEORY
C     FOR EACH LOWER CASE K IN THE DISORDER FUNCTION WE COMPUTE A SET OF
C     CAPITAL K'S AND A SET OF WEIGHT  FRACTION CRYSTALLINITY XCR FOR
C     FOR EACH UPPER LIMIT OF INTEGRATION.
      KBEGIN = INT(1)
      DO 20 I=1,NKPTS
      KCOUNT = 0
      DO 21 J=2,NINT
      KCOUNT = KCOUNT + 1
      KK = INT(J)
      A1 = 0.
      A2 = 0.
      A3 = 0.
      A4 = 0.
      DO 22 K = KBEGIN,KK
      A1 = A1 + YS(K)
      A2 = A2 + YC(K)
C
C     X1 IS S**2 X F**2 AVERAGE
C
      X1 = (SCOF0 + SCOF1*X(K) + SCOF2*X(K)**2.)*X(K)**2.
C
C     X2 IS X1 X D, THE DISORDER FUNCTION.
C
      X2 = X1*EXP(-XK(I)*X(K)**2.)
      A3 = A3 + X1
      A4 = A4 + X2
   22 CONTINUE
      A1 = A1 - 0.5*YS(1) - 0.5*YS(KK)
      A2 = A2 - 0.5*YC(1) - 0.5*YC(KK)
      XO1 = (SCOF0 + SCOF1*X(1) + SCOF2*X(1)**2.)*X(1)**2.
      XO2 = XO1*EXP(-XK(I)*X(1)**2.)
      A3 = A3 - 0.5*XO1 - 0.5*X1
      A4 = A4 - 0.5*XO2 - 0.5*X2
      XKAP = A3/A4
      XCR = (A1*A3)/(A2*A4)
      XLOW = X(KBEGIN)
      XUP = X(KK)
      DEGXCR(KCOUNT) = XCR
      WRITE (6,1000) XCR, XK(I), XLOW, XUP, XKAP
 1000 FORMAT (//,23H WEIGHT FRACTION XCR = ,1PE10.3,10X,22H DISORDER PAR
     @AMETER = ,1PE10.3,10X,15H LOWER LIMIT = ,1PE10.3,15H UPPER LIMIT =
     % ,1PE10.3/9H KAPPA = ,1PE10.3)
   21 CONTINUE
      A1 = 0.
```

```
      DO 50 J = 1,KCOUNT
   50 A1 = A1 + DEGXCR(J)
      XCRAVG = A1/FLOAT(KCOUNT)
      A1 = 0.
      DO 51 J = 1,KCOUNT
   51 A1 = A1 + (DEGXCR(J) - XCRAVG)**2.
      A1 = A1/FLOAT(KCOUNT)
      A1 = SQRT(A1)
      CV = (A1/XCRAVG)*100.
      WRITE(6,1002) XCRAVG,A1,CV
 1002 FORMAT(40X,* AVERAGE XCR = *,1PE10.3,* RMS DEVIATION *,1PE10.3,* P
     1ERCENT VARIATION = *,1PE10.3)
      WRITE (6,1001)
 1001 FORMAT(//)
   20 CONTINUE
   99 RETURN
      END
```

```
      SUBROUTINE ORIENT
      REAL X(2000), Y(2000), YS(2000), YC(2000)
      REAL YSN(2000), XO(2000), LAMBDA, VARN(20,200)
      INTEGER MESG(8), ICOND (8)
      COMMON /ZZZ/YSN,XO,NP,MESG,ICOND,LAMBDA,VARN
      COMMON /ZZ/X,Y,YS,YC
      PIOV = 3.14159/180.
      READ(5,100) NBEGIN, NUP
  100 FORMAT (2I4)
      DLPHI = ABS (X(2) - X(1))
      XNUM = 0.
      XDENOM = 0.
      WRITE(6,1000)
 1000 FORMAT(* ENTERING ORIENTATION SUBROUTINE *)
      BKGRND = 150.
      DO 4 I=NBEGIN,NUP
    4 BKGRND = AMIN1(BKGRND,YSN(I))
      DO 1 I = NBEGIN, NUP
      XX = FLOAT(I - NBEGIN)*DLPHI
      A1 = PIOV * XX
      A2 = YSN(I) - BKGRND
      F1 = SIN(A1)
      F2 = F1**2
      F3 = SIN(A1)
      IF (I.NE.NBEGIN.OR.I.NE.NUP)  GO TO 2
      A = A2*F2*F3/2.
      D = A2*F3/2.
      GO TO 3
    2 A = A2*F2*F3
      D = A2*F3
    3 XNUM = XNUM + A
      XDENOM = XDENOM + D
    1 CONTINUE
      ASINSQ = XNUM/XDENOM
      FX = 1. - 3.*ASINSQ/2.
      B1 = SQRT(ASINSQ)
      BETA = ASIN(B1)
      BETA = BETA/PIOV
      WRITE (6,200)
  200 FORMAT(//)
      WRITE(6,201) NBEGIN,NUP
  201 FORMAT(37H EVALUATION OF THE ORIENTATION BEGINS,10X,22H GOING FROM
     1 DATA POINT,I4,14H TO DATA POINT,I4/)
      WRITE (6,202) XX
  202 FORMAT (30X,33H THE PHI RANGE EXTENDS FROM 0 TO ,F7.3,8H DEGREES,/
     130X,47H WITH THE FIRST ANGLE ADJUSTED TO ZERO DEGREES.,/)
      WRITE (6,203)  FX,BETA
  203 FORMAT (30H HERMANS ORIENTATION FACTOR = ,F8.5,30H AND THE ORIENTA
     2TION ANGLE IS , F6.3)
      RETURN
      END
```

```
      SUBROUTINE HELIXX
C
C---- ORIENTATION AND SPIRAL ANGLES ASSUMING GAUSSIAN DISTRIBUTIONS
C
    1 READ(5,5)H,DELH
      READ(5,5)EPS,GAM
      READ(5,5)X,Y
      PI=3.14159
      T=PI/180.
      EPS1 = EPS*T
      GAM1=GAM*T
      EPS2=EPS1*EPS1
      GAM2=GAM1*GAM1
   10 D1=2.*H*EPS1
      D2=2.*H*GAM1
      C1=X*EXP(H*EPS2)
      C2=Y*EXP(H*GAM2)
      C12=C1*C1
      C22=C2*C2
      IF(C12)22,20,20
   20 IF(C22)22,23,23
   23 X1=C1+SQRT(C12-1.)
      X2=C2+SQRT(C22-1.)
      FI1 = ALOG(X1)/D1
      FI2 = ALOG(X2)/D2
      AF=ABS(FI1-FI2)
   11 WRITE(6,15)H,FI1,FI2,AF
   12 CONTINUE
      IF(AF-1.E-04)14,14,22
   14 ALPH2 = ALOG(2.)/H
      ALPHA=SQRT(ALPH2)/T
      FG1=FI1/T
      FG2=FI2/T
      WRITE(6,25)EPS,GAM,X,Y,H,FG1,FG2,ALPHA
      WRITE(7,25)EPS,GAM,X,Y,H,FG1,FG2,ALPHA
      GO TO 99
   22 H=H+DELH
      GO TO 10
    5 FORMAT(2F8.4)
   15 FORMAT(4F10.5)
   25 FORMAT(8F9.5)
   99 RETURN
      END
```

SAMPLE INPUT DATA

DISORDER PARAMETER AND DEGREE OF CRYSTALLINITY

```
STRPLT
CRSFRA
RUN 65.74 MYLAR 1000A  DISORDER DATA
 (S**2)*I WITH SEGMENTED STRAIGHT LINE BKGRND
1.54180
     3.200     6.586     3.300     6.589     3.400     5.204     3.500     5.900
     3.600     7.986     3.700     8.337     3.800     8.340     3.900     8.344
     4.000     7.305     4.100     9.744     4.200    10.097     4.300    10.451
     4.400    10.457     4.500    11.857     4.600     9.770     4.700    10.125
     4.800    10.829     4.900    11.884     5.000    11.542     5.100    11.199
     5.200    12.256     5.300    14.366     5.400    12.973     5.500    14.736
     5.600    14.044     5.700    14.405     5.800    14.415     5.900    14.425
     6.000    16.196     6.100    16.560     6.200    16.925     6.300    16.585
     6.400    17.304     6.500    19.084     6.600    20.868     6.700    19.823
     6.800    22.673     6.900    23.401     7.000    25.195     7.100    25.927
     7.200    28.437     7.300    31.664     7.400    31.336     7.500    38.492
     7.600    45.305     7.700    50.703     7.800    67.191     7.900    81.206
     8.000    93.816     8.100   100.000     8.200    92.922     8.300    85.832
     8.400    79.807     8.500    68.372     8.600    69.163     8.700    66.710
     8.800    64.254     8.900    57.817     9.000    54.985     9.100    49.251
     9.200    45.317     9.300    42.463     9.400    37.787     9.500    36.011
       ↑         ↑         ↑         ↑         ↑         ↑         ↑         ↑
       ↓         ↓         ↓         ↓         ↓         ↓         ↓         ↓
    28.000    14.695    28.100    11.575    28.200    13.186    28.300    12.689
    28.400    12.721    28.500    13.283    28.600    11.718    28.700    12.281
    28.800    10.705    28.900    12.878    29.000     9.144    29.100     9.706
    29.200    10.811    29.300     9.212    29.400    10.320    29.500    10.346
    29.600     6.004    29.700     7.113    29.800     6.033    29.900     3.849
    30.000     6.063    30.100     3.315    30.200     4.431    30.300     3.886
    30.400     5.008    30.500     3.905    30.600     2.796999999.999
DSORPA
   3
  44 119
 119 147
 170 197
 3  1147245
190.0 0.1 0.2 0.3 0.4 0.5 0.6 0.7 0.8 0.9 1.0 1.1 1.2 1.3 1.4 1.5 1.6 1.7 1.8
  17 0.10   3 810 4
 0.947 0.811 0.641 0.481 0.350 0.251 0.180 0.130 0.071 0.040 0.024 0.015 0.010
 0.007 0.005 0.004 0.003
 5.760 5.126 4.358 3.581 2.976 2.502 2.165 1.950 1.685 1.536 1.426 1.322 1.218
 1.114 1.012 0.900 0.821
 7.796 7.250 6.482 5.634 4.814 4.094 3.492 3.010 2.338 1.944 1.714 1.566 1.462
 1.374 1.296 1.220 1.144
PLOTCV
ENDPLT
ENDRUN
```

CRYSTALLITE SIZE VIA WILSON VARIANCE

```
STRPLT
 RUN 36.75 MYLAR 400A CRYSTALLITE SIZE
 CU K ALPHA
1.54180
  40025      13
  40050      14
  40075      14
  40100      14
  40125      15
  40150      16
  40175      15
  40200      13
  40225      15
  40250      15
  40275      13
  40300      16
  40325      15
  40350      15
  40375      15
  40400      16
  40425      15
  40450      15
  40475      17
  40500      17
  40525      14
  40550      16
  40575      14
  40600      16
    ↑          ↑
    |          |
    |          |
    ↓          ↓
  44825      10
  44850      10
  44875      14
  44900      15
  44925      12
  44950      14
  44975      11
  45000      14
  45025      12
  45050      10
  45075      12
  45100      14
9999999
CRYSIZ
  13 187
 0.025 0.90
PLOTCV
001
000000
ENDPLT
END RUN
```

HERMANS' ORIENTATION FACTOR

```
STRPLT
PHISCN
RUN 46.75   MYLAR          PHI SCAN  TWO THETA=       (CORRECTED)
CU K ALPHA
   4500      17
   9000      21
  13500      20
  18000      18
  22500      20
  27000      20
  31500      20
  36000      22
  40500      26
  45000      23
  49500      27
  54000      33
  58500      36
  63000      43
  67500      60
  72000      81
  76500     105
  81000     118
  85500     131
  90000     130
  94500     122
  99000     100
 103500      80
 108000      61
 112500      41
 117000      30
 121500      29
```

```
 342000      14
 346500      13
 351000      13
 355500      17
 360000      16
 364500      12
9999999
ORNTAT
  19  39
PLOTCV
ENDPLT
ENDRUN
```

APPENDIX H

STUDYING PET FILMS WITH POLARIZED LIGHT

A molecule will have a polarizability which varies with the direction of an applied electric vector passing through it. However, in a liquid or gas the molecules are distributed and oriented at random, thus it seems reasonable to regard them as having a mean polarizability $\bar{\alpha}_M$, which is an additive function of the atomic polarizabilities. The Lorentz-Lorenz equation can be written as

$$\frac{n^2-1}{n^2+2} \cdot \frac{M}{D} = \frac{4}{3} \pi N_o \bar{\alpha}_M = \left[R_M\right] \qquad (23)$$

where n is the refractive index, M is the molecular weight, D the density of the medium, N_o Avogadro's number, and $[R_M]$ the molecular refractivity. In a crystal the atoms have a particular spatial relationship to one another. The effect of neighboring dipoles on the polarization of any atom varies with the direction of the electric vector. However, this effect falls off very rapidly with the distance between the atoms concerned and in a qualitative treatment it is sufficient to regard it as operating only between atoms which are linked by chemical bonds, i.e., atoms in the closest proximity to one another.

Consider the simple case of a line of atoms which are chemically linked and more widely separated from other atoms in a transverse direction. If the electric vector of light is parallel to the line joining the atomic centers and dipoles are in line (-+-+-+-+), such an arrangement of charges results in the moments of the dipoles being increased by induction above the value they would have if the effects of immediate neighbors cancelled out. If the electric vector of light is perpendicular to the line joining the atomic centers and the charges of like sign are adjacent, by induction the dipole moments are reduced from the values corresponding to the normal polarizabilities. Thus, if diatomic molecules were arranged parallel or nearly parallel to

one another, such a material would have a larger refractive index for light vibrating transverse to this direction. Whether such a material is uniaxial or biaxial depends on the side to side packing of the molecular chains. However, such crystals have a positive optical sign. Materials which have a negative optical sign, such as the PET films herein investigated will have the lower polarizability along the molecule and the higher polarizability normal to this direction. The PET films investigated were biaxial, with the slow direction along the trace of the optic axis plane. This means that the higher refractive index and thus the higher polarizability is along the trace of the optic axis plane. In other words, in view of the above discussion, the molecules align themselves perpendicular to the trace of the optic axis plane or normal to the ($\bar{1}05$) reciprocal lattice planes. All this was confirmed with mechanical measurements which showed that the direction of highest strength was normal to the trace of the optic axis plane.

☆ U. S. GOVERNMENT PRINTING OFFICE: 1976 — 657-630/848